THE DETERMINATION OF FAILURE OCCURRING IN THE STATOR COIL WINDING DUE TO THE OVER-VOLTAGE USING MATLAB SOFTWARE

A Thesis

Presented to

the Faculty of the College of Science & Technology

Morehead State University

In Partial Fulfillment of the Requirements for the Degree

Master of Science in Vocational Education / Technology

by

Ali Reza Alavizadeh

December 1, 2000

Accepted by the faculty of the College of Science & Technology, Morehead State University, in partial fulfillment of the requirements for the Master of Science in Vocational Education / Technology degree.

Ahmad Zargari

Director of Thesis

Master's Committee: _Ahmad Zargari_____ , Chair

James E. Smallwood

Wayne A. Mueller

_1-8-2001_

Date

ABSTRACT

THE DETERMINATION OF FAILURE OCCURRING IN THE STATOR COIL
WINDING DUE TO THE OVER VOLTAGE USING MATLAB SOFTWARE

Ali Reza Alavizadeh, M.S.
Morehead State University, 2000

Director of Thesis: Dr. Ahmad Zargari

This Thesis covers the study of the thermal effect of the voltage surge on the

heat distribution of the stator coil winding. For this study, one turn of the stator coil

winding located at the overhang area of the stator was selected with consideration

given to the impact of the insulator material and curvature of the wire in the overhead

area. MATLAB Software was chosen to solve the transient heat differential equation

using the Finite Element Method. Although the calculated temperatures did not

demonstrate any significant temperature increments leading to thermal failure in the

wire, they did show that the temperature reaches its maximum in the wire where the

curvature is the highest. The temperature in both the conductor and the insulator

were increased by the choice of material insulators, which possessed less thermal

conductivity. Also, as the curvature of the wire increased, the temperature increased

in both the conductor and the insulator. The inner side of the bent part of the wire

possessed higher temperature than the outer side and this was true regardless of the

insulator material and the curvature of the wire. The impact of the voltage surge appeared as a sudden increment in the wire temperature for both conductor and insulator, and as expected the temperature of the conductor was higher than the insulator. By changing the material property and the curvature, the nodal temperatures were changed accordingly but the temperature distribution remained the same.

Accepted by: _Ahmad Zargari_____ , Chair

James E. Smallwood

Wayne A. Morella

TABLE OF CONTENTS

ACKNOWLEDGEMENTS

The author wishes to acknowledge all those individuals who assisted in completion of this Thesis. Their continuos support and guidance toward successful completion of this Thesis is highly appreciated.

Sincere appreciation is expressed to Dr. Ahmad Zargari, my Thesis Advisor, for his guidance and encouragement. His useful and effective assistance was always a positive help toward finishing the Thesis. Without him, this Thesis would not have been completed. Special thanks are extended to the Masters Committee members, Dr. Wayne A. Morella, and Dr. James E. Smallwood for their willingness to lend their educational and research expertise through constructive criticism and guidance during the Thesis.

I am also grateful to Dr. William R. Grise and Dr. Rodney B. Stanley for providing their technical guidance from the beginning of the research to its completion. Thanks are also extended to Dr. Charles J. Whidden, Dr. Benjamin K. Malphrus, and Mr. Michael Combs for sharing their academic and technical experiences and constructive guidance.

Sincere gratitude is expressed to Dr. S. Ali Ahmadi and Dr. Dora C. Ahmadi for their constructive comments and support during this Thesis. I also wish to thank Ms. Debbie Claxon for providing her useful editorial consultation.

CHAPTER ONE

Introduction

Electric motors play a significant role in our industrial world. They are used in refrigerators, air conditioners, fans, hair dryers, and automobiles. Electric motors are categorized into two different groups: DC motors and AC motors. DC motors are those which work with Direct Current (DC), while AC motors are those that work with Alternative Current (AC). Generally, electric motors consist of a fixed coil called *Stator* and a moving coil called *Rotor*. Figure 1 shows some rotor coils and Figure 2 (next page) shows a stator coil.
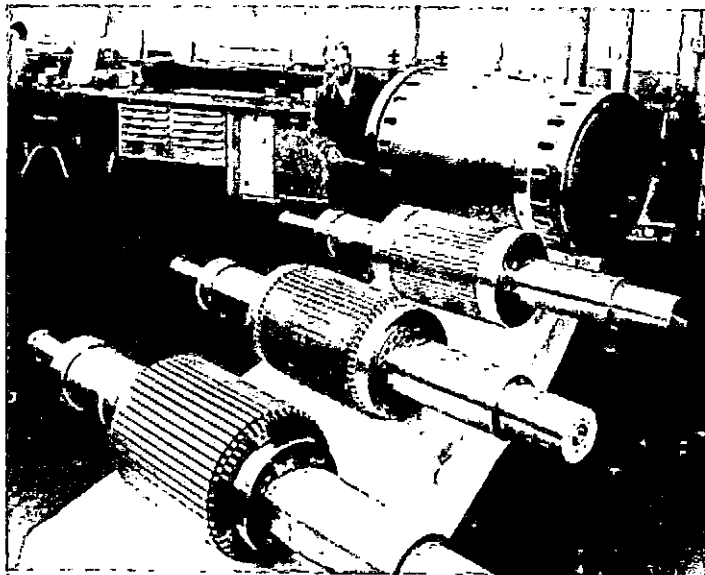

Figure 1. Rotor for a 2500-kW 3-kV two pole 400-Hz motor in different stages of production. (Courtesy Brown Company).
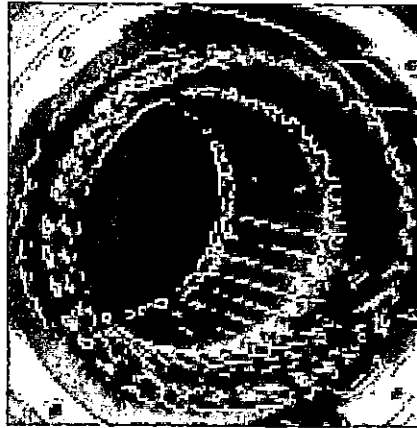
Figure 2. A typical stator coil winding.

When voltage surge is loaded on the input of an electric device such as a refrigerator, it may damage some components in the circuitry of the device. Electric motors, like other electric devices, are vulnerable to over-voltage. The coil inside the motor (either rotor or stator) may be damaged due to a sudden increase in input voltage. Electric discharge, lightning, or short circuit may cause over-voltage. In order to prevent coil damage due to the over-voltage phenomenon there is a device called Voltage Suppressor to reduce the effect of voltage surge. Another device, called Lightning Arrester, is used to control the storm-generated lightning strikes. None of these devices, of course, are perfect. They just reduce the effect of the surge and do not totally prevent the coil failure.

Other factors could indirectly impact the coil winding, such as mechanical stress exerted on the wires by the slot walls. When this type of stress occurs, both

conductor and insulators experience a pressure, which leads to the temperature increasing in both of them. Therefore, when voltage surge is loaded across the coils, it creates extra temperature inside the wires. Figure 3 shows a real case in which the failure has occurred due to the voltage surge.
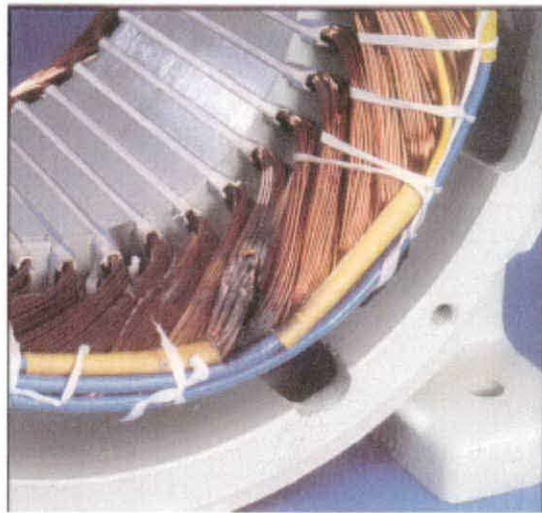
Figure 3. The coil winding failure as a result of voltage surge.

The impact of the voltage surge on the coil winding appears with the sudden increasing of the temperature within the conductors and insulators. The wires turn to turn or even the winding may be grounded in the slot as shown in Figures 4 (next page) and 5 (next page) due to voltage surge.

In addition, there are different sources of thermal stress as well as mechanical stress. Sufficient attention should be paid to choose proper material for insulator *Coefficient of Linear Expansion* (CLE). This coefficient determines the rate of

expansion of the insulator's dimension with respect to the temperature increase. If the difference between the insulator's CLE and conductor's CLE is too much, the conductor and the insulator will not expand with the same rate. Therefore, additional stress will be
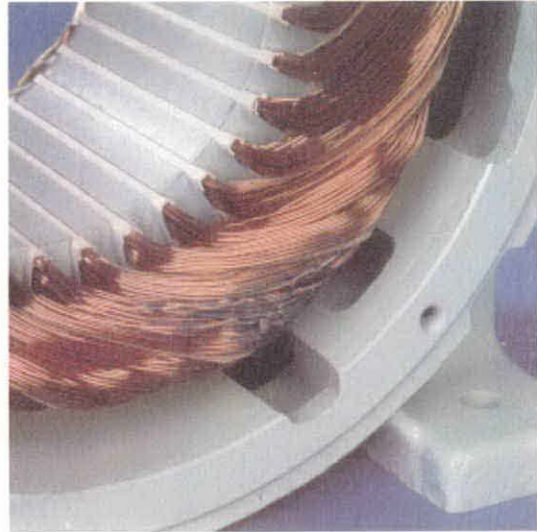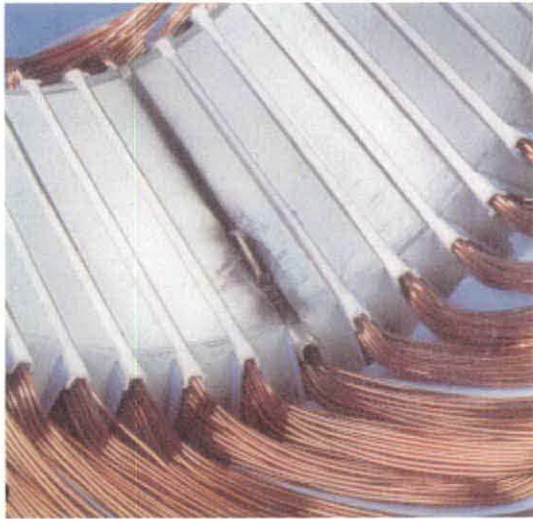
Figure 4. Winding grounded in the Slot.   Figure 5. Winding shorted turn-to-turn.

produced and exerted to both the conductor and insulator due to this difference. If the wire is bent sharply at the corners of the slots, then the cross-section of the wire at that particular point will decrease. Consequently, the resistance will increase because the resistance has an inverse relation with the cross-section of the wire. Therefore, the wire is subject to more thermal stress, resulting in a higher expected chance for failure. In order to observe the places in which the failure occurs, the heat equation

within the wire will be solved. A computer program can be implemented for assistance in solving the equation.

General Area of Concern

Voltage surge is a general cause of failure in the electrical machines and it is not limited to motors. In any electric or electronic circuit, a discharge of a capacitor may cause over-voltage. For example, capacitors store electric energy. If, by accident, a capacitor is discharged, the stored energy inside the capacitor is loaded onto the circuit. This extra load appears as a voltage peak on the circuit voltage. Some components in the circuit work within some specific range of input voltage and now, they receive extra voltage. Therefore, they cannot handle it and failure occurs.

Lightning may produce over-voltage. If transmission lines are struck by lightning, this natural phenomenon may damage the cables, transformers, or other electric devices in the circuitry. A typical voltage, to the order of a hundred thousand volts is exerted on the coils in transformers. If they are not equipped with proper circuitry such as lightning arresters, the coil will burn or damage. When lightning strikes the telephone or other communication lines or devices (like antennas), the data and information carried in the lines are distorted and usually destroyed.

Statement of the Problem

The purpose of this Thesis is to determine the place(s) on the stator coil winding that fail due to over-voltage using MATLAB Software. This study is an attempt to determine the temperature distribution among the wires in the stator coil winding of an electric motor using MATLAB Software.

Significance of the Study

Voltage surge has many negative results. It causes damage of the circuitry and electric machines; damages such as burning the coil winding, burning the electronic/ electric components such as ICs, transistors, capacitors and so forth. In the electric motor, voltage surge causes burning of the winding and, as a result, some failures such as turn-to-turn shorted damage, and grounding will happen.

In some cases, it may be impossible to do experiments under real conditions. For instance, in the case of the lightning, one deals with the high voltage from the order of a hundred thousands volts. Working with high voltages is dangerous.

In order to avoid the probable dangers, the real case should be modeled to a smaller size. A circuit is made to produce an impulse and then the output impulse is sent to the stator coil winding. Then the response of the coil can be observed. Another alternative way is to simulate the real situation with computer. Writing or using a software program, which is able to simulate the case of voltage surge, would be useful to analyze the cause and effect of the surge. Using computer simulation allows one to obtain similar results without actually working with the high voltage.

Also, the computer's program can be used in the future and it may be developed to solve more general problems.

There are some software available which have the capability of doing general analyses such as mechanical and thermal analyses. For instance, ANSYS Finite Element Analysis Software is capable of performing several tasks. Using this package, one can also have *Coupled Filed Analysis* (CFA). In CFA, different agents that contribute in the case are coupled and are analyzed. For example, engaging both mechanical and thermal agents to observe the response of the stator coil winding to the over-voltage.

Wires, which have several insulators, should be properly designed. The order of and the materials used in making the insulators are very important. If the order of coating the insulators on the conductor is changed, the heat distribution within the wire entirely will be changed accordingly. Hence, making some comparisons between different analysis is important. It helps manufacturers to improve their products more sufficiently and reliably.

Research Questions

In the present Thesis, three questions are going to be answered regarding the voltage surge phenomenon:

- Where on the wire does the failure happen due to the over-voltage?

- What is the impact of the bent on the heat distribution within the wire?

- What is the impact of the insulator material on the heat distribution within the wire?

Assumptions

The findings of this Thesis depends on the following assumptions:

1- It is assumed that the wires in the stator coil winding are not bent sharply. Therefore, there is a smooth curve in the overhang areas.

2- The wires in the coil winding have only one insulator layer.

Limitations

There are five factors limiting the study:

1- The wires in the coil winding have just one insulator.

2- Just one turn of the stator coil winding is analyzed.

3- The impact of all other agents such as a magnetic field is not considered.

4- Only one value was chosen for the voltage surge (i.e. 50,000 V).

5- Only one material was chosen for the conductor (i.e. Copper).

Definition of Terms

-   *Convection:* One of the ways that heat can be transferred is

convection. It happens when objects with temperature differences are

both in contact with a fluid. Fluid in contact with a high-energy object

gains energy and becomes warmer and, in most cases, it expands and

becomes less dense than the surrounding cooler fluid. Therefore, the

warmed fluid rises toward the cooler object. It reaches the cooler object

and loses energy and, consequently, it becomes denser and falls.

Convection described here is called free; the convection can be forced, as

when a furnace blower causes circulation to heat the room of a house

(Halliday, & Resnick, 1986).

-   *Diffusivity:* Özisik (1980) has stated, "The thermal diffusivity is the

property of the medium and has the dimension of length^2 / time, which

may be given in m^2/hr or m^2/s"(p. 7). The diffusivity is the property of the

medium. It describes the speed of rate of heat propagation into the solid

with change in temperature during time (Özisik, 1980).

-   *Finite Element Method:* It is one of the ways used to solve the differential

equations by means of numerical methods. The strategy is to decompose a

complicated structure into simple small parts and analyze them

individually (Liu, 1998). Using a finite element model gives a piecewise approximation to the equation (Huebner, Thornton, & Byrom, 1995).

- *Electrical Conductivity*: It is the reciprocal of the resistivity, which is a characteristic of a material rather than of a particular specimen of it (Halliday, & Resnick, 1986). Each type of conductive material has its own unique characteristic called resistivity and denoted by ρ (Floyd, 1991).

- *Heat Conduction:* It is the transfer of energy arising from the temperature difference between two adjacent points of a body. The equation governing the heat conduction is described as (Halliday, & Resnick, 1986):

$$H = -kA \frac{dT}{dx} \qquad (1)$$

Where H (measured in Joule per second for instance) is the time rate of heat transfer across the body of area A, dT/dx is the temperature gradient, and k is a constant called *thermal conductivity*.

- *Isotropic Materials*: They are materials in which the physical properties are the same in any chosen direction inside them. For example, if a

material is isotropic, the electrical conductivity is the same in any direction (Sears, 1958).

-   *Laplace Equation*: It is a differential equation named after French mathematician, Pierre Simon de Laplace (1749-1827). It describes physical phenomena such as electromagnetic propagation, mechanical wave propagation, electric potential of a charge distribution and so forth. The equation is written as follows (Özisik, 1980):

$$\nabla^2 \; T\,(\vec{r},\,t) = 0 \qquad\qquad (2)$$

Where T is a desired variable and ∇^2 is called *Laplacian Operator*. The form of Laplacian depends on the coordinate system chosen. For instance, in the Cartesian coordinate system, its form is given by Equation (3) (Arfken, 1971).

$$\nabla^2 \; T = \frac{\partial^2 T}{\partial x^2} + \frac{\partial^2 T}{\partial y^2} + \frac{\partial^2 T}{\partial z^2} \qquad\qquad (3)$$

-   *MATLAB*: The name MATLAB stands for Matrix Laboratory. It is an interactive software, which has been used recently in scientific and engineering fields (MATLAB User's Guide, 1993). MATLAB is not a

computer language in the normal sense, but it does most of the work of a

computer programming language (Kwon, & Bang, 1997).

- *Steady State and Transient*: steady state is a state or condition of a system

or process that does not change in time. Transient is a temporary

oscillation that happens in a circuit because of a sudden change of voltage

or of load (Marriam-Webster's Collegiate Dictionary, 1993). In the

Transient case, the time variation is involved.

- *Stress:* Stress is defined as the force acting across any given surface per

unit area in the material. If the force is a pull perpendicular to the area of

the material, it is called *Tension* (Symon, 1964). Stress may be

mechanical or thermal. When the coil is being wound, the wires are

pulled along the slots in the stator slots. As there are several turns run

inside each slot, there may be some force exerted by the walls of the slots

on the wires. Even the wires may exert force on each other. This force

acts as a stress on the wires.

- *Thermal Conductivity:* it is a constant, which is a characteristic of the

substances (Carslaw, & Jaeger, 1959). A material with a large thermal

conductivity, is a good heat conductor and substance with a small thermal

conductivity, is a poor heat conductor (Halliday, & Resnick, 1986).

- *Thermal expansion coefficient*: Halliday, and Resnick (1986) have defined Thermal expansion coefficient as: "a fractional change in length per degree temperature change".

Summary

Chapter one provided an introduction to the topic of this Thesis. The general area of concern was addressed. After stating the problem, several research questions, with Thesis assumptions and limitations of the study were expressed. The last part of the chapter listed the definition of the terms.

CHAPTER II

REVIEW OF LITERATURE

In this chapter, literature concerning voltage surge will be presented. Then, some articles and papers related to this Thesis will be discussed. The concept of the Finite Element Analysis and approximation methods used for solving the differential equations will be addressed too. Finally, the historical background of the Finite Element Method will be discussed

Review of Literature

Lightning, as an external surge, develops over a short-range time. In order to check the power system stability, high voltage surges are simulated in the laboratories using "impulse". Malik, Al-Arainy, and Qureshi (1998) have defined the impulse as follows: "a unidirectional voltage (or current) rising quickly to its peak value and then decaying slowly to zero"(p. 282). Figure 6 (next page) shows one of the typical circuits used for producing an impulse. The shape of output waveform is shown also (Malik et al, 1998, p. 287). The output of such a circuit is applied to the power system component and the response of the component is recorded and analyzed.
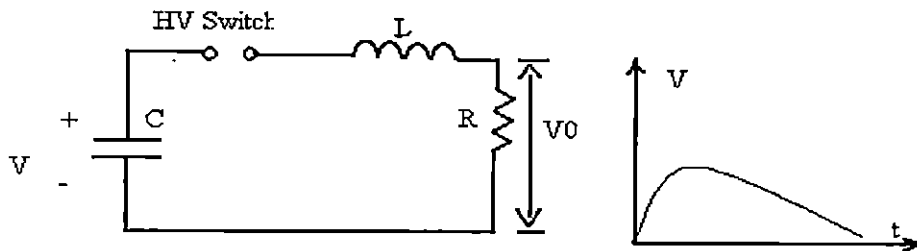
Figure 6. The circuit diagram and output voltage waveform (Malik et al, 1998, p. 287).

Using the same idea, Narang, Gupta, Dick, and Sharma (1989) analyzed and predicted the surge distribution in the motor stator coil winding. In their procedure, measurement was performed on one phase of the stator coil winding while the rest of the phases were grounded to the stator frame. They used a repetitive low-voltage surge generator. They have also compared the experimental results with ones that were obtained by using a computer model for the problem. In their procedure, they considered the turn conductors as transmission lines; each coil was segmented into five distinct sections with uniform geometry.

Oyegoke (1997) used the concept of the transmission line and compared three different approaches for calculating the transient voltage distribution within the stator coil winding. He compared them with the experimental results. Those three methods are *Multiconductor Transmission Line and Scatter Matrix Concept (MTLSMC)*, *Multiconductor Transmission Line and Averaging Techniques Concepts (MTLAC)*, and *Multiconductor Transmission Concept for Circuit Simulators (MTLCCS)*. The

author has concluded: "Also, it has been seen that computation of the peak voltage across turns using the *mtlatc* [sic] and *mtlsmc* gives a very close to experimental results". The author provided a graph, which indicated the transient voltage wave across the coil versus time.

Rajagopal, Seetharamu, and Ashwathnarayana (1998) and Sarkar, Mukherjee, and Sen (1991) considered the transient analysis from another point of view. In both, the whole induction motor including rotor, shaft, and stator were considered and meshed. Rajagopal et al (1998) presented two-dimensional transient finite element analysis of the induction motor. They developed a *Galerkin's weighted residual* technique for analyzing the induction motor. The model was applied to one squirrel cage Totally Enclosed Fan Cooled (TEFC) machine of 3.7 kW and another surfaced-cooled machine with 5.7 kW. They concluded that the model could be applied to all small and medium TEFC motors or any other machine with similar construction. In their paper, just the thermal effect was considered and they did not mention the over-voltage effect and its impact on raising the temperature. A similar approach is seen in Sarkar et al (1991) research, but it was in the steady state case and the time duration was not considered in their approach. They have also used three-dimensional analysis and a three-dimensional arch-shaped prism element for modeling both the rotor and the stator.

Finite Element Method (FEM)

Liu (1998) has defined FEM as follows:

> The *finite element method* (FEM), or *finite element analysis* (FEA),
> is based on the idea of building a complicated object with simple
> blocks, or, dividing a complicated object into small and manageable
> pieces. Application of this simple idea can be found everywhere in
> everyday life as well as in engineering.
> *Examples*:
> - Lego (kids' play)
> - Buildings
> - Approximation of the area of a circle:
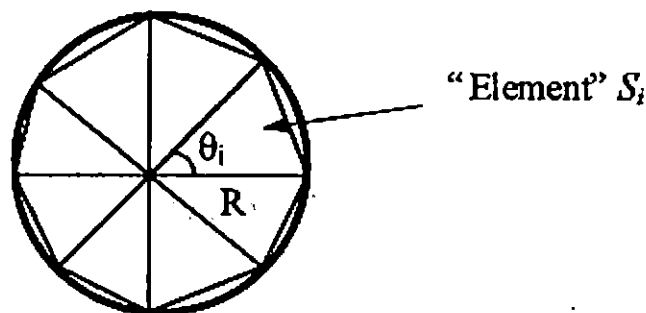
"Element" S_i

Area of one triangle: $= S_i = \dfrac{1}{2} R^2 \sin \theta_i$

Area of the circle: $= \displaystyle\sum_{i=1}^{N} S_i = \dfrac{1}{2} R^2 N \sin \left(\dfrac{2\pi}{N}\right) \rightarrow \pi R^2 \ as\ N \rightarrow \infty$

where N = total number of triangles (elements).

The main goal is to solve some differential equation that describes the physical behavior of the model under certain conditions. Usually, finding the answers for differential equations in complicated models is not easy. However, there are approximation techniques to solve them, such as *Method of Weighted Residual.*

Method of Weighted Residual

This method is explained through solving the following typical differential

equation:

$$\frac{d^2}{dx^2}f - f = -x, \quad 0 < x < 1 \quad , \quad f(0) = 0, \text{ and } f(1) = 0 \quad (4)$$

In this method, a trial function (with unknown coefficients) is chosen and

implemented in the differential equation (Kwon, & Bang, 1997). Usually the form of

the trial function is not as simple as the one used here to show the method. The trial

function is defined: $u = a x (1 - x)$. Simple calculation shows that this function

satisfies the boundary conditions. So it is put into the Equation 4.

$$R = \frac{d^2}{dx^2}u - u + x = -2a - a x(1 - x) + x \quad (5)$$

R is called *The Residual Error*. In order to obtain the unknown parameter a,

Equation 5 should be solved. To this end, a *weighted function* (called w) is chosen

and the weighted averaged of the residual over the interval [0,1] is set to zero.

Therefore:

$$I = \int_0^1 w R \, dx = \int_0^1 w \left(\frac{d^2u}{dx^2} - u + x \right) dx \quad (6)$$

$$I = \int_0^1 w \left[-2a - \alpha x \left(1 - x \right) + x \right] dx = 0 \qquad (7)$$

Next, Function w should be determined. For this, there are several ways to estimate the weighted function, and the resultant approximation solution differs depending on the weighted function. One of those ways is *Galerkin's Method*. In this method, the weighted function is calculated from the trial function itself (Kwon, & Bang, 1997):

$$w = \frac{du}{da} \qquad (8)$$

Using this method for the above example yields $w = x \left(1 - x \right)$. Substituting w in Equation 7, obtained $a = 0.2272$ so that $u = 0.2272x \left(1 - x \right)$ (Kwon, & Bang, 1997).

Piecewise Continuous Trial Function

Function u obtained in the previous section is not the *exact* one because it has just been estimated, but it can be improved. For this, more terms can be added to the trial function and each of the added functions would have an unknown constant. Therefore, the same number of weighted functions, as the number of constants, would be added.

Assuming the trial function for the unknown exact answer is not an easy task. This is especially true when the shape of the problem is more complicated or the domain contains complicated boundary conditions. In order to overcome these problems, the trial function is described using piecewise continuous functions (Kwon, & Bang, 1997). Consider the following function:

$$g_i(x) = \begin{cases} \dfrac{x - x_{i-1}}{x_i - x_{i-1}} & x_{i-1} \le x \le x_i \\[2mm] \dfrac{x_{i+1} - x}{x_{i+1} - x_i} & x_i \le x \le x_{i+1} \\[2mm] 0 & \text{otherwise} \end{cases}$$

Writing the trial function (u) in term of $g_i(x)$ results:

$$u(x) = a_1 g_1(x) + a_2 g_2(x) \qquad\qquad (9)$$

Now, the interval [0,1] is divided into three subintervals and g_is are introduced based on this division as shown by Figure 7 (next page).
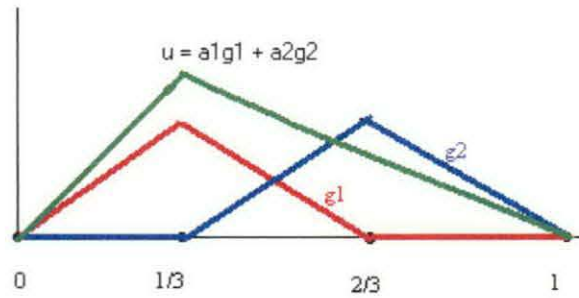
Figure 7. The interval [0,1] is divided into three equal sub-domains.

$$g_1(x) = \begin{cases} 3x & 0 \le x \le \dfrac{1}{3} \\[2ex] 2\text{-}3x & \dfrac{1}{3} \le x \le \dfrac{2}{3} \\[2ex] 0 & \dfrac{2}{3} \le x \le 1 \end{cases}$$

$$g_2(x) = \begin{cases} 0 & 0 \le x \le \dfrac{1}{3} \\[2ex] 3x\text{-}1 & \dfrac{1}{3} \le x \le \dfrac{2}{3} \\[2ex] 3\text{-}3x & \dfrac{2}{3} \le x \le 1 \end{cases}$$

Using Equation 9 results:

$$u = \begin{cases} a_1(\,3\,x\,) & 0 \le x \le \frac{1}{3} \\[2em] a_1(\,2-3\,x\,)+a_2(\,3\,x-1\,) & \frac{1}{3} \le x \le \frac{2}{3} \\[2em] a_2(\,3-3\,x\,) & \frac{2}{3} \le x \le 1 \end{cases}$$

For computing the residual error, the weighted functions must be defined. The *Galerkin's* method is used to calculate the weighted functions (Kwon, & Bang, 1997). Using Equation 8 yields:

$$w_1 = \begin{cases} 3\,x & 0 \le x \le \frac{1}{3} \\[2em] 2-3\,x & \frac{1}{3} \le x \le \frac{2}{3} \\[2em] 0 & \frac{2}{3} \le x \le 1 \end{cases} \qquad (10)$$

$$w_2 = \begin{cases} 0 & 0 \le x \le \frac{1}{3} \\[2em] 3\,x-1 & \frac{1}{3} \le x \le \frac{2}{3} \\[2em] 3-3\,x & \frac{2}{3} \le x \le 1 \end{cases} \qquad (11)$$

From Equation 6, obtained, $I = \int_0^1 w\,R\,dx = \int_0^1 w\,(\frac{d^2u}{dx^2} - u + x)dx$. Using the integration by part technique results:

$$I = \int_0^1 (-\frac{dw}{dx}\frac{du}{dx} - w\,u + x\,w)\,dx + (w\,\frac{du}{dx}\Big|_0^1) = 0 \qquad (12)$$

And using Equations 10 and 11, finally yielded:

$$I_1 = \int_0^1 (-\frac{dw_1}{dx}\frac{du}{dx} - w_1\,u + x\,w_1)\,dx + (w_1\,\frac{du}{dx}\Big|_0^1) = 0$$

$$I_2 = \int_0^1 (-\frac{dw_2}{dx}\frac{du}{dx} - w_2\,u + x\,w_2)\,dx + (w_2\,\frac{du}{dx}\Big|_0^1) = 0$$

By solving these two integrals, the values for a_1 and a_2 will be determined. Using a_1 and a_2 in Equation 9 leads to the trial function (Kwon, & Bang, 1997).

Galerkin's Finite Element Function

In the previous section, the trial function was computed by using some piecewise continuous functions. These functions are characterized by some parameters (similar to a_1 and a_2). Now the piecewise continuous functions are defined by means of the values of the trial function at each node. In other words,

these functions are defined in terms of nodal variables. Considering the same

example above, and try to solve it (Kwon, & Bang, 1997). Figure 8 shows an interval

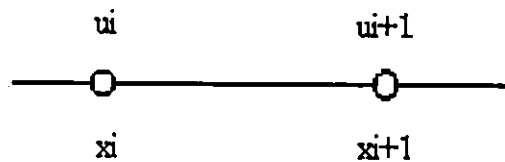in the domain of the problem (which is [0,1]). This "sub-domain" is called *Element*.

$$u_i \qquad\qquad u_i{+}1$$

$$x_i \qquad\qquad x_i{+}1$$

Figure 8. A sub-domain of the total domain.

Now, the trial function is defined as below:

$$u = c_1 x + c_2 \qquad\qquad (13)$$

At each node the value of the function u is:

$$u\,(x_i) = c_1 x_i + c_2 = u_i \qquad\qquad (14)$$

$$u\,(x_{i+1}) = c_1 x_{i+1} + c_2 = u_{i+1}$$

Where u_i and u_{i+1} are nodal values (refer to Figure 8). Solving these equations yield:

$$c_1 = \frac{u_{i+1} - u_i}{x_{i+1} - x_i} \qquad (15)$$

$$c_2 = \frac{u_i x_{i+1} - u_{i+1} x_i}{x_{i+1} - x_i}$$

By substituting these parameters into Equation 13, obtained:

$$u = H_1(x) u_i + H_2(x) u_{i+1} \qquad (16)$$

where

$$H_1(x) = \frac{x_{i+1} - x}{h_i} \qquad (17)$$

$$H_2(x) = \frac{x - x_i}{h_i} \qquad (18)$$

$$h_i = x_{i+1} - x_i$$

Equations 17 and 18 are called *linear shape functions* (Kwon, & Bang, 1997).

It is seen that u is computed in terms of nodal values u_i and u_{i+1}. First, the domain is

divided into three elements with corresponding nodal values as shown in Figure 9.

Element 1   Element 2   Element 3

$$
\begin{array}{cccc}
u1 & u2 & u3 & u4 \\
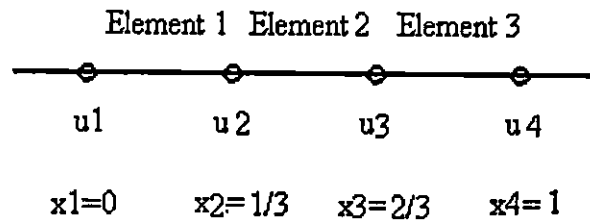x1=0 & x2=1/3 & x3=2/3 & x4=1
\end{array}
$$

Figure 9. The domain is divided into three elements.

Because there are three elements, three residues exist as follows:

$$ I = \sum_{i=1}^{3} \int_{x_i}^{x_i+1} (- \frac{dw}{dx} \frac{du}{dx} - w\,u + x\,w)\, dx + (w\, \frac{du}{dx}\Big|_0^1) = 0 \qquad (19) $$

Next, the proper expressions for w and u are substituted. As there are two u's,

there will be two w's. They are: $w_1 = H_1(x)$ and $w_2 = H_2(x)$. For u's, Equation 15

is used. Consequently:

$$ I = -\int_{x_i}^{x_i+1} \left\{ \begin{bmatrix} H_1' \\ H_2' \end{bmatrix} [H_1'\quad H_2'] + \begin{bmatrix} H_1 \\ H_2 \end{bmatrix} [H_1\quad H_2] \right\} dx \begin{bmatrix} u_i \\ u_{i+1} \end{bmatrix} + \int_{x_i}^{x_i+1} x \begin{bmatrix} H_1 \\ H_2 \end{bmatrix} dx \qquad (20) $$

Which is the matrix form of Equation 19 (Kwon, & Bang, 1997).

Equation 4 is one-dimensional, which means one variable. The more general

case would be a two-dimensional equation. Equation 21 demonstrates a two-

dimensional differential equation (Kwon, & Bang, 1997):

$$\frac{\partial^2 k(x, y)}{\partial x^2} + \frac{\partial^2 k(x, y)}{\partial y^2} = g(x, y) \qquad \text{in } \Omega \qquad (21)$$

Ω is a two-dimensional domain in which the equation is defined. The

boundary conditions are:

$$k = k_0 \qquad\qquad \text{on } \Gamma_e \qquad (22)$$

$$\frac{\partial k}{\partial n} = n_0 \qquad\qquad \text{on } \Gamma_n \qquad (23)$$

Where k_0 is a known value and n_0 is the flux boundary condition. This flux is

measured in the direction of the outward unit vector n_0 at the boundary. Figure 10

(next page) demonstrates a typical two-dimensional boundary condition. Γ_e and Γ_n

are the essential and natural boundary conditions for the differential Equation 21.
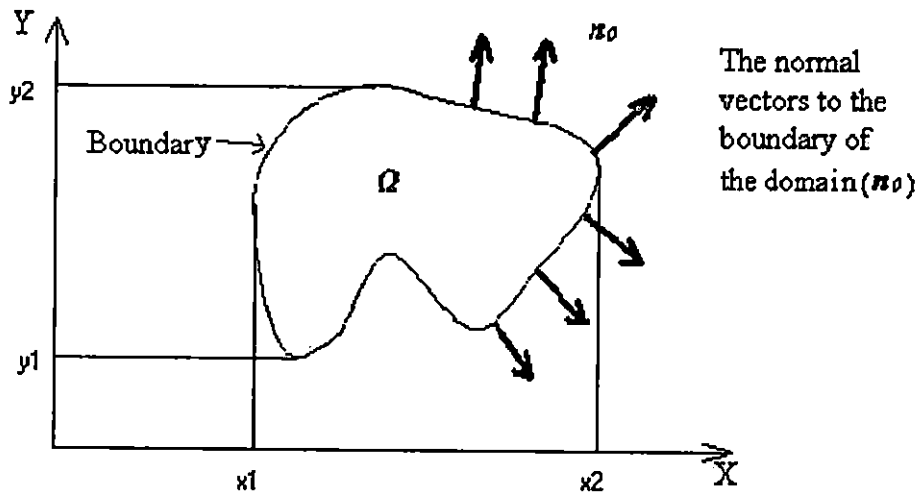
Figure 10. The domain Ω used to solved Equation 21. The curve that encloses the domain is the boundary Γ.

The trial function is chosen to be f. Using the weighted residual method for the two-dimensional domain yields (Kwon, & Bang, 1997):

$$I = \int_{\Omega} w \left(\frac{\partial^2 f}{\partial x^2} + \frac{\partial^2 f}{\partial y^2} - g(x,y) \right) d\Omega$$

$$= \int_{\Omega} w \left(\frac{\partial^2 f}{\partial x^2} + \frac{\partial^2 f}{\partial y^2} \right) d\Omega - \int_{\Omega} w g(x,y) d\Omega \quad (24)$$

For calculating the integral in Equation 24, the integration by part is applied to the first two terms in the integrands. Equations 25 and 26 illustrate the results (Kwon, & Bang, 1997):

$$\int_\Omega w\left(\frac{\partial^2 f}{\partial x^2}\right)d\Omega = -\int_{y1}^{y2}\int_{x1}^{x2}\frac{\partial w}{\partial x}\frac{\partial f}{\partial x}dxdy + \int_{y1}^{y2}\left[w\frac{\partial f}{\partial x}\right]_{x1}^{x2}dy \qquad (25)$$

$$\int_\Omega w\left(\frac{\partial^2 f}{\partial y^2}\right)d\Omega = -\int_{x1}^{x2}\int_{y1}^{y2}\frac{\partial w}{\partial y}\frac{\partial f}{\partial y}dxdy + \int_{x1}^{x2}\left[w\frac{\partial f}{\partial y}\right]_{y1}^{y2}dx \qquad (26)$$

The last two terms in Equations 25 and 26 are calculated at the boundary of the domain Ω. After calculation, they become: $\oint_\Gamma w\frac{\partial f}{\partial x}n_x d\Gamma$ and $\oint_\Gamma w\frac{\partial f}{\partial y}n_y d\Gamma$ respectively. n_x and n_y are the components of the normal vector n which is perpendicular to the boundary Γ. Then Equations 25 and 26 are added. Therefore, (Kwon, & Bang, 1997):

$$\int_\Omega w\left(\frac{\partial^2 f}{\partial x^2}+\frac{\partial^2 f}{\partial y^2}\right)d\Omega = -\int_\Omega\left(\frac{\partial w}{\partial x}\frac{\partial f}{\partial x}+\frac{\partial w}{\partial y}\frac{\partial f}{\partial y}\right)d\Omega + \oint_\Gamma w\left(\frac{\partial f}{\partial x}n_x+\frac{\partial f}{\partial y}n_y\right)d\Gamma \qquad (27)$$

The boundary integral can be written as: $\dfrac{\partial f}{\partial n} = \dfrac{\partial f}{\partial x} n_x + \dfrac{\partial f}{\partial y} n_y$. Using this in Equation 27 yields:

$$\int_\Omega w\left(\frac{\partial^2 f}{\partial x^2} + \frac{\partial^2 f}{\partial y^2}\right) d\Omega = -\int_\Omega \left(\frac{\partial w}{\partial x}\frac{\partial f}{\partial x} + \frac{\partial w}{\partial y}\frac{\partial f}{\partial y}\right) d\Omega + \oint_\Gamma w\frac{\partial f}{\partial n} d\Gamma \qquad (28)$$

Next, the first term in Equation 24 is replaced with Equation 28. Therefore, (Kwon, & Bang, 1997):

$$I = -\int_\Omega \left(\frac{\partial w}{\partial x}\frac{\partial f}{\partial x} + \frac{\partial w}{\partial y}\frac{\partial f}{\partial y}\right) d\Omega - \int_\Omega wg(x,y) d\Omega + \int_{\Gamma_n} w\frac{\partial f}{\partial n} d\Gamma \qquad (29)$$

There are different finite elements used to discretize a two-dimensional domain. One of the simplest elements is the three-nodded triangle, as in Figure 11 (next page).
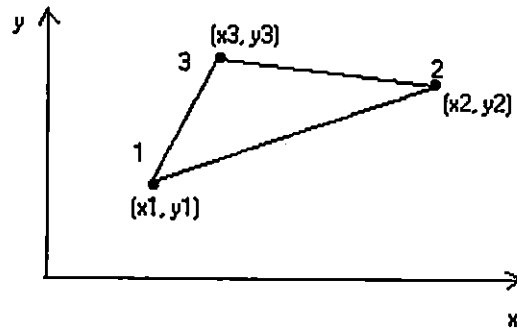
Figure 11 . A typical triangle element.

The interpolation function used for the triangular element is written as a linear polynomial with two independent variables. Equation 30 demonstrates the interpolation function.

$$f = c_1 + c_2 x + c_3 y \qquad\qquad (30)$$

Or in matrix form:

$$f = \begin{bmatrix} 1 & x & y \end{bmatrix} \begin{bmatrix} c1 \\ c2 \\ c3 \end{bmatrix} \qquad\qquad (31)$$

Constants c_1 through c_3 should be calculated. This function has three values at three nodal points 1, 2, and 3 in Figure 11. The values are f_1, f_2, and f_3 respectively and are shown as the matrix form in Equation 32.

$$\begin{bmatrix} f1 \\ f2 \\ f3 \end{bmatrix} = \begin{bmatrix} 1 & x1 & y1 \\ 1 & x2 & y2 \\ 1 & x3 & y3 \end{bmatrix} \begin{bmatrix} c1 \\ c2 \\ c3 \end{bmatrix} \tag{32}$$

Solving the linear equation in Equation 32 with respect to cs yields (Kwon, & Bang, 1997):

$$\begin{bmatrix} c1 \\ c2 \\ c3 \end{bmatrix} = \frac{1}{2A} \begin{bmatrix} x2y3 - y3x2 & x3y1 - x1y3 & x1y2 - x2y1 \\ y2 - y3 & y3 - y1 & y1 - y2 \\ x3 - x2 & x1 - x3 & x2 - x1 \end{bmatrix} \begin{bmatrix} f1 \\ f2 \\ f3 \end{bmatrix} \tag{33}$$

In which A is the area of the rectangular area shown in Figure 11 and can be calculated as:

$$A = \frac{1}{2} \begin{vmatrix} 1 & x1 & y1 \\ 1 & x2 & y2 \\ 1 & x3 & y3 \end{vmatrix} \tag{34}$$

By substituting Equation 33 into Equation 31, the trial function will be obtained :

$$f = H_1(x, y)f_1 + H_2(x, y)f_2 + H_3(x, y)f_3 \qquad (35)$$

in which the shape functions H_i are calculated as (Kwon, & Bang, 1997):

$$H_1 = \frac{1}{2A} \left[(x_2y_3 - x_3y_2) + (y_2 - y_3)x + (x_3 - x_2)y \right] \qquad (36)$$

$$H_2 = \frac{1}{2A} \left[(x_3y_1 - x_1y_3) + (y_3 - y_1)x + (x_1 - x_3)y \right] \qquad (37)$$

$$H_3 = \frac{1}{2A} \left[(x_1y_2 - x_2y_1) + (y_1 - y_2)x + (x_2 - x_1)y \right] \qquad (38)$$

Next, the first integral in Equation 29 is calculated as:

$$M^e = \int_\Omega \left(\frac{\partial w}{\partial x} \frac{\partial f}{\partial x} + \frac{\partial w}{\partial y} \frac{\partial f}{\partial y} \right) d\Omega$$

$$= \int_\Omega \left(\begin{bmatrix} \dfrac{\partial H1}{\partial x} \\ \dfrac{\partial H2}{\partial x} \\ \dfrac{\partial H3}{\partial x} \end{bmatrix} \begin{bmatrix} \dfrac{\partial H1}{\partial x} & \dfrac{\partial H2}{\partial x} & \dfrac{\partial H3}{\partial x} \end{bmatrix} + \begin{bmatrix} \dfrac{\partial H1}{\partial y} \\ \dfrac{\partial H2}{\partial y} \\ \dfrac{\partial H3}{\partial y} \end{bmatrix} \begin{bmatrix} \dfrac{\partial H1}{\partial y} & \dfrac{\partial H2}{\partial y} & \dfrac{\partial H3}{\partial y} \end{bmatrix} \right) d\Omega \qquad (39)$$

Calculating Equation 39 yields a matrix called *element matrix*. This matrix and its

components are demonstrated in Equations 40 through 49 (Kwon, & Bang, 1997):

$$[M^e] = \begin{bmatrix} m11 & m12 & m13 \\ m21 & m22 & m23 \\ m31 & m32 & m33 \end{bmatrix} \tag{40}$$

$$m_{11} = \frac{1}{4A} \, [(x_3 - x_2)^2 + (y_2 - y_3)^2] \tag{41}$$

$$m_{12} = \frac{1}{4A} \, [(x_3 - x_2)(x_1 - x_3) + (y_2 - y_3)(y_3 - y_1)] \tag{42}$$

$$m_{13} = \frac{1}{4A} \, [(x_3 - x_2)(x_2 - x_1) + (y_2 - y_3)(y_1 - y_2)] \tag{43}$$

$$m_{21} = m_{12} \tag{44}$$

$$m_{22} = \frac{1}{4A} \, [(x_1 - x_3)^2 + (y_3 - y_1)^2] \tag{45}$$

$$m_{23} = \frac{1}{4A} \, [(x_1 - x_3)(x_2 - x_1) + (y_3 - y_1)(y_1 - y_2)] \tag{46}$$

$$m_{31} = m_{13} \tag{47}$$

$$, \quad m_{32} = m_{23} \tag{48}$$

$$m_{33} = \frac{1}{4A} \ [(x_2 - x_1)^2 + (y_1 - y_2)^2] \tag{49}$$

The second integral in Equation 29 would be calculated as:

$$\int_\Omega \begin{bmatrix} H1 \\ H2 \\ H3 \end{bmatrix} g(x, y) d\Omega \tag{50}$$

The amount of this integral depends on the form of Function $g(x, y)$. The third integral in Equation 29 is performed over the boundary of the domain Ω. One of the common boundary conditions is the heat convection which is written as $(\partial f / \partial n) = h \times (f - f_0)$. In this formula, h represents the heat convection coefficient and f_0 represents the ambient temperature. Rewriting this equation to obtain a more general case yields $(\partial f / \partial n) = af + b$ (Kwon, & Bang, 1997). Therefore, the last integral in Equation 29 will become:

$$\int_{\Gamma_n} w \frac{\partial f}{\partial n} d\Gamma = \int_{\Gamma'} w\{a(x, y)u + b(x, y)f_0\}d\Gamma \tag{51}$$

The Differential Equation of Heat Conduction in the Solid

The equation governing the heat conduction within a solid is written as:

$$\nabla^2 T - \frac{1}{\kappa}\frac{\partial T}{\partial t} = 0 \tag{52}$$

Where:

$T = T(x, y, z, t)$: the temperature in the solid

$\rho = Density\ of\ the\ solid$

$K = Conductivity$

$\kappa = Diffusivity\ (= \dfrac{K}{\rho c})$

The form of ∇^2 (*Laplacian*) depends on the coordinate system. In the

Cartesian coordinate system, the Laplacian is written as:

$$\nabla^2 T = \frac{\partial^2 T}{\partial x^2} + \frac{\partial^2 T}{\partial y^2} + \frac{\partial^2 T}{\partial z^2} \tag{53}$$

This is the general form of the Laplacian in the Cartesian coordinate system.

If the problem being considered is a two-dimensional one, then the variable T would

be independent of z. Therefore, Equation 53 will be decreased to:

$$\nabla^2 T = \frac{\partial^2 T}{\partial x^2} + \frac{\partial^2 T}{\partial y^2} \tag{54}$$

Carslaw, and Jaeger (1959) have computed "the equation of conduction in a thin wire heated by an electric current" in one dimension. They have stated that this is obtained as:

$$\frac{\partial}{\partial t} T = \kappa \frac{\partial^2}{\partial x^2} T - v(T - T_0) + \frac{jI^2}{\rho c \omega^2} \tag{55}$$

In their formalism, T is temperature and $v = (Hp)/(\rho c \omega)$ and $\kappa = K/\rho c$ (Carslaw, & Jaeger, 1959). They have defined H as *surface conductance* (Carslaw, & Jaeger, 1959, p. 19). I is the current passing through the wire. j is a constant indicating the number of calories in *joule*. It is assumed that the solid is isotropic. Therefore, for a two-dimensional problem, Equation 55 would be changed to:

$$\frac{\partial}{\partial t} T = \kappa (\frac{\partial^2 T}{\partial x^2} + \frac{\partial^2 T}{\partial y^2}) - v(T - T_0) + \frac{jI^2}{\rho c \omega^2} \tag{56}$$

As the voltage surge produces heat inside the wire, a term representing this effect should be added. Because the output of a RC circuit is used to represent the voltage surge, the output voltage of such a circuit is used to make the proper term. Referring to the Ohm's Law, the heat produced in a wire having resistance R due to

some voltage $V(t)$ is calculated as: $(V(t)^2 \times t)/R$. Therefore, this term will be added to

Equation 56. Equation 57 indicates the result:

$$\frac{\partial}{\partial t} T = \kappa \left(\frac{\partial^2 T}{\partial x^2} + \frac{\partial^2 T}{\partial y^2} \right) + \frac{V^2(t)}{R} t + \frac{jI^2}{\rho c \omega^2} \qquad (57)$$

Term $v(T - T_0)$ is omitted in this equation because this term describes the

heat convection and the convection has already been considered (the last term in

Equation 29). Because there are two different types of material (conductor and

insulator), Equation 57 should be solved within both of the materials. Therefore, the

constants κ, ρ, c, ω should be changed properly, depending on the property of the

area. On the other hand, it is apparent that there is neither electric current nor voltage

surge within the insulator. If κ_c, ρ_c, c_c, and ω_c represent the conductor constants and κ_i

represents the insulator thermal conductivity, the governing equation of a wire having

one layer as insulator would be:

In the conductor: $\qquad \frac{\partial}{\partial t} T = \kappa_c \left(\frac{\partial^2 T}{\partial x^2} + \frac{\partial^2 T}{\partial y^2} \right) + \frac{V^2(t)}{R} t + \frac{jI^2}{\rho_c c_c \omega_c^2} \qquad (58)$

In the insulator: $\qquad \frac{\partial}{\partial t} T = \kappa_i \left(\frac{\partial^2 T}{\partial x^2} + \frac{\partial^2 T}{\partial y^2} \right) \qquad (59)$

Next, the weighted residual method should be applied to both Equations 58

and 59. Applying this method to Equation 58 yields:

$$I = \int_\Omega w\kappa_c(\frac{\partial^2 T}{\partial x^2}+\frac{\partial^2 T}{\partial y^2})\,d\Omega + \int_\Omega w\frac{V^2(t)}{R}t\,d\Omega + \int_\Omega w\frac{jI^2}{\rho_c c_c \omega_c^2}\,d\Omega -$$

$$\int_\Omega w\frac{\partial T}{\partial t}\,d\Omega \tag{60}$$

Where Ω and Γ represent the domain and the boundary respectively. The

same procedure should be performed for Equation 59 but only the procedure for

Equation 58 is detailed. In order to calculate the integrals in Equation 60, the domain

Ω should be determined. Figure 12 demonstrates a linear triangle in the Cartesian

coordinate system. This element is chosen to be the domain. The sides of the triangle
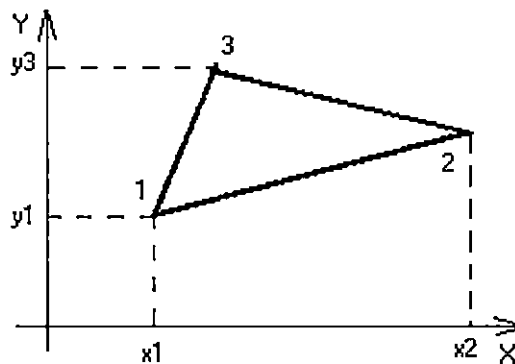
are the boundary Γ.

Figure 12. The domain Ω used to calculate integral I in Equation 60

Therefore:

$$I = \iint\limits_{x\,y} w\kappa_c\left(\frac{\partial^2 T}{\partial x^2}+\frac{\partial^2 T}{\partial y^2}\right)dx\,dy + \iint\limits_{x\,y} w\frac{V^2(t)}{R}t\,dx\,dy +$$

$$\iint\limits_{x\,y} w\frac{jI^2}{\rho_c c_c \omega_c^2}\,dx\,dy - \iint\limits_{x\,y} w\frac{\partial T}{\partial t}\,dx\,dy \qquad (61)$$

Using the integration by parts yields:

$$I = -\iint\limits_{x\,y}\left(\frac{\partial w}{\partial x}\frac{\partial T}{\partial x}+\frac{\partial w}{\partial y}\frac{\partial T}{\partial y}\right)dx\,dy + \int_\Gamma w\frac{\partial T}{\partial n}\,d\Gamma +$$

$$\iint\limits_{x\,y} w\frac{jI^2}{\rho_c c_c \omega_c^2}\,dx\,dy - \iint\limits_{x\,y} w\frac{\partial T}{\partial t}\,dx\,dy \qquad (62)$$

Since $T(x, y, t) = H_1(x, y)\,T_1(t) + H_2(x, y)\,T_2(t) + H_3(x, y)\,T_3(t)$, Equation 62 becomes:

$$I = \iint\limits_{x\,y} \left\{ \begin{bmatrix} H'_{1x} \\ H'_{2x} \\ H'_{3x} \end{bmatrix} \begin{bmatrix} H'_{1x} & H'_{2x} & H'_{3x} \end{bmatrix} + \begin{bmatrix} H'_{1y} \\ H'_{2y} \\ H'_{3y} \end{bmatrix} \begin{bmatrix} H'_{1y} & H'_{2y} & H'_{3y} \end{bmatrix} \right\} dxdy \begin{bmatrix} T_1 \\ T_2 \\ T_3 \end{bmatrix} -$$

$$-\iint\limits_{x\,y} \frac{jI^2}{\rho_c c_c \omega_c{}^2} \begin{bmatrix} H_1 \\ H_2 \\ H_3 \end{bmatrix} dxdy + \int\limits_{x_1}^{x_2} c_x \begin{bmatrix} \dfrac{x_2 - x}{x_2 - x_1} \\ \dfrac{x - x_1}{x_2 - x_1} \\ 0 \end{bmatrix} dx + \int\limits_{y_1}^{y_3} c_y \begin{bmatrix} \dfrac{y_3 - y}{y_3 - y_1} \\ \dfrac{y - y_1}{y_3 - y_1} \\ 0 \end{bmatrix} dy \; -$$

$$\iint\limits_{x\,y} \frac{V^2(t)}{R} t \begin{bmatrix} H_1 \\ H_2 \\ H_3 \end{bmatrix} dxdy + \iint\limits_{x\,y} \begin{bmatrix} H_1 \\ H_2 \\ H_3 \end{bmatrix} \begin{bmatrix} H_1 & H_2 & H_3 \end{bmatrix} \begin{bmatrix} T'_1 \\ T'_2 \\ T'_3 \end{bmatrix} dxdy = 0 \qquad (63)$$

In this equation, c_x and c_y are the thermal convection along the sides, which are parallel to x axis and y axis respectively. The last term in Equation 63 deals with the time-integration. It shows the time variation of the temperature. Using Equations 36, 37, and 38 the last term in Equation 63 becomes (Kwon, & Bang, 1997):

$$\iint\limits_{x\,y} \begin{bmatrix} H_1 \\ H_2 \\ H_3 \end{bmatrix} \begin{bmatrix} H_1 & H_2 & H_3 \end{bmatrix} \begin{bmatrix} T'_1 \\ T'_2 \\ T'_3 \end{bmatrix} dxdy = \frac{A}{12} \times \begin{bmatrix} 2 & 1 & 1 \\ 1 & 2 & 1 \\ 1 & 1 & 2 \end{bmatrix} \qquad (64)$$

In which A is the area of the linear triangle. Now, Equation 63 is rewritten as:

$$[P]\left\{\dot{T}\right\}^t + [Q]\,\{T\}^t = \{V\}^t \qquad (65)$$

In which:

$$[P] = \iint\limits_{x\,y} \begin{bmatrix} H_1 \\ H_2 \\ H_3 \end{bmatrix} [H_1 \quad H_2 \quad H_3]\, dxdy \qquad (66)$$

$$[Q] = \iint\limits_{x\,y} \left\{ \begin{bmatrix} H'_{1x} \\ H'_{2x} \\ H'_{3x} \end{bmatrix} [H'_{1x} \quad H'_{2x} \quad H'_{3x}] + \begin{bmatrix} H'_{1y} \\ H'_{2y} \\ H'_{3y} \end{bmatrix} [H'_{1y} \quad H'_{2y} \quad H'_{3y}] \right\} dxdy \qquad (67)$$

$$\{V\} = -\iint\limits_{x\,y} \frac{jI^2}{\rho_c c_c \omega_c^2} \begin{bmatrix} H_1 \\ H_2 \\ H_3 \end{bmatrix} dxdy + \int\limits_{x_1}^{x_2} c_x \begin{bmatrix} \dfrac{x_2 - x}{x_2 - x_1} \\[4pt] \dfrac{x - x_1}{x_2 - x_1} \\[4pt] 0 \end{bmatrix} dx + \int\limits_{y_1}^{y_3} c_y \begin{bmatrix} \dfrac{y_3 - y}{y_3 - y_1} \\[4pt] \dfrac{y - y_1}{y_3 - y_1} \\[4pt] 0 \end{bmatrix} dy \ - \qquad (68)$$

$$- \iint\limits_{x\,y} \frac{V^2(t)}{R} t \begin{bmatrix} H_1 \\ H_2 \\ H_3 \end{bmatrix} dxdy$$

In Equation 65, the superscript *t* indicates that the temperature *T* varies with

time. $\dot{T}$ indicates the derivative of the temperature with respect to the time. There are

several ways to calculate the integrals having the time variation. The one used for

this study is *the backward difference method.*

The Backward Difference Method

Equation 65 is written at time t. If the time is changed by amount Δt, then

Equation 65 will turn to:

$$[P] \left\{ \overset{\bullet}{T} \right\}^{t+\Delta t} + [Q] \{T\}^{t+\Delta t} = \{V\}^{t+\Delta t} \qquad (69)$$

The derivative of Function T is:

$$\{\overset{\bullet}{T}\}^{t+\Delta t} = \frac{\{T\}^{t+\Delta t} - \{T\}^{t}}{\Delta t} \qquad (70)$$

Using Equation 70 in Equation 69 yields:

$$([P] + \Delta t [Q])\{T\}^{t+\Delta t} = \Delta t \{V\}^{t+\Delta t} + [P]\{T\}^{t} \qquad (71)$$

The last integral in Equation 68 contains a term representing the output

voltage of the RC circuit (Figure 6). Basically, the output voltage of any RC circuit is

in the form of Equation 72 (next page).

$$V(t) = V_0 \, e^{-\frac{1}{RC}t} \qquad\qquad (72)$$

In which V_0 is the voltage across the capacitor before being connected to the resistor. R is the resistance.

Historical Background of Finite Element Analysis

Before the advent of computers, scientists had to solve differential equations using complicated solution concepts such as series, *Bessel Functions, Laplace Transformation* and so on. Solving the equation using these concepts required simplifying the problem. They were also time-consuming and human error became another source of inaccuracy. Even if they could solve the equation, with these concepts, the answer was not too realistic (Hoole, 1989).

The advent of the digital computer and sophisticated software made it possible to obtain the answer in a few minutes. Computers became more effective and reliable and, therefore, their usage has expanded in solving equations and problems. These schemes are known as *approximation* methods, since it is possible to increase the accuracy as much as desired, according to the available computer technology.

True, these digital, approximate solutions may be less accurate than the closed form solution from classical analysis for simple problem shapes such as the circle or the triangle. However; in the real world, numerical scheme yields more accurate solutions in view of the classical methods' dependence on simplifying assumptions

(Hoole, 1989). As a historical background of Finite Element Method, Hoole (1989)

has stated the following:

> Finite elements made their earliest appearance in 1941. Hrenikoff
> (1941) and later McHenry (1943) introduced the concept of replacing a
> continuum by a latticelike assembly of bars, in analogy with a structure
> of steel struts. In consequence, although the method is generally
> applicable to the solution of any differential equation in a continuum,
> the terminology of the science of finite elements is laced with the
> terminology of structural analysis.

The method was expanded and improved, and the interpolation

functions were introduced to describe the nodal variables within the elements.

Gradually the method was implemented in various branches of engineering,

such as electrical and mechanical engineering. For example, in the Electrical

field, Silvester (1969) used high-accuracy triangular finite elements for

solving the Laplace's differential equation. In his article, he presented details

about the high-order polynomial with the triangular element shape. He also

developed a computer program used for analyzing the general high-order

finite element waveguide. About Silvester and his role in improving the

Finite Element Method, Hoole (1989) implies:

> He introduced high-order polynomial triangular elements (Silvester
> 1969), the idea of ballooning for open boundary problems (Silvester,
> Lowther, Carpenter, and Wyatt 1977), and the concept of universal
> matrices (Silvester 1978, 1982a, 1982b) on which most of the current
> finite elements research effort in electrical engineering is based.
> Thanks largely to his endeavors, by the middle of the 1970s the method
> was acknowledged as one of the best for the solution of large field
> problems in electromagnetics [sic].

Zienkiewicz, Lyness, and Owen (1977) developed a computer program to

formulate the three-dimensional magnetic field problem. Their work is also

related to the electrical field. In the electro-heat problems, Armor and Chari (1976) analyzed the heat flow in the stator core by implementing a three-dimensional finite element.

Summary

In chapter II, the literature used for this Thesis was reviewed. There were similar papers in which the transient analysis had been discussed. One of the approximation methods for solving the differential equations was introduced (*Weighted Residual Method*). The methods to calculate the trial function were stated. Finally, a brief history of the finite element method was explained.

CHAPTER III

METHODOLOGY

This chapter consists of methods and procedures used in conducting the present Thesis. The following items are addressed: restatement of the problem, restatement of the research questions, research instruments and methods, and the summary of the chapter.

Restatement of the Problem

The purpose of this Thesis is to determine the place(s) where the stator coil winding wires fail due to over-voltage using MATLAB Software. This study is an attempt to determine the temperature distribution among the wires in the stator coil winding of an electric motor using MATLAB Software.

Restatement of the Research Questions

When the over-voltage phenomenon occurs, some place(s) damage. There are several agents responsible for the failure, such as resistance of the wires, and the shape of the coil winding. There are three questions to be answered:

- Where on the wire does the failure happen due to over-voltage?

- What is the impact of the bent on the heat distribution within the wire?

- What is the impact of the insulator material on the heat distribution within the wire?

Research Instrument and Procedure

One turn of a stator coil winding was chosen. The wire had one insulator

layer. The wire was divided into three parts: two straight cylinders that ran inside the

slot of the stator core and one curved part (over hang part) that went from one slot

into another as shown by Figure 13. Point *I* indicates the place where the input

voltage is applied and point *O* indicates the output.

As shown in Figure 13, the wire had symmetry around axis *YY'*. Therefore,

half of the wire (for instance the right side of the wire) was considered for analyzing.

Figure 14 (next page) demonstrates the left hand-side of the wire.
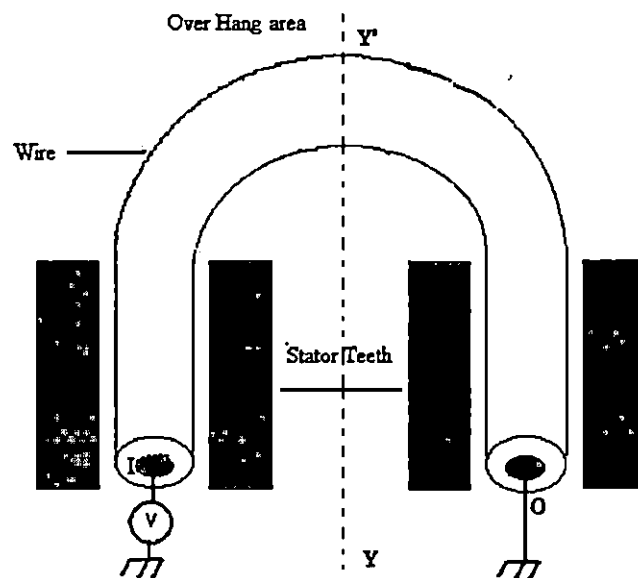
Figure 13. A wire in the slot of a stator coil winding.
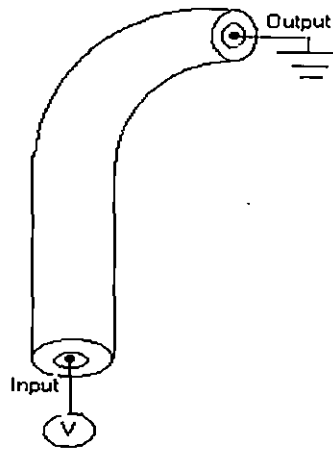
Figure 14. The left hand side of the wire shown in Figure 13.

Since the temperature distribution across and along the wire was being studied, a cross-section along the wire was considered. Therefore, the wire was divided into two identical parts as shown in Figure 15.
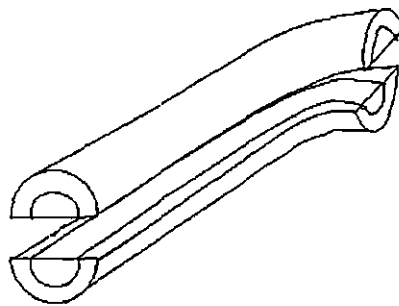

Figure 15. The wire was divided into two identical parts. The shaded area shows the conductor.

Figure 16, shows the same cross-section shown in Figure 15 from the top view. This

area was basically the domain in which the analysis was performed.
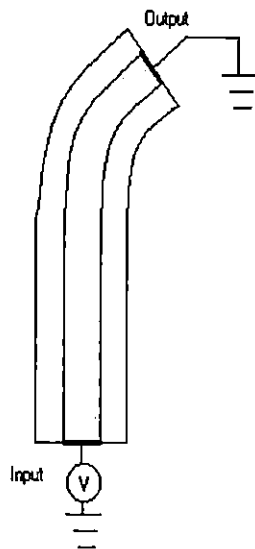
<u>Figure 16.</u> The cross-section of the wire from the top view.

Next, the domain needed to be meshed. Because the domain was two-

dimensional, the two-dimensional element was used. The element chosen for the

current study was the linear triangle element.

The Computer Program and It Components

The main steps spanned to do finite element analysis were:

    1- Dividing the domain of analysis into small linear triangles.

    2- Numbering the nodes created in the domain.

3- Calculating the element vector and element matrix and making the system vector and system matrix.

4- Applying the constraints existing in the problem to the system vector and matrix in order to obtain the main matrix equation.

5- Solving the matrix equation.

6- Plotting the results for different points within the wire.

In order to perform all of the above tasks, nine different MATLAB functions were written. In this analysis, the domain shown in Figure 16 was divided into 600 linear triangles. The total number of the nodes was three 336. Figure 17 demonstrates the meshed domain (it shows the bent part partially).
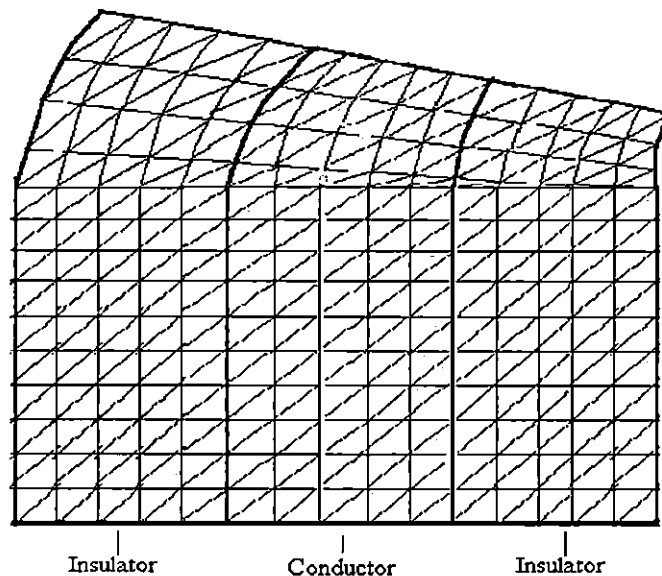

Figure 17. The domain was meshed using the triangle element.

Figure 17 was used to design the parts of the computer program, which deals with the meshing and coordinates of the nodes. The computer program consisted of nine functions, which are all called from the main program. The name and the functionality of each function are explained as follows:

1- *ss_cylinder* (the main function)

All of the variables' declarations and initializations are made in this function. This function also calls the other functions to perform their tasks one by one. The constraint nodes, the corresponding values, and the flux at the boundaries are determined in this function.

A list of all variables and their tasks are defined. This list is useful for debugging and tracing the program. Most of the variables are global, which means that any of the functions, which are called from the main program, can use them. There are some local variables that are defined within certain functions. Appendix A-1 shows the names of all the variables used in the MATLAB program.

Another list gathered in the first stage of this function is the names of all matrices and vectors. This list is useful for understanding and tracing the whole program. Appendix A-2 demonstrates the names of all the involved matrices and vectors. Appendix A-3 shows the functions used in the MATLAB program.

The initialing of the variables, matrices, and vectors are the next stage. Some of these variables, such as the thermal conductivity of the wire (named *con_k* in the

main program) are constants. Therefore; these values remain unchanged. If another

kind of material is used for the analysis, the related variables should be modified.

This modification is performed easily in the *"Initialing the variables, vectors, and*

matrices" part of Function *ss_cylinder*. In the main program, the matrix solution is

solved and the results will be plotted. Plotting is the last part of the program.

The algorithm flowchart of Function *ss_cylinder* is shown in Figure 18.
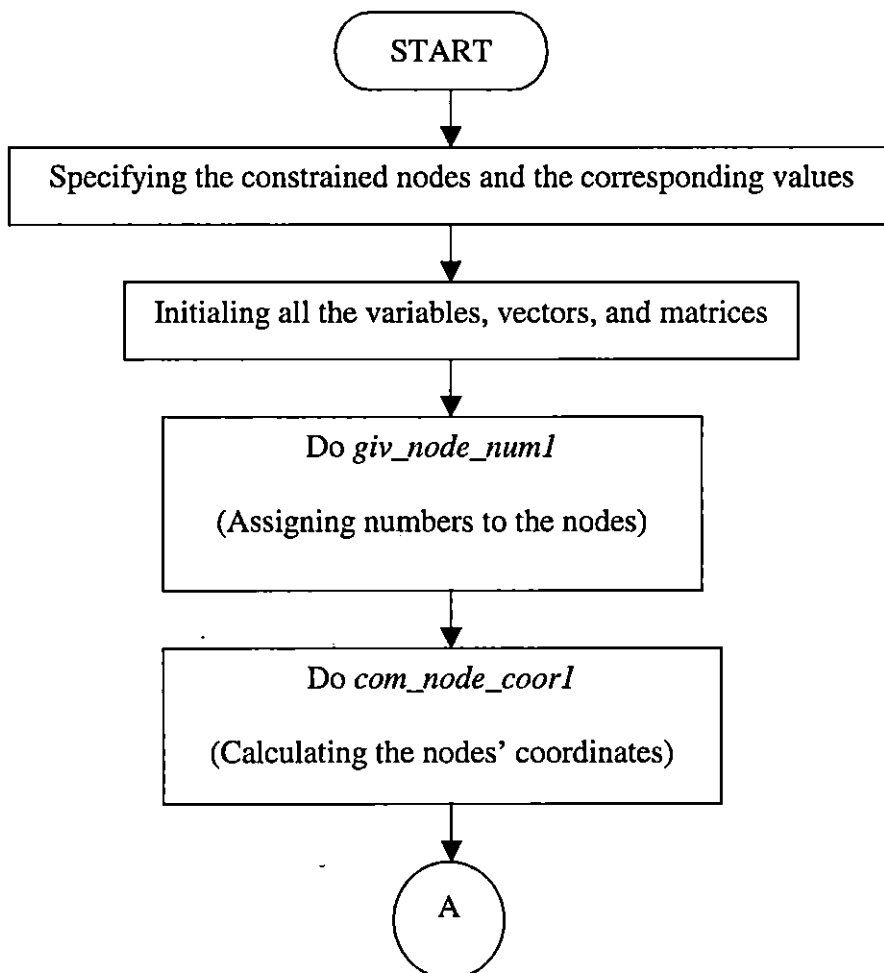

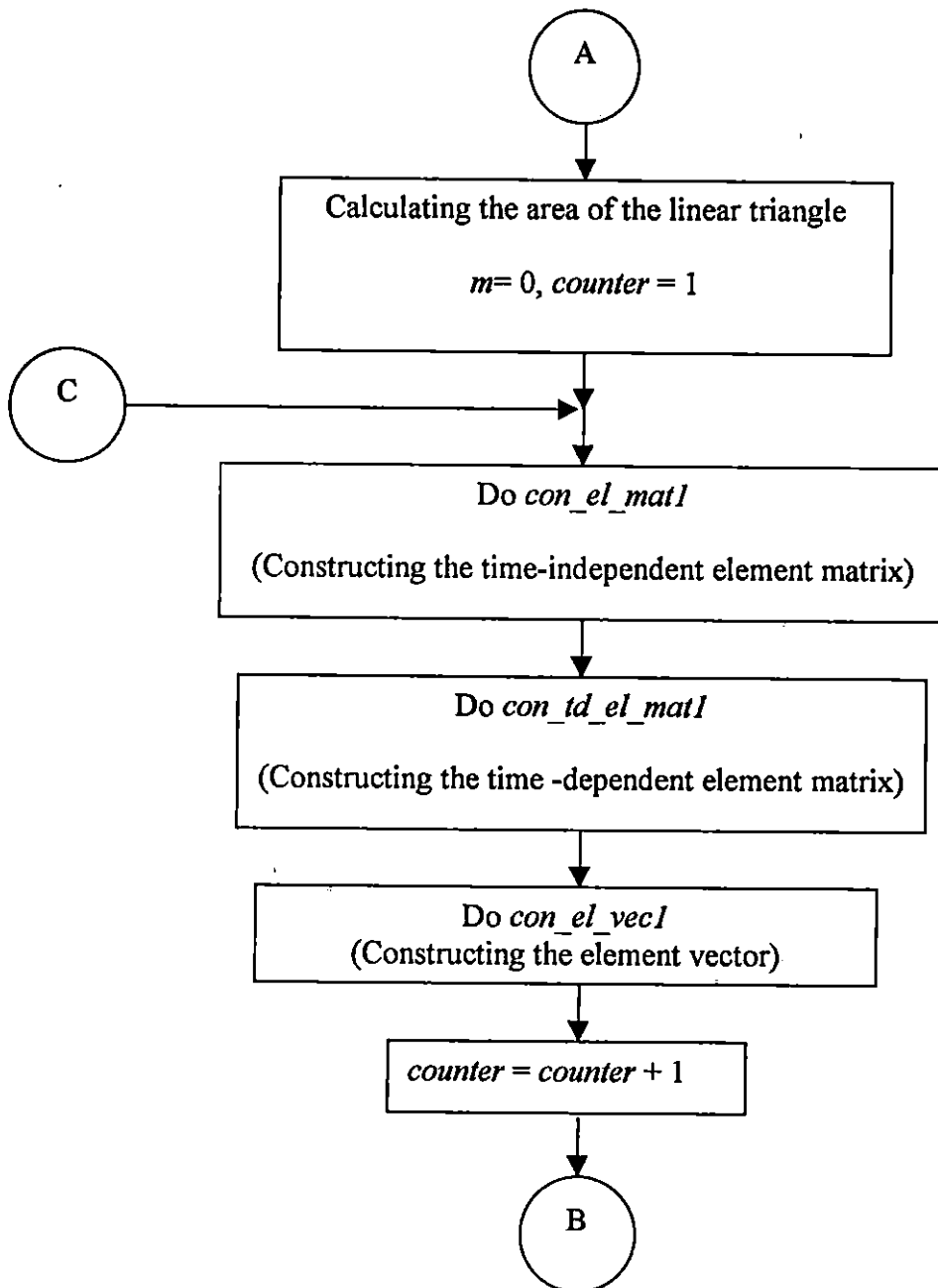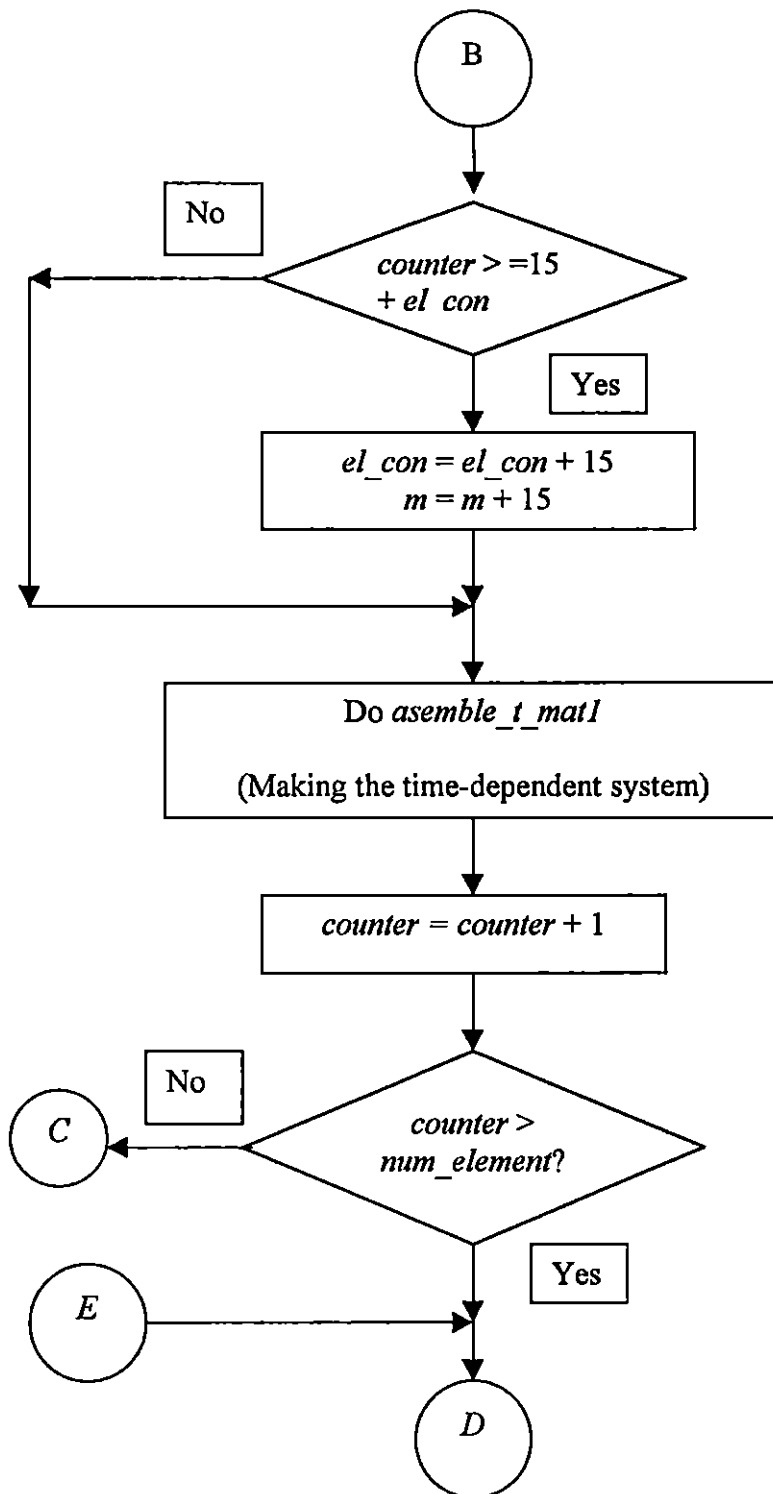Figure 18. The algorithm flowchart for function *ss_cylinder*

Figure 18 (continued)

Figure 18 (Continued)

```
                          ( D )
                            │
                            ▼
        ┌───────────────────────────────────────────┐
        │           Filling el_flux_mat             │
        │                                           │
        │    (The matrix containing the nodes with  │
        │                  the                      │
        │           flux boundary condition)        │
        └───────────────────────────────────────────┘
                            │
                            ▼
        ┌───────────────────────────────────────────┐
        │    Calculating the coordinates of the     │
        │                  nodes                    │
        │    which have flux boundary condition     │
        └───────────────────────────────────────────┘
                            │
                            ▼
            ┌───────────────────────────────────┐
            │   Filling el_mat1 and el_vec1     │
            └───────────────────────────────────┘
                            │
                            ▼
```

No

$$i >= num\_flux\_node - 2?$$
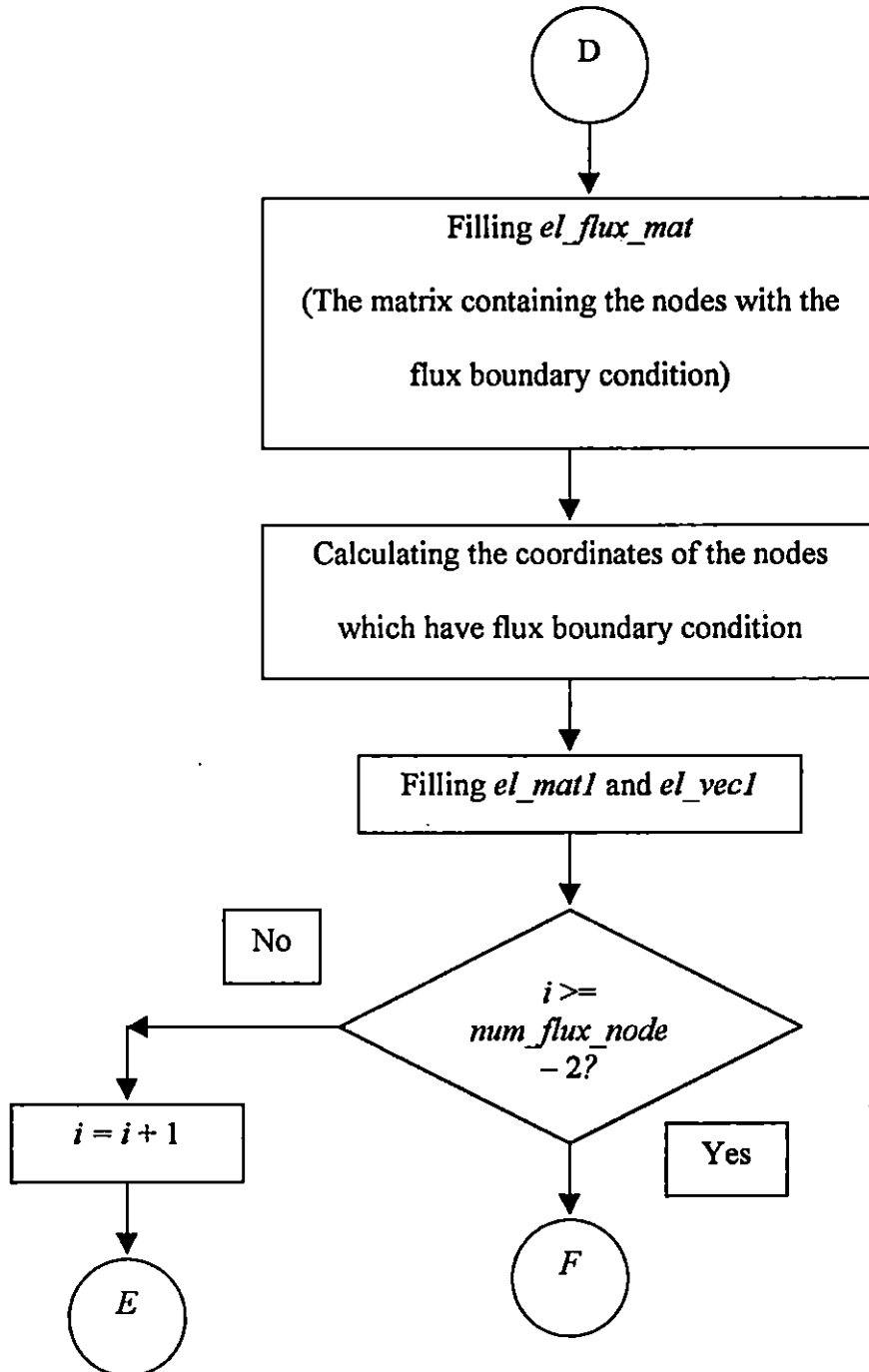
Yes

$i = i + 1$
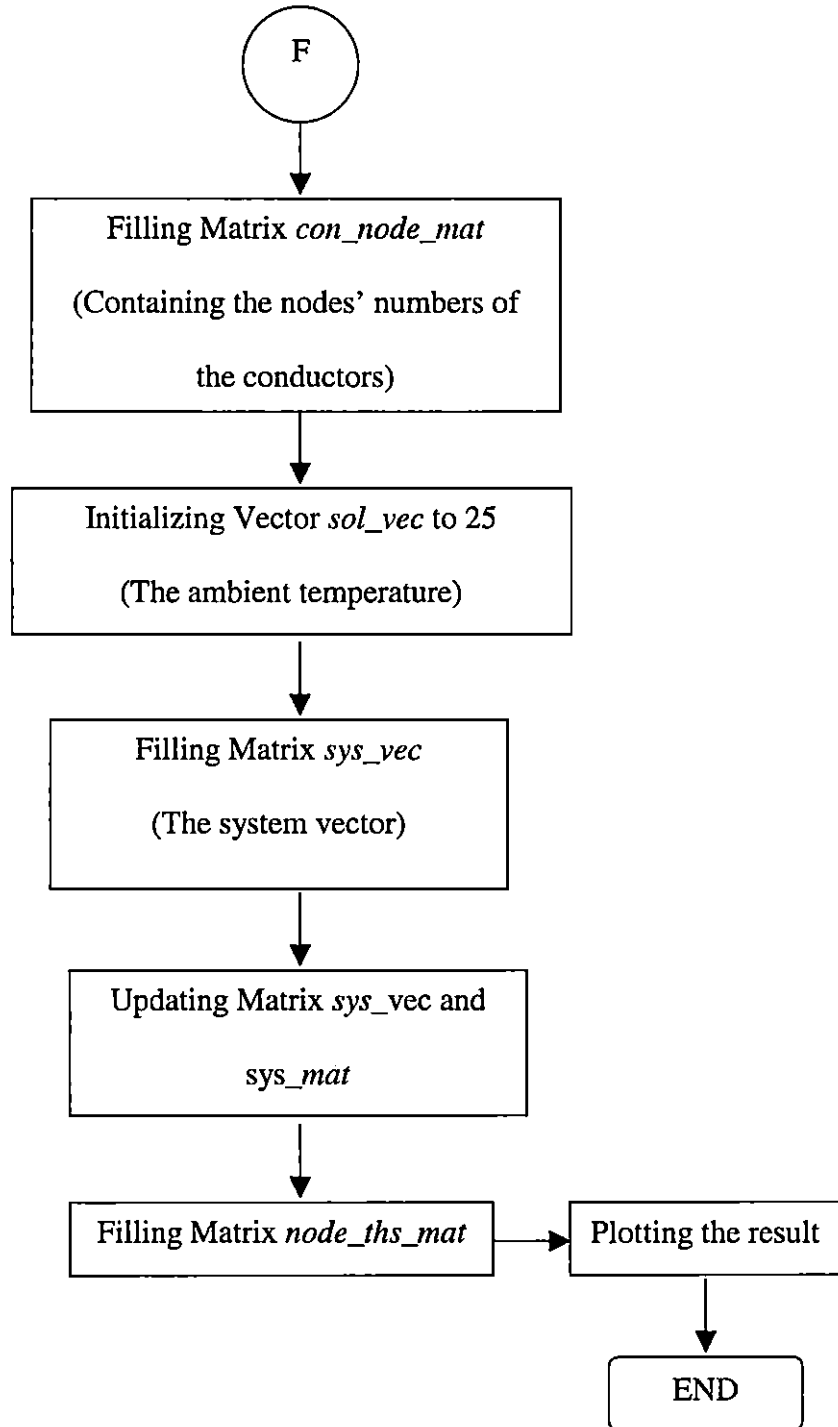
(E)

(F)

Figure 18 (continued)

Figure 18 (continued)

2. give_nod_number

This function assigns numbers to the nodes. The total number of the nodes along the axis x and the axis of the symmetry are 16 and 11 respectively. To start numbering the nodes, the node located at the origin of the coordinate system is chosen to be number one. Figure 19 demonstrates this case.
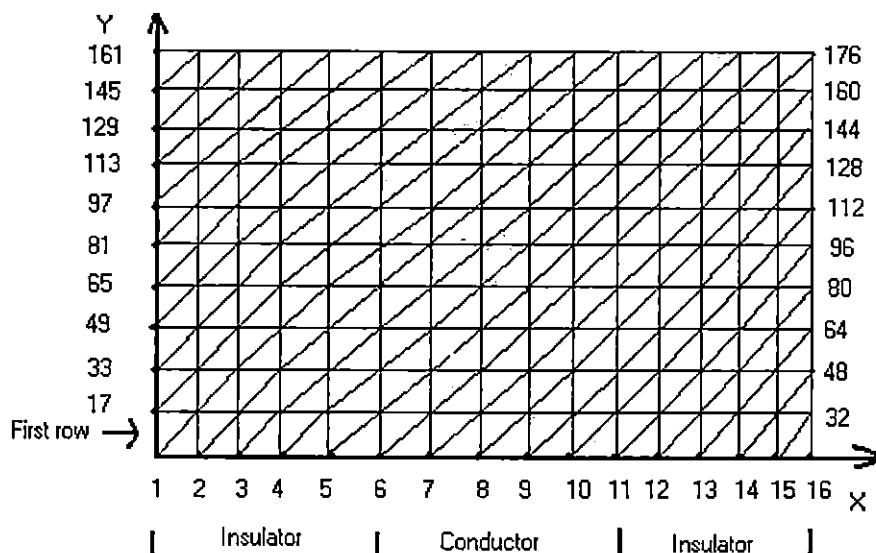

Figure 19. The numbered nodes on the domain. The interior numbers are not specified to avoid confusion.

The above figure is for the straight part of the wire. For the curved part, the numbering is started from number 177 to number 336. The number of the nodes and element in the curved part is the same as the straight one.

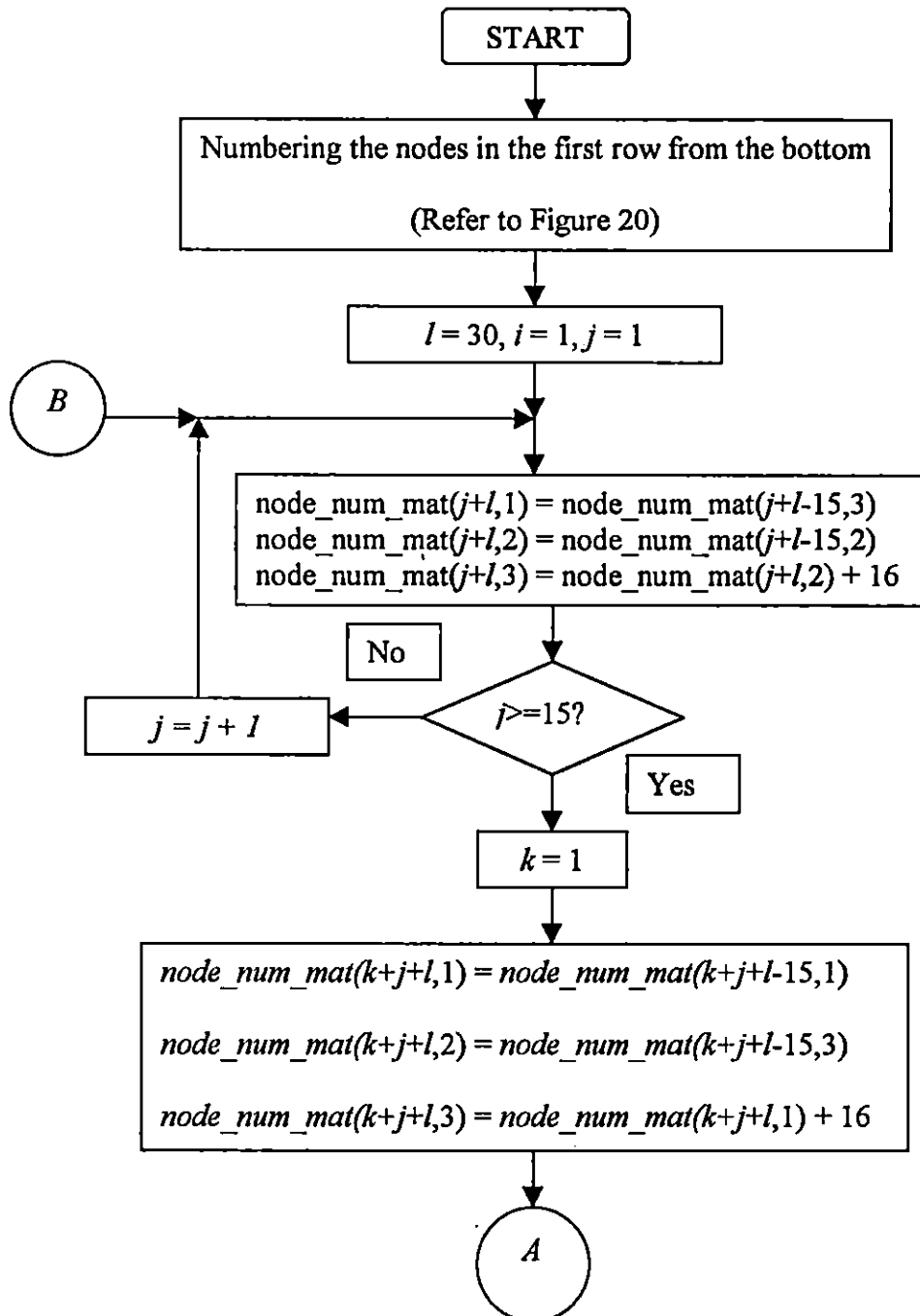The algorithm used to assign numbers to each node in the domain is shown in Figure

19.

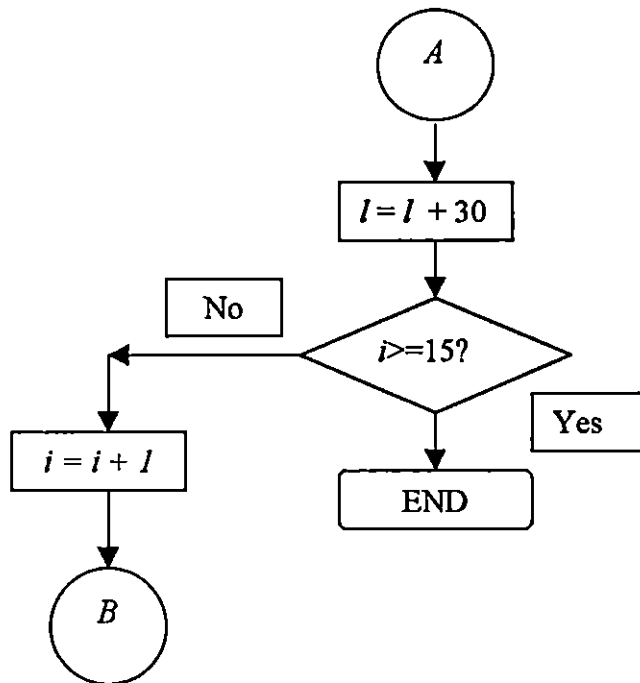Figure 20. The algorithm flowchart for Function *give_node_num1*

Figure 20 (continued)

3. Com_node_coor1.m

After numbering the nodes, the coordinates (positions) of the nodes on the

domain are determined. Function *com_node_coor1* performs this task. This

function has some input parameters that are passed by means of the main

program. These parameters are *node_coor_mat*, *wire_dia*, *cyl_hei*, *arc_len*, and

arc_ang. This function has one output which is Matrix *node_coor_mat1*. Its

main function is to fill matrix *node_coor_mat*. Figure 21 (next page) shows the

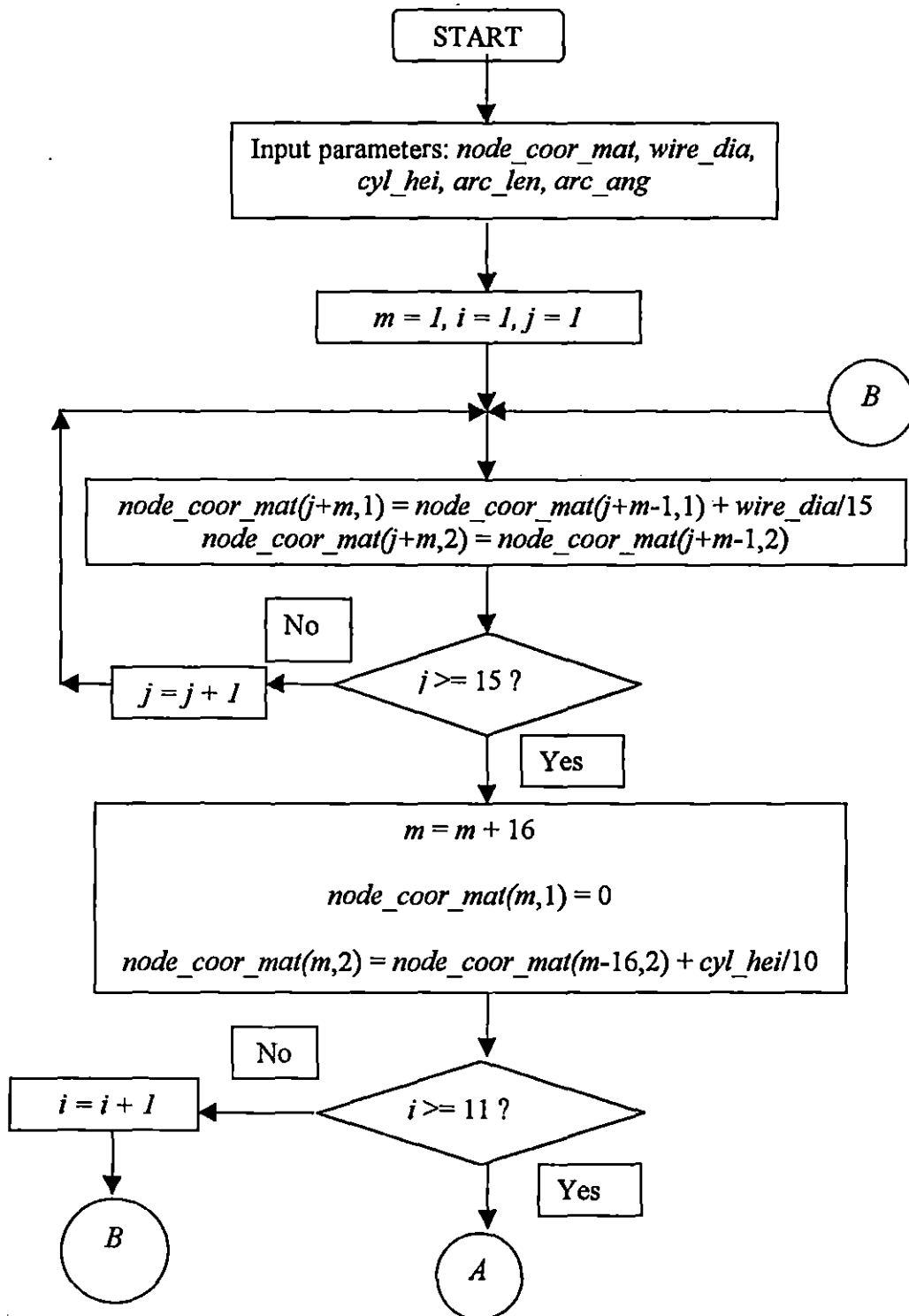algorithm flowchart of Function *com_node_coor1*.

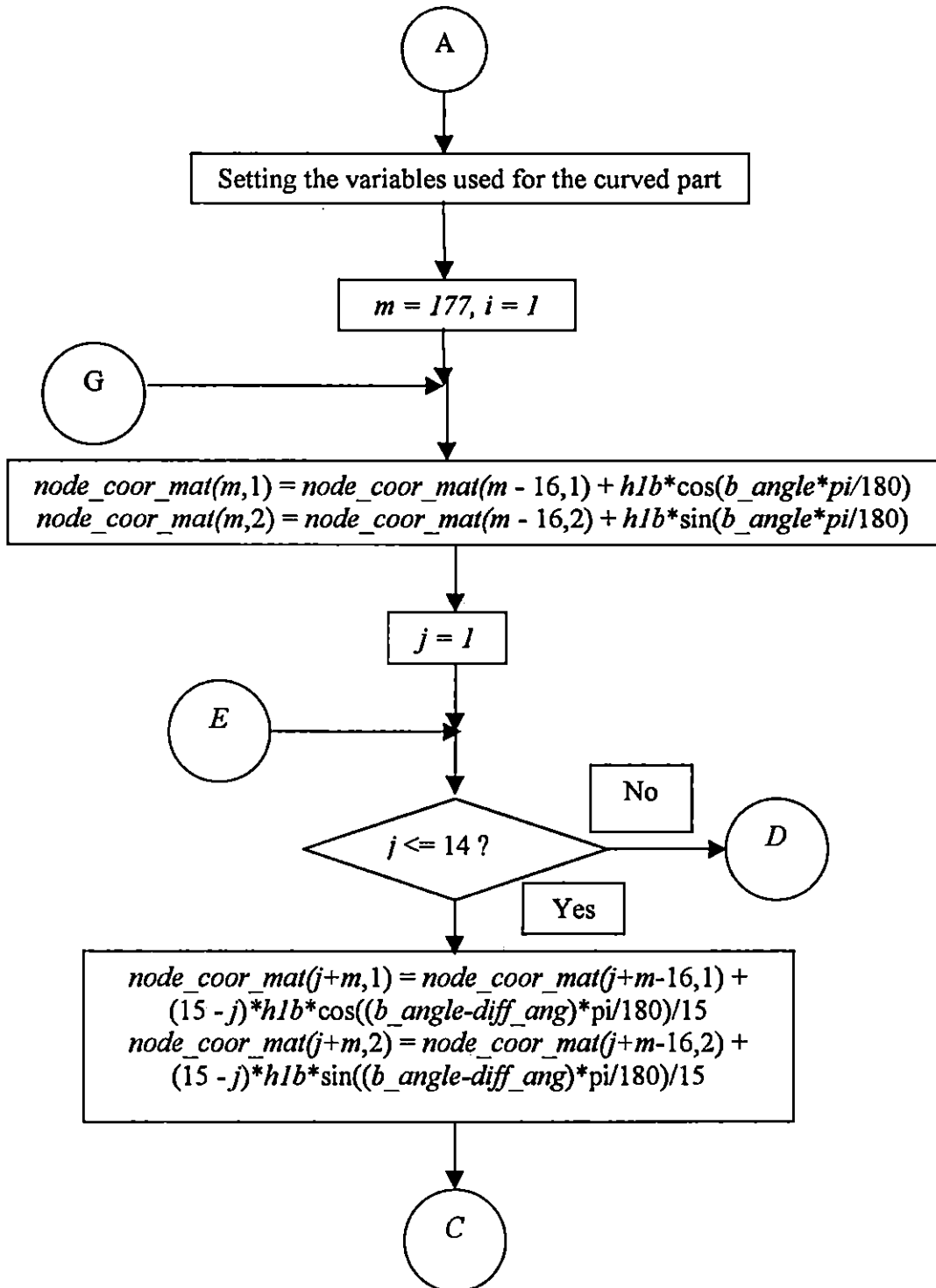Figure 21. The flowchart for Function *com_node_coor.m*.

$$A$$

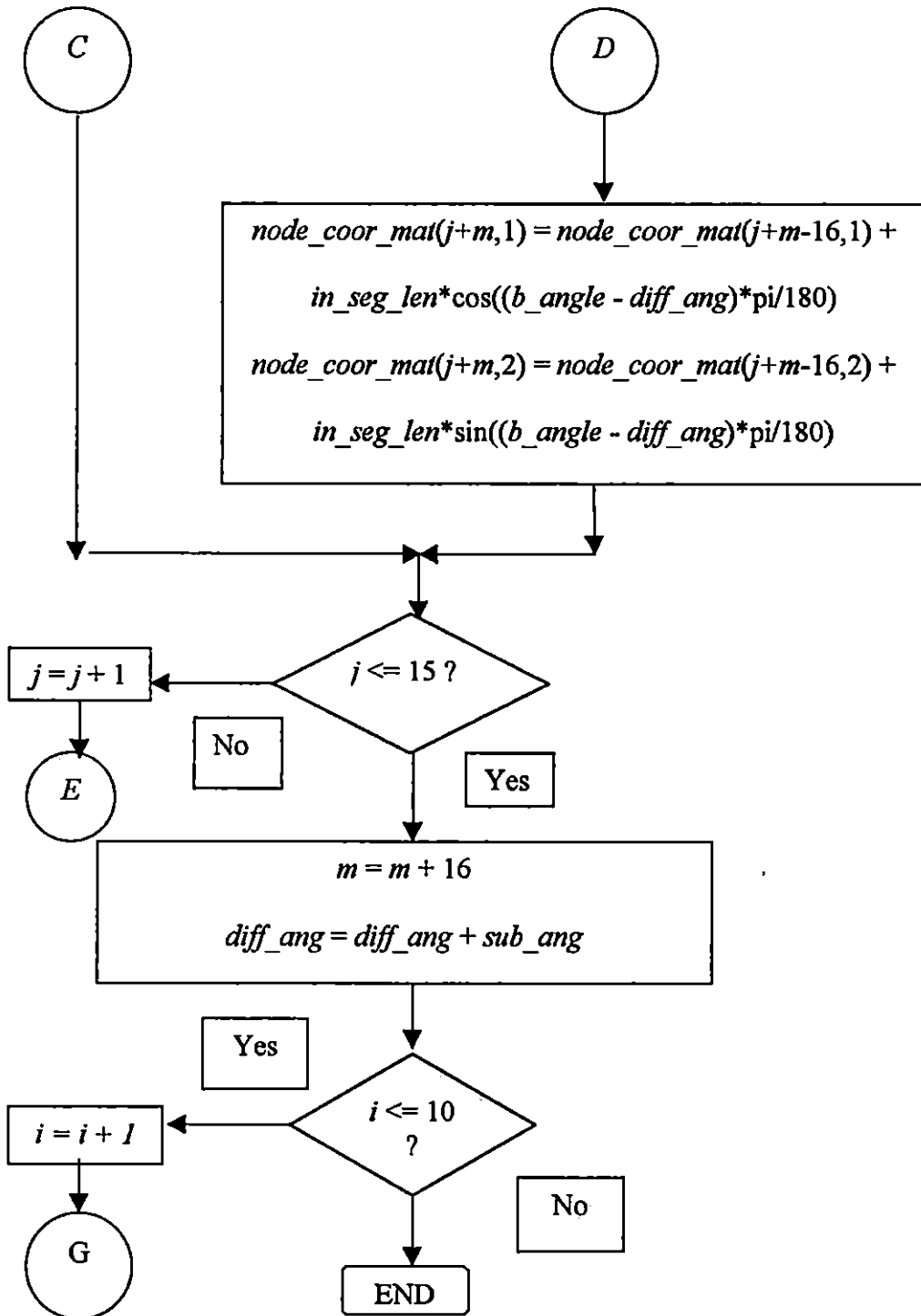Setting the variables used for the curved part

$$m = 177, i = 1$$

$$G$$

$$node\_coor\_mat(m,1) = node\_coor\_mat(m - 16,1) + h1b*\cos(b\_angle*pi/180)$$
$$node\_coor\_mat(m,2) = node\_coor\_mat(m - 16,2) + h1b*\sin(b\_angle*pi/180)$$

$$j = 1$$

$$E$$

$$j <= 14 \ ?$$

No

$$D$$

Yes

$$node\_coor\_mat(j+m,1) = node\_coor\_mat(j+m-16,1) +$$
$$(15 - j)*h1b*\cos((b\_angle-diff\_ang)*pi/180)/15$$
$$node\_coor\_mat(j+m,2) = node\_coor\_mat(j+m-16,2) +$$
$$(15 - j)*h1b*\sin((b\_angle-diff\_ang)*pi/180)/15$$

$$C$$

Figure 21 (continued)

Figure 21 (continued)

The variables used in this figure are the same as the ones used in the programs. The description of each variable is listed in Appendix A-1.

4. con_el_malt

This function constructs the matrix element. Using matrices *node_coor_mat*, *node_num_mat*, and *el_mat*, it generates Matrix element *el_mat*. This matrix is a 3×3 matrix.

5. con_td_el_mat1

In this function, a 3×3 matrix called *td_el_mat* is generated. This matrix is the same for all the elements in the domain and eventually it is combined with the time-dependent system matrix (i.e. *td_sys_mat*).

6. con_el_vec1.m

This function, calculates the element vector for the triangle linear element. The inputs of this function are *el_vec, node_coor_mat, node_num_mat, counter,* and *tri_area.* The output is Vector *el_vec.*

7. asemble_mat1.m

When both the element vector and the element matrix are built, they should be assembled in order to obtain the system matrix and system vector. This task is done by Function *asemble_mat.m.* The inputs of this function are *sys_mat,*

node_num_mat, el_mat, el_vec, sys_vec, and *counter* and the outputs are *sys_vec*

and *sys_mat.* The first part of the function builds the system matrix and the

second part builds the system vector.

8. asemble_t_mat1.m

The task of this function is to fill matrix *td_sys_mat.* Basically, this function

calculates the time-dependent integral existing in Equation 62 (the last integral).

The input parameters of this function are *td_sys_mat, td_el_mat, node_num_mat,*

and *counter.* The output is *td_sys_mat.*

9. node_t_h.m

There are two different types of reports: temperature distribution along the

wire, and temperature distribution across the wire. This function gets the nodal

values from the main program and fills Matrix *node_ths_mat.* This matrix is

used to plot the graph of the temperature versus the length of the wire.

The program is written using the MATLAB software since it is relatively easy to

learn and the length and simplicity of the codes compared with other languages is an

advantage of MATLAB. Since most engineering problems deal with matrix

calculation and MATLAB software is geared toward solving problems involving

matrices calculation, it is definitely a useful tool for solving engineering problems

(Kwon, & Bang 1997).

Summary

In this chapter, the problem and research questions were restated. Then the procedure used for solving the problem was explained. The details of the computer programs and the algorithms used to write the program were also addressed.

.

CHAPTER IV

FINDINGS

In this chapter, the results and findings of the analysis are shown and discussed. First, the names of the materials and their physical properties are explained and then the result for each of them is going to be demonstrated individually.

Materials' Specifications

The analysis was performed using different kinds of materials as the insulator. The conductor chosen was Copper. The conductor specifications are shown in Table 1.

Table 1

The Physical Properties of the Conductor Used in the Analysis

AWG	Length (m)	Diameter (m)	Thermal Conductivity (J/m.s.K)	Electrical Conductivity (Ω^{-1}-m^{-1})
18	0.12	0.001	405.12	5.98e+007

The coefficient of convection chosen was 5 in this study. The wire consists of two parts: the straight part and the bent one. The length shown in the above table indicates the total length of the wire.

Three different insulators were used for the present study. The thickness was the same: 0.0005 m. The thermal conductivity of the insulators is demonstrated in Table 2 (RBC Industries, 1997).

Table 2

The Physical Properties of the Insulators Used in the Analysis

Name	Thermal Conductivity (cal/sec/cm^2/°C/cm×10^{-4})
Epoxy Resin (*RBC*-5520)	5
Epoxy Resin (*RBC*-5200)	5.3
Epoxy Resin (*RBC*-5400)	27.0

The values in the above table should be converted into SI system of units, which is *W/m²c*. To do so, it is sufficient to multiply them by 419 to convert them. The curvature of the wire (the amount of its bent) was considered in the analysis.

Therefore, the arbitrary values for it were plugged into the computer program. These values were 15°, 25°, and 35°. The arbitrary voltage surge was chosen as 50,000 V.

The first analysis was performed with the assumption that there was not any voltage surge. The reason for doing this analysis was to observe the heat distribution along the wire layers in the normal case. The materials' properties listed in Table 2 were plugged into the computer program one by one. Once the material was chosen, the curvature was chosen, and with this data, the computer program was run to obtain the temperature distribution for those specific values. Then, having the same material property, the curvature was changed and again, the program was run for all the different material properties with different curvatures.

Since observing temperature in different points in the wire was desired, the sets of the three nodes were picked up from different parts of the wire. Figure 22 (next page) shows the location of the three sets of nodes in the wire. Table 3 (next page) shows the associated numbers for the discussed nodes.

It should be mentioned that the nodes in the inner side and outer side of the wire were in correspondence with each other. They were at the same distance from the center of the wire. Also, all the nodes belonging to the same set were located at the same cross-section as seen in Figure 22 (next page). For choosing each of these sets in the program, there was a parameter named *plot_key* in Function *ss_cylinder*. For set number one, *plot_key* was set to two. For set number two, *plot_key* was set to three and for set number three, *plot_key* was set to four.
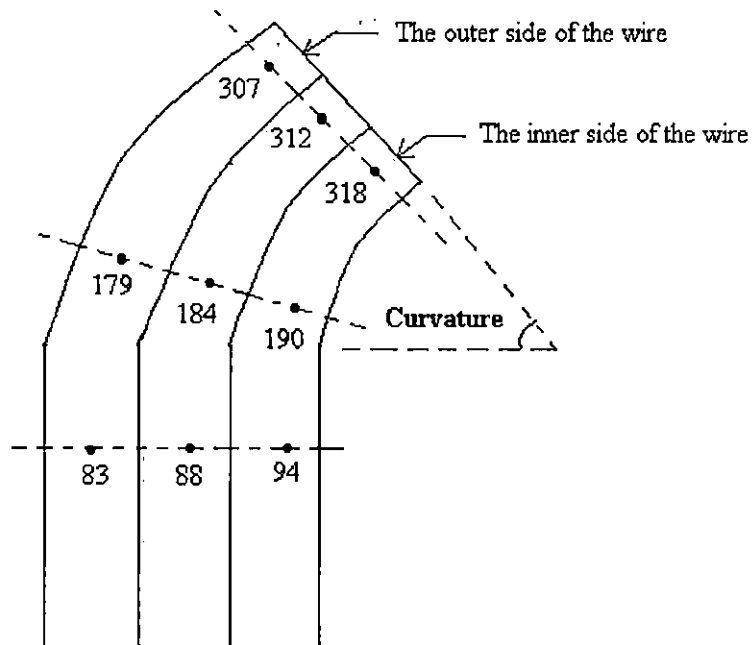
Figure 22. The nodes chose to observe the temperature in both insulator and conductor.

Table 3

The Node Numbers of the Three Nodes Chosen for the Analysis

Set number	outer side node	conductor	inner side node
1	83	88	94
2	179	184	190
3	307	312	318

To begin, first those codes in the program, which calculate the time-dependent

part, were commented. Those codes are in Function *ss_cylinder* (refer to Appendix

B) and begin at line number 303. Figure 23 shows this commented part of the

program.
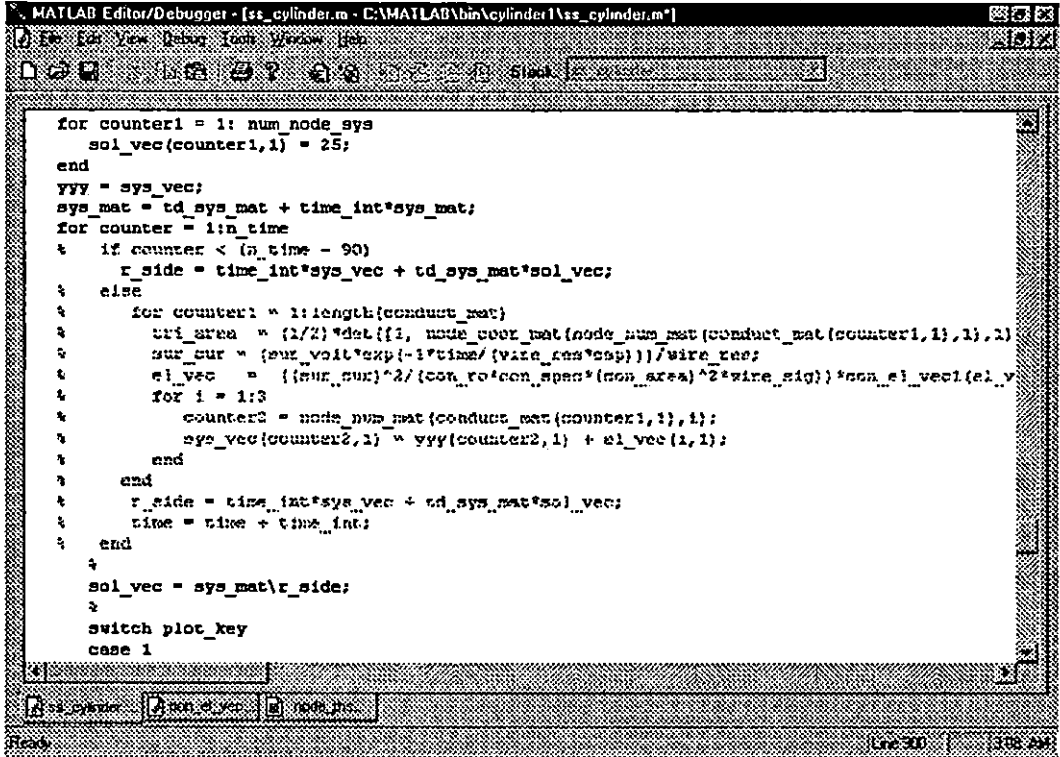
Figure 23. The commented part of *ss_cylinder* function which are green in color.

Then, the values were plugged in one by one. For this purpose, the variable

insl_k (refer to Table 2) was set for each material. The initial time (*ini_time*) and the

terminal time (*fin_time*) were set to 0 and 0.02 seconds respectively.

The first insulator used for the analysis without the surge was Epoxy Resin

(*RBC*-5520). The curvature angle was set to 15°. Figure 24 demonstrates the

temperature for this case. As the Figure shows, when the current starts passing

through the wire, the temperature in both the conductor and insulator increases from

the ambient temperature (25°C) up to 25.00045 °C and 25.00044 °C for conductor
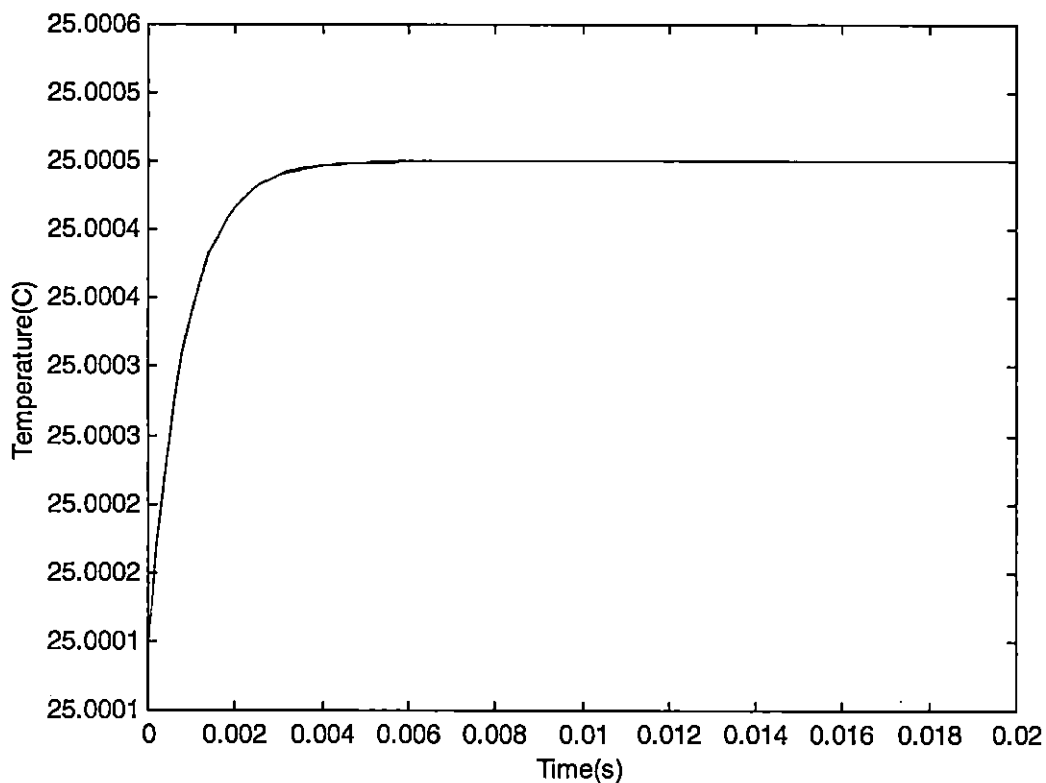
and insulator respectively.

Figure 24. The temperature distribution in both conductor and insulator with the

nodes in the set number one (angle = 15°).

Those values can be found in the time-history matrix, *node_ths_mat*. As expected, the temperature of the conductor was higher than the insulator since the conductor was surrounded by the insulator and, therefore, the insulator blocks the heat flow from the conductor toward the ambient.

Another result from this analysis was that the difference between the temperature of the insulator and conductor was not very much. As seen in Figure 24, the graphs of the insulator and conductor look to be coincided but they actually are not. The actual difference will be revealed by changing the scale of the graph. Figure 25 shows the result of the change.
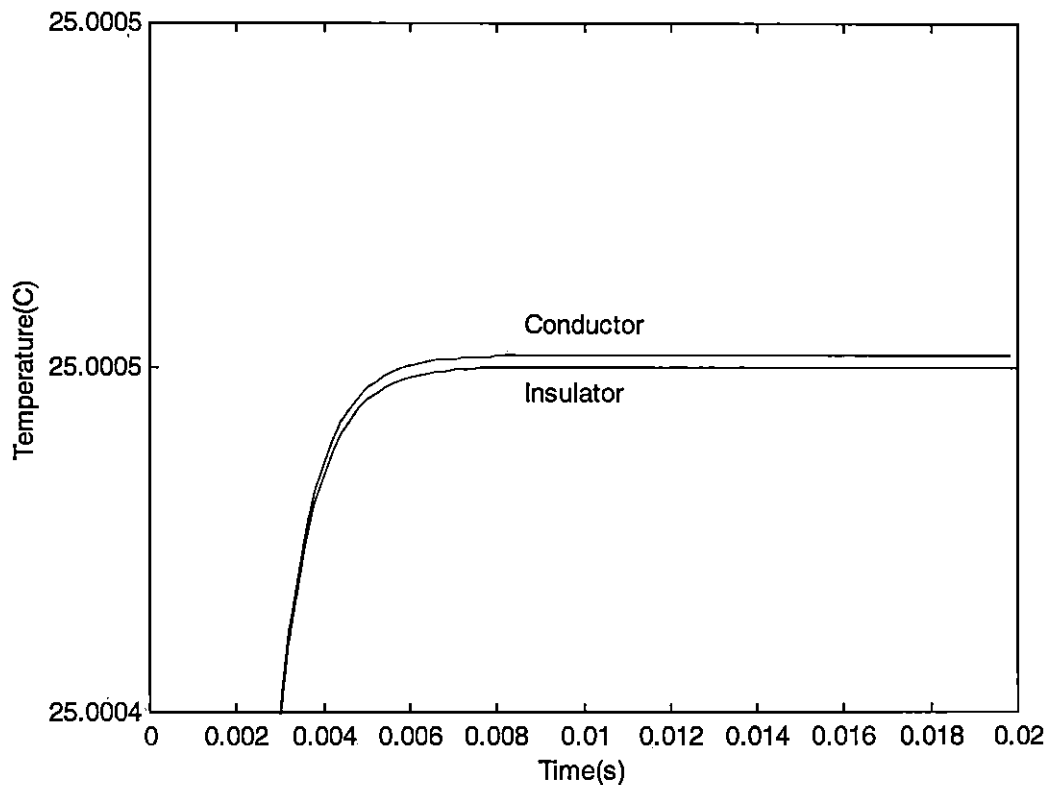
Figure 25. The same distribution shown in Figure 24, but using different axial scales.

The temperature was not really the same between conductor and insulator. However, as seen in Figure 25, the temperature of both nodes in the inner side and outer side of the wire were the same. This should be true since this analysis belongs to node set number one, which deals with the nodes lying in the straight part of the wire. Consequently, the rate of the temperature change in the corresponding nodes was identical.

After enough time passed, the temperature, either in conductor and insulator, was established and did not change. This was acceptable since the rate of the heat producing in the wire due to the current was balanced with the rate of the heat flowing out of the wire to the ambient.

In order to observe the temperature distribution in other parts of the wire, the analysis was repeated for the node sets number 2 and 3 leaving the rest of the parameters unchanged. Figures 26 (next page) and 27 (next page) show the heat distributions for set 2 and 3 respectively.
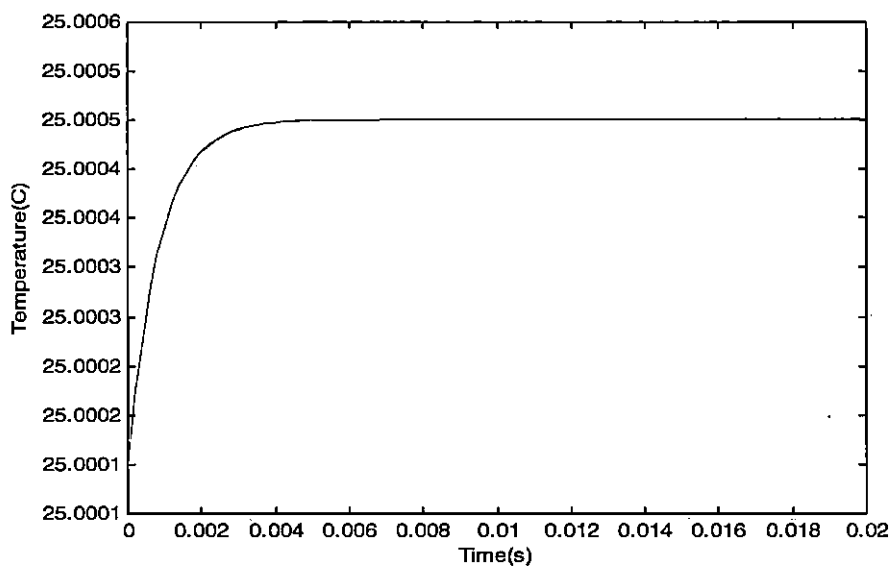
Figure 26. The temperature distribution in both conductor and insulator with the node
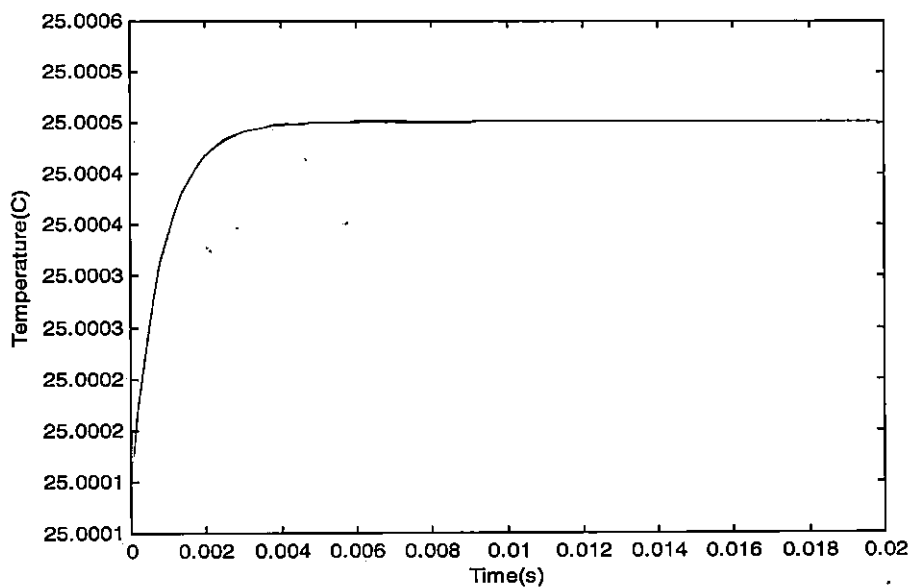
set number 2 (angle = 15°).

Figure 27. The temperature distribution in both conductor and insulator with the

nodes in the set number three (angle = 15°).

Although the shape of the graphs in Figure 26 and 27 are similar, they do not demonstrate the same temperature distribution. By changing the axial scale of these figures, Figures 28 and 29 (next page) better demonstrate the temperature sdistribution.
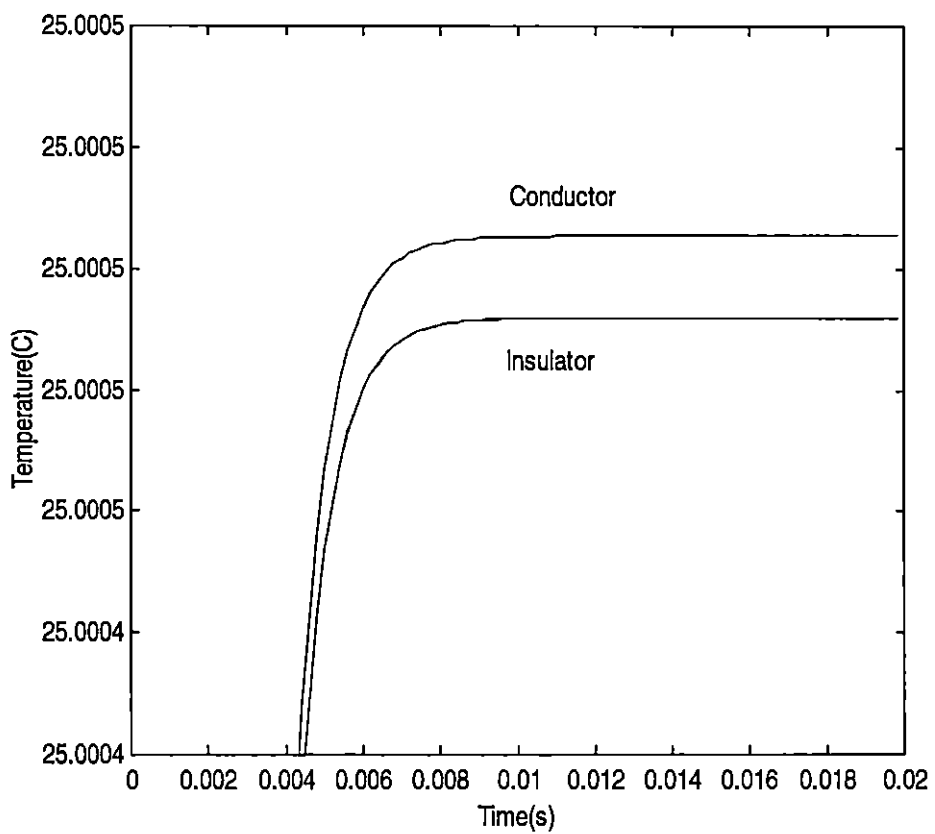

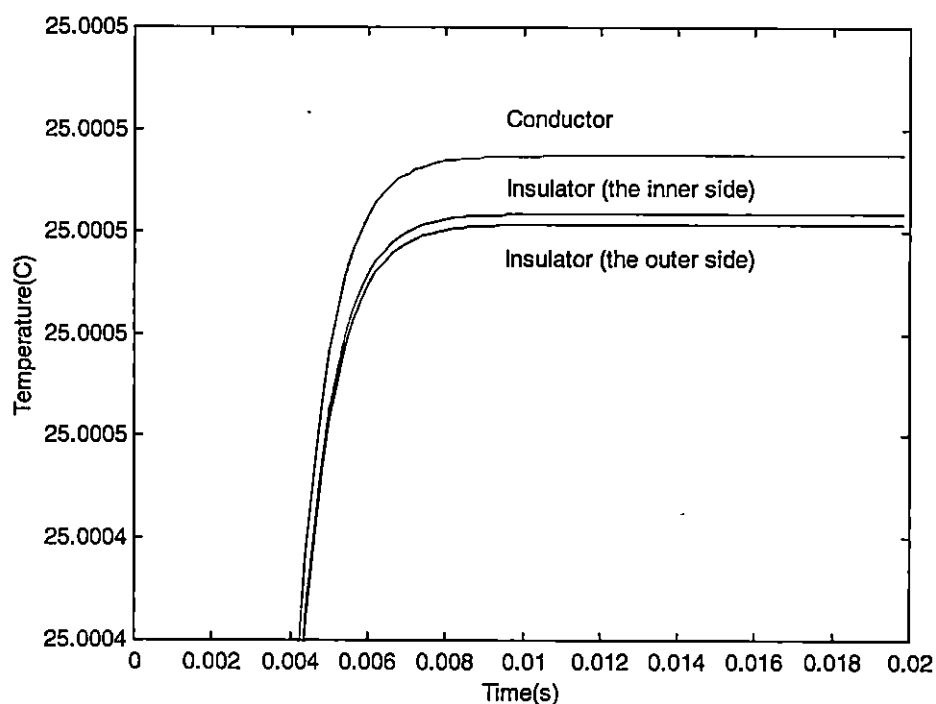Figure 28. The same distribution as in Figure 26 but with different scale.

Figure 29. The same distribution as in Figure 27 but with different scale.

An interesting thing in Figure 29 is the distinguishing which appeared

between the temperature of the inner side and the outer side of the wire insulator.

The reason for this separation was that since the wire was bent, the nodes in the inner

side were under more pressure than the nodes in the outer side. Therefore, the

temperatures in the nodes representing the inner side were higher than the outer ones.

As seen in both Figures 28 and 29, the temperature difference between

conductor and insulator was not much. Actually, it was from the order of ten to the

power of negative four. Even when checking the matrix *node_ths_mat* for the value

of the temperature, it showed that the temperature difference was negligible. The

reason was that since the electrical resistivity of the copper was very small (1.68 ×

10^{-8} Ω-m), the rate of the heat production within the conductor was not big.

Therefore, any raise in the temperature was conducted outward since copper had a

good thermal conductivity too. This case was valid along the wire as confirmed by

the Figures 24, 26, and 27.

The temperature was also observed from another perspective. In this

perspective, the temperature variation was observed along the wire (at different

positions in both conductor and insulator) at some specific instant of time. This

specific time could be any moment in the time interval, which is interval [0, 0.02]. In

order to obtain such a graph, Parameter *plot_key* in Function *ss_cylinder* (refer to

Appendix B) was set to one. It was corresponded to the moment t = 1.2 ms. The rest

of the parameters such as the insulator material, the curvature, and the voltage surge

remained unchanged. Figure 30 (next page) shows such a case.
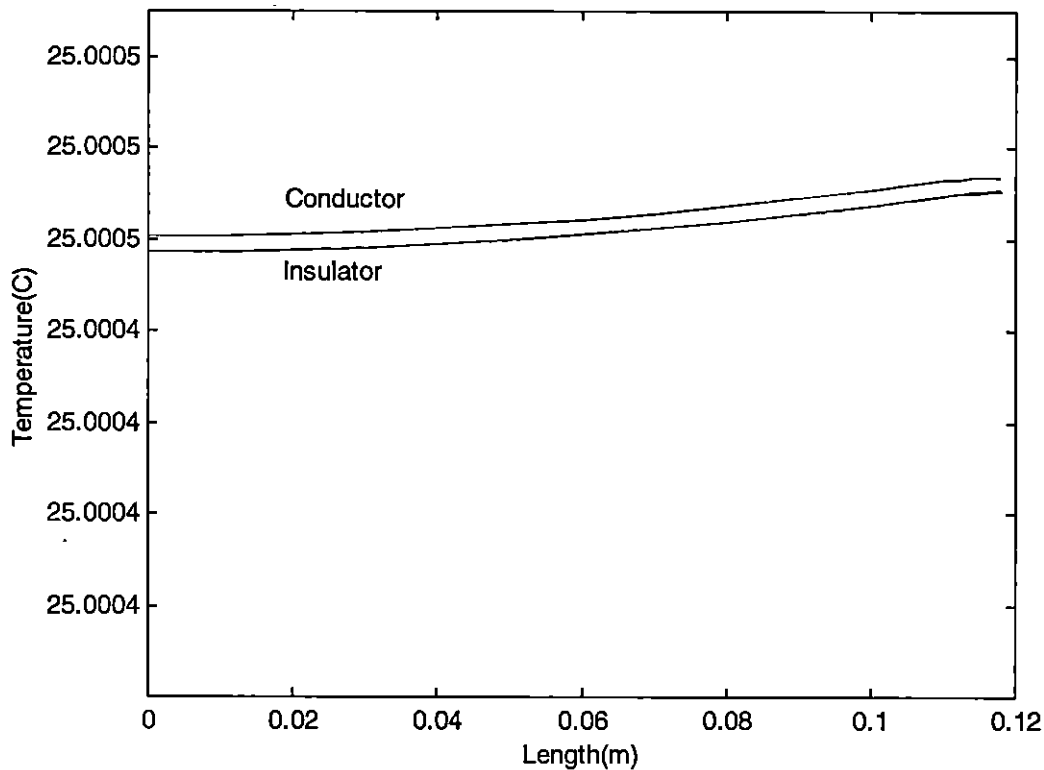
Figure 30. The change of the temperature along the wire (angle = 15°).

As Figure 30 shows, there was no difference between the temperature of the

inner side of the wire (in the insulator layer) and the outer ones. However, this was

true only in the straight part. In the bent part, the temperature of the inner area

became a little bit more than the outer one. This difference was observed by

changing the scales in the graph. Figure 31 (next page) is demonstrating the same

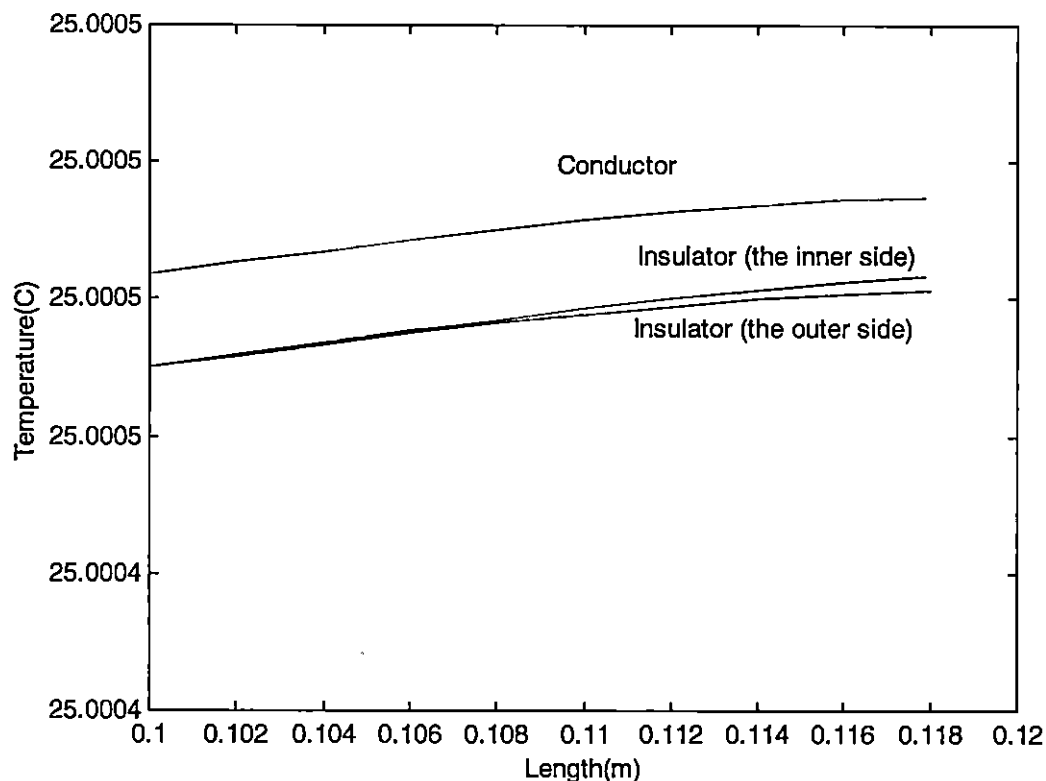distribution, but using a different scale.

Figure 31. The same distribution as Figure 30, but in the bent part of the wire and with different scale (angle = 15°).

As mentioned before, due to the low electrical resistivity of the conductor, the temperature raise was very small. Therefore, it cannot be shown in the graph although it is possible to view the node temperature values by changing the output format of the data. By default, MATLAB sets the format to be *short*. It means that the output format of the result would have four digits as decimals. In order to change the format, at the command line, the command *format long G* was executed. This command set the format to fifteen digits (either fixed or floating). Therefore, the

matrix containing the answers (*node_thy_mat*) changed and the values were displayed with the new format. Table 4 shows a part of Matrix *node_thy_mat* for three arbitrary nodes 259, 264, and 270 (column 17 of Matrix *node_thy_mat*).

Table 4

The Temperature at Some Typical Nodes (Angle = 15°)

Node number	Temperature (°C)
259 (Insulator-the outer side)	25.00041760
264 (Conductor)	25.00041792
270 (Insulator- the inner side)	25.00041762

Referring to the above table, the change in the temperature occurred in the higher order of the decimal digits and, therefore, MATLAB rounded the extra decimal digits. This explains why the temperature difference was not obvious in Figure 30.

Also shown in Figure 30, the temperatures of the nodes, which were located in the bent part (the area of the graph between points 0.1 and 0.12 on the X-axis in Figure 30), were more than the straight ones. Consequently, the impact of the curvature appeared as a raise in the temperature in both conductor and insulator. To inspect the impact of the curvature angle on the temperature pattern, the angle was

changed to 25 degrees and the rest of the parameters left unchanged. Figure 32
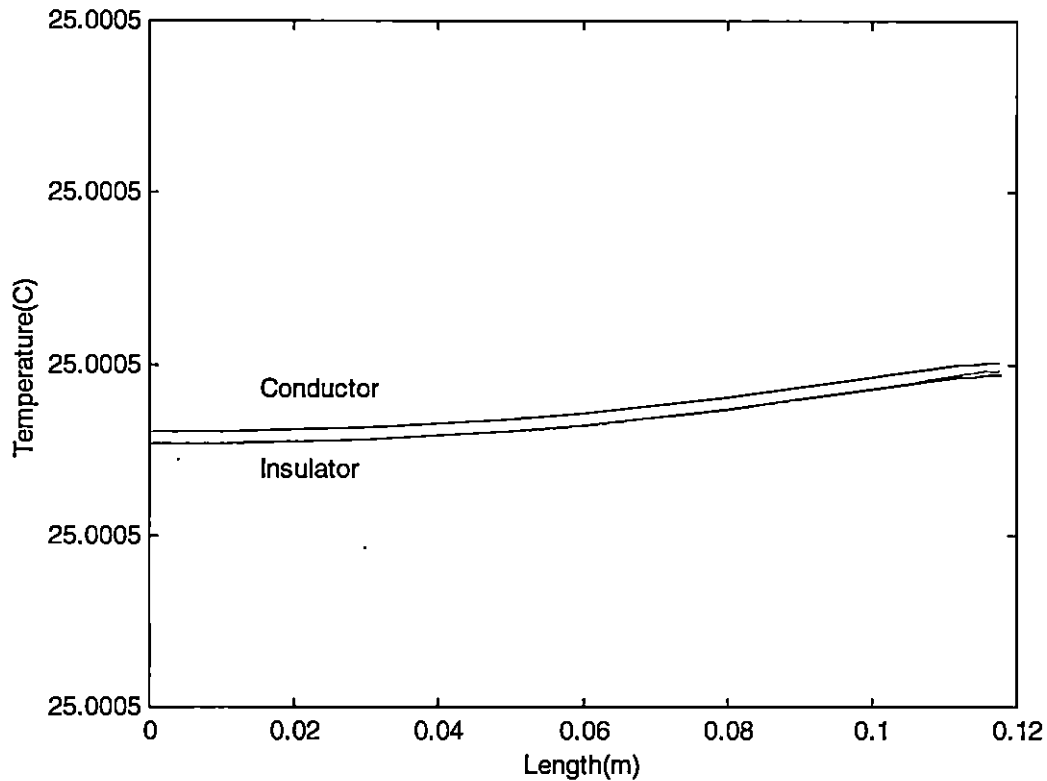
represents the result.

Figure 32. The change of the temperature along the wire (angle = 25°).

The temperature of the conductor was higher than the insulator. By changing

the output format of the data, the order of the temperature was revealed. Using *long*

G format, the temperature for the similar nodes shown in Table 4 were obtained.

Table 5 (next page) represents the result.

Table 5

The Temperature at Some Typical Nodes (Angle = 25°)

Node number	Temperature (°C)
259 (Insulator-the outer side)	25.00043975
264 (Conductor)	25.00047499
270 (Insulator- the inner side)	25.00044002

As seen in the above table, the temperature of the node which was in the inner side of the wire was higher than the outer ones. The pattern implied that at bent the temperatures of the inner nodes in the insulator were higher than the similar nodes in the outer side of the insulator. Still, as expected, the temperature of the conductor was highest. The problem of having very small values of the temperature was considered. As mentioned before, this was due to the low resistivity of the conductor.

By changing the angle from 25 to 35, the graph in Figure 33 (next page) was produced. The shape of the graph was the same as Figure 32, however, there was a small rise in the nodal temperature.
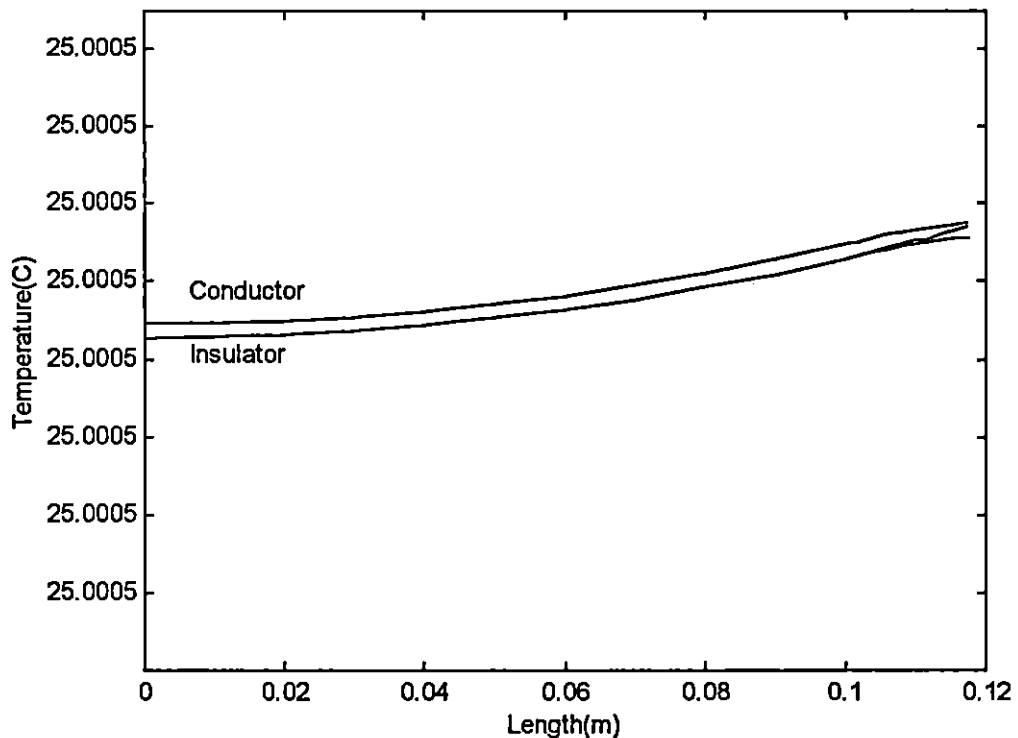
Figure 33. The change of the temperature along the wire (angle = 35°).

Figure 34 (next page) shows a re-scaled version of Figure 33 giving a closer look. In this figure, a small peak is observed in the insulator temperature distribution (the inner side of the insulator). It means that the temperature became higher in that area and then came down. Again, as the curvature of the wire increased, the temperature increased as well. The location of the small peak is approximately at $x = 0.11$m and its value is 25.00045659 °C.
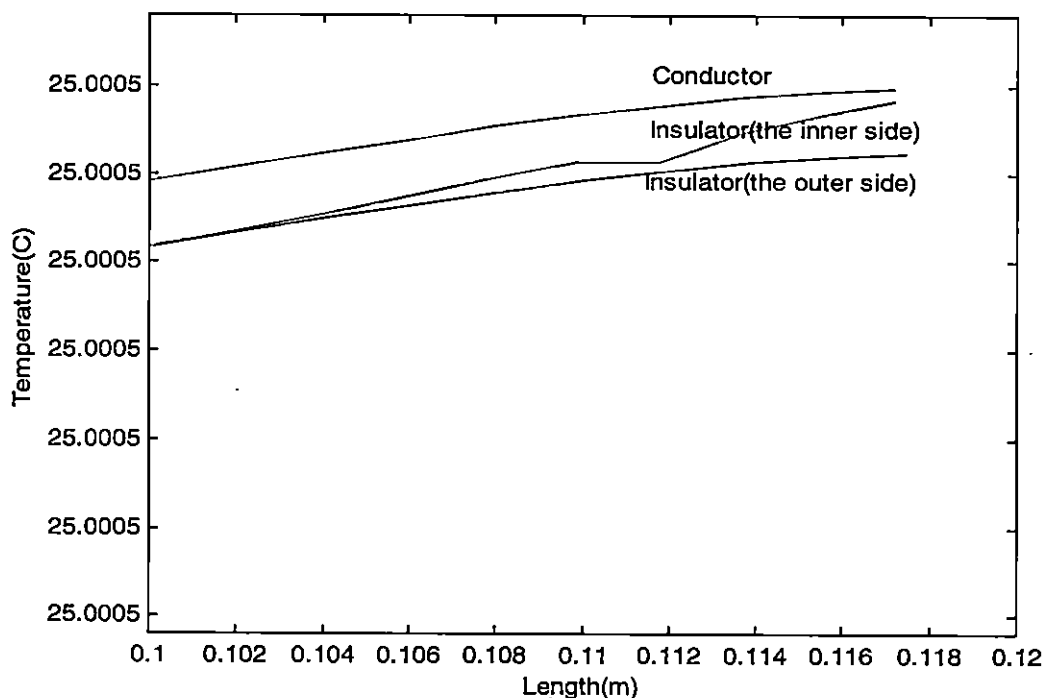
Figure 34. The same distribution as shown in Figure 33, but in the bent area.

Therefore, it was concluded that the temperature in the wire (in both

conductor and insulator) increased when the curvature of the wire increased. Also,

the nodes located in the bent part of the wire gained more temperature than the nodes

in the straight part. As observed, the temperature in the inner side of the wire

insulator was more than the temperature in the outer side and, of course, the

temperature of the conductor, in any case, was the highest one.

In order to observe the impact of the insulator material on the wire

temperature, the above analyses were performed again changing the parameter

representing the material property of the insulator. The parameter describing the

insulator behavior was thermal conductivity. In Function *ss_cylinder*, this multiplier was described by Parameter *ins1_k* (refer to Appendix A-1).

Having the same values for the rest of the parameters and setting the angle to be 15°, Epoxy Resin (*RBC*-5200) was chosen as the insulator. In Function *ss_cylinder*, the parameter describing this material was uncommented and the previous parameter (Epoxy Resin RBS 5520) was commented. Figure 35 (next page) shows the result of the analysis.

The shape of this figure is similar to *RBC*-5520 (with all other parameters the same). But the nodal temperatures are different. For instance, Table 6 compares the temperatures among three arbitrary nodes of *RBC*-5520 and *RBC*-5200.

Table 6

A Comparison Between the Temperatures of Some Arbitrary Nodes for Different Insulator Materials

	Temperature (°C)	
Node number	*RBC*-5520	*RBC*-5200
259 (Insulator-the outer side)	25.00045097	25.00041002
264 (Conductor)	25.00045131	25.00041031
270 (Insulator- the inner side)	25.00045100	25.00041003

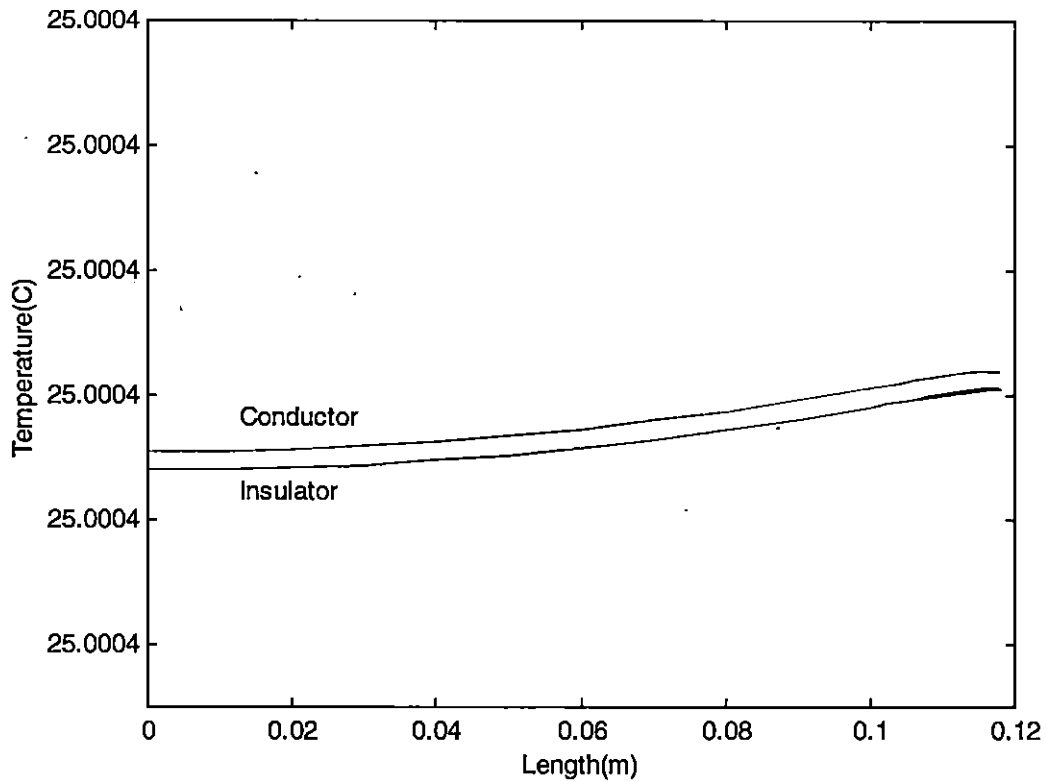These data were obtained from Matrix *node_thy_mat.*

Figure 35. The change of the temperature along the wire for *RBC*-5200 (angle = 15°).

Figure 36 (next page) shows the results of the analysis with only the angle changed from 15 degrees to 25 degrees.
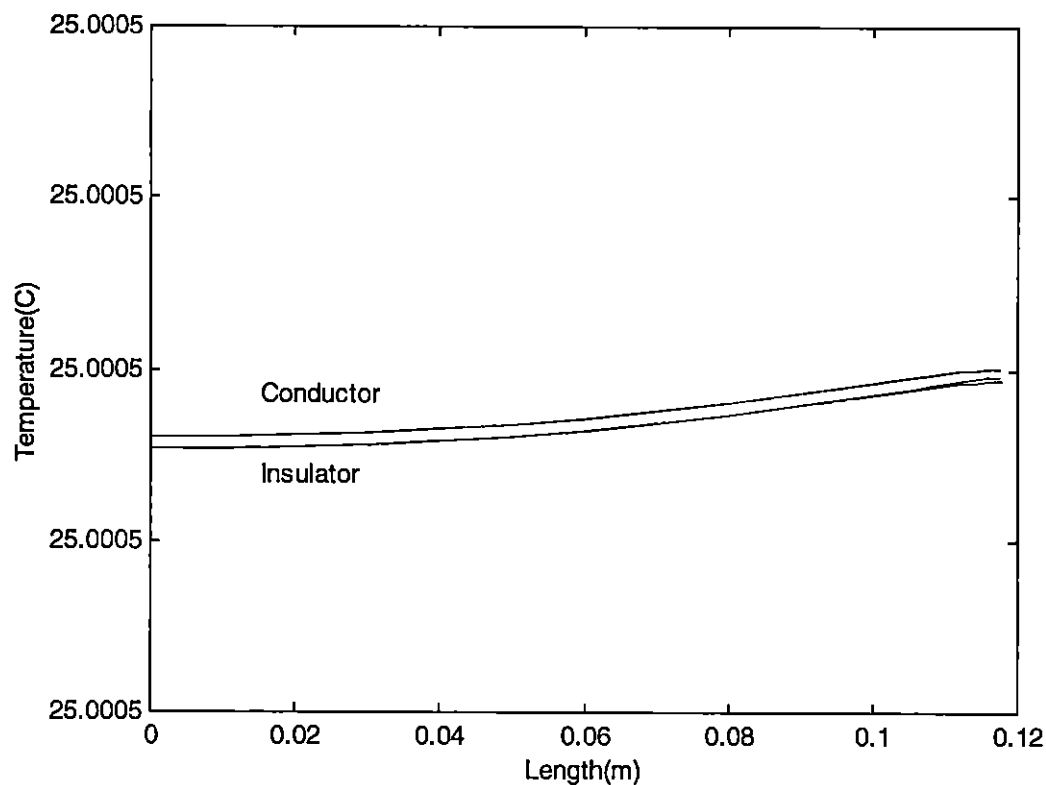
Figure 36. The change of the temperature along the wire for *RBC*-5200 (angle = 25°).

The last angle change to 35° was plugged into the program with the rest of the parameters left unchanged. Figure 37 (next page) illustrates that, in this analysis, the temperature increases when the angle increases.
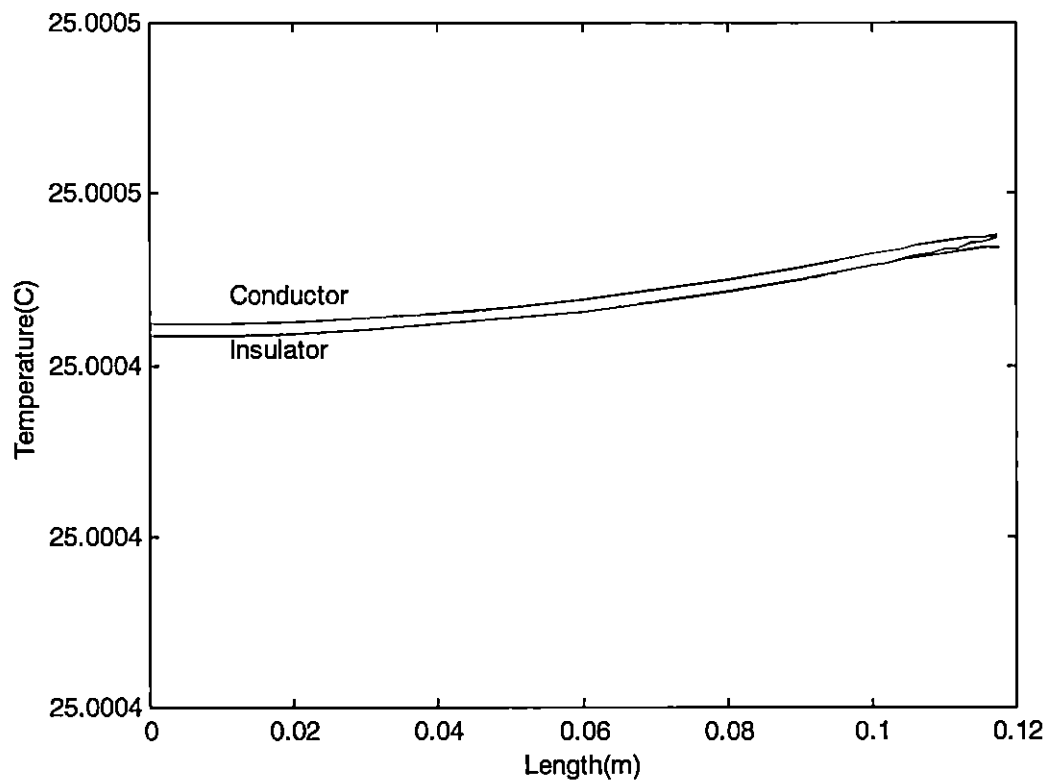
Figure 37. The change of the temperature along the wire for *RBC*-5200 (angle = 35°).

Epoxy Resin (RBC-5400) was the last material used. The same procedure was

performed with the value of the angle changed each time. The results of the first

analysis (i.e. 15 °) is illustrated in Figure 38 (next page).
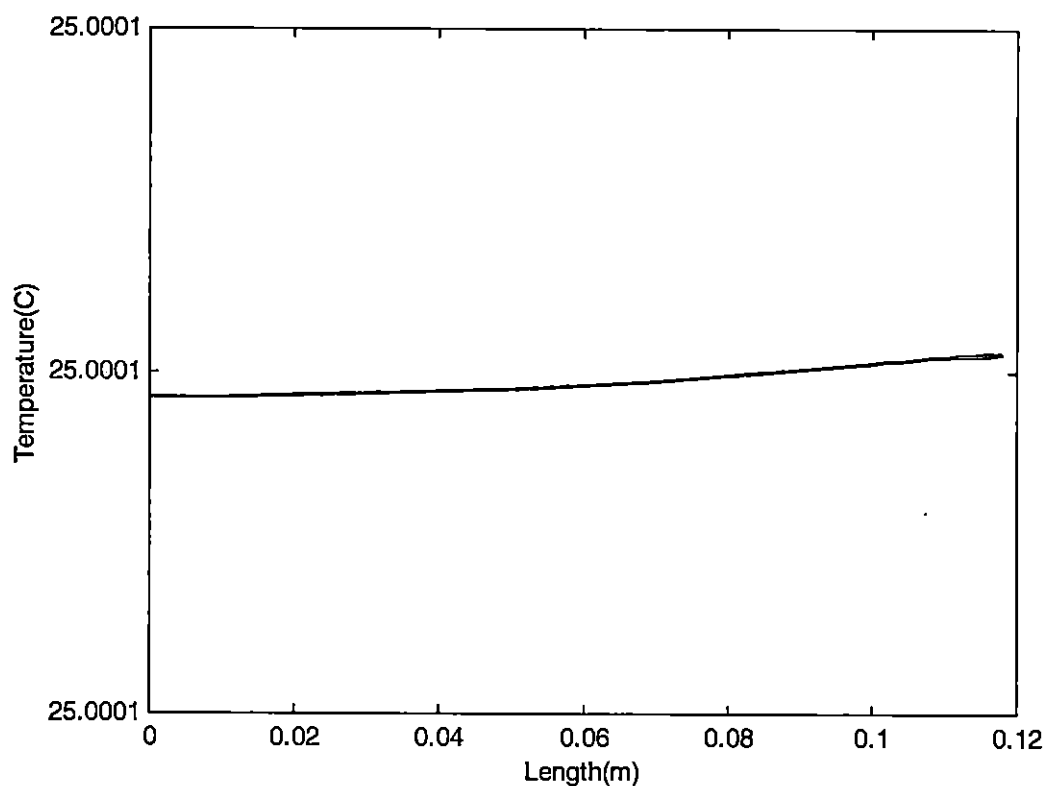
Figure 38. The change of the temperature along the wire for RBC-5400 (angle = 15°).

Since the thermal conductivity of RBC-5400 is relatively high, the heat is

conducted to the ambient quicker as compared to the two previous insulators.

Therefore, the nodal temperatures are small. Referring to Figure 38, the maximum

temperature occurs at the end of the wire where the bent is maximum. Referring to

Matrix node_thy_mat, the.maximum values are 25.00008054 °C in the conductor and

25.00008049 °C and 25.00008048 °C for inner nodes and outer nodes respectively.

The results of changing the angle from 15° to 25° are shown in Figure 39.

Figure 39. The change of the temperature along the wire for *RBC*-5400 (angle = 25°).

In Figure 39, the temperature difference between the insulator and conductor

is very small and is not readily distinguishable. Although, as expected, the

temperature at the far end of the wire, where it is bent, tends to be higher than other

places. The temperature difference is more clearly revealed when the scale of the

graph is changed as is demonstrated in Figure 40 (next page).
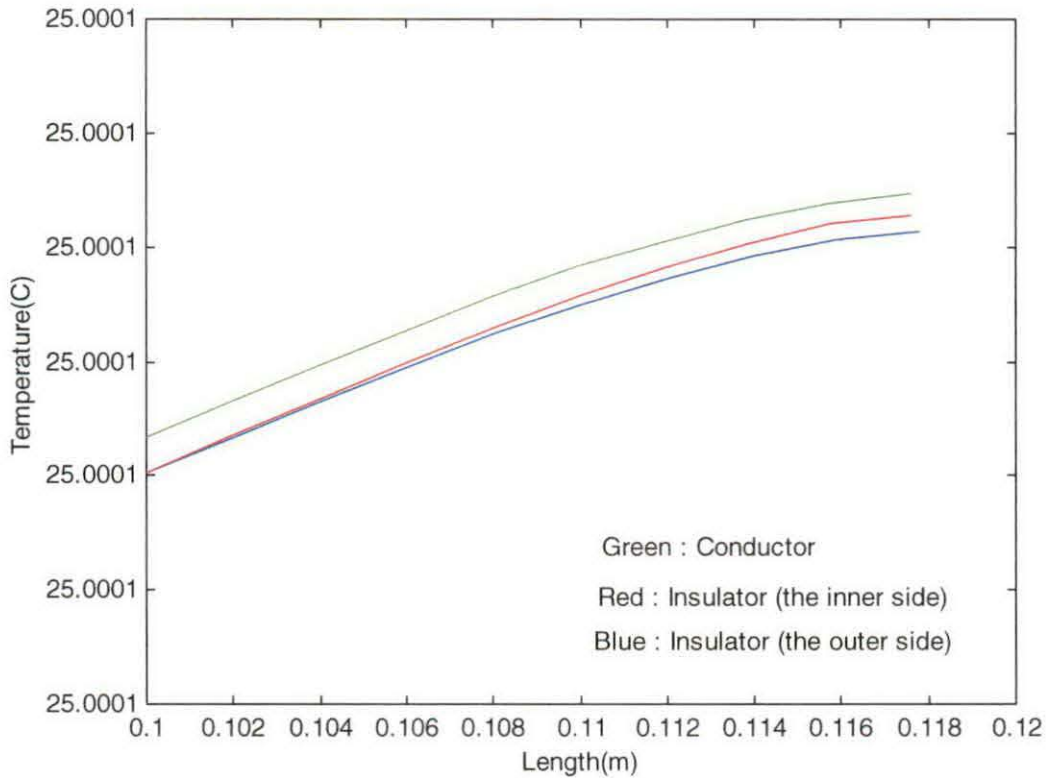
Figure 40. The same figure as Figure 39, but with different scale and showing the bent part of the wire (angle = 25°).

As expected, the temperature of the inner side is higher than the outer side. Also, the temperature at this part of the wire is the highest one compared with other parts, and can be seen by observing the values of the temperatures in Matrix *node_thy_mat*. Referring to Matrix *node_thy_mat*, the maximum temperature in the conductor is 25.00008509 °C and for the insulator (both the inner side and the outer side) are 25.00008505 °C and 25.00008502 °C respectively.

Again, all the parameters were unchanged except the angle of the wire, which

was set at 35°. The distribution result is illustrated in Figure 41.
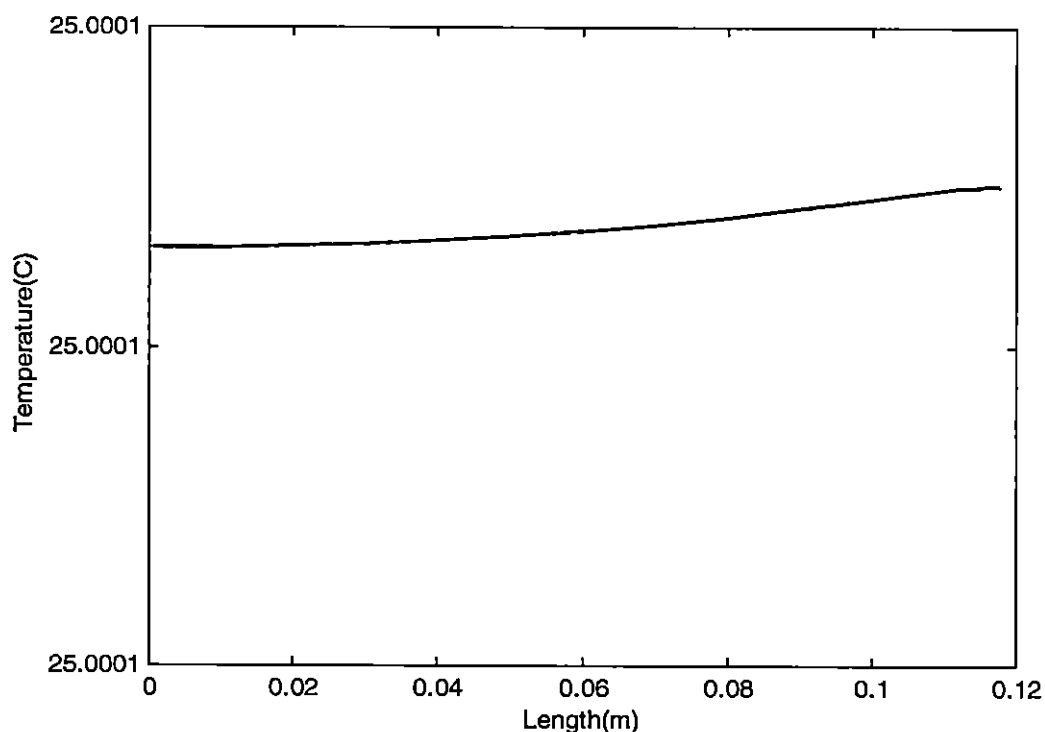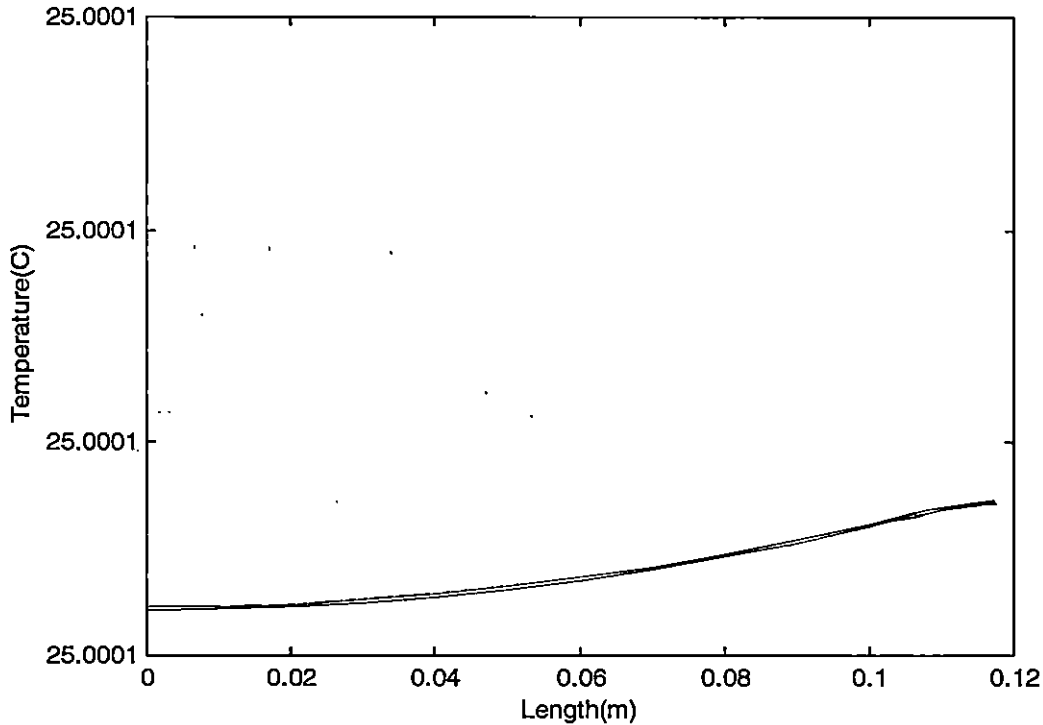

Figure 41. The change of the temperature along the wire for *RBC*-5400 (angle = 35°).

Here, again, the difference between the insulator and conductor is very small.

However, it is still obvious that the temperature increases as the curvature of the wire

increases. A closer view of the bent part of the wire can be seen by changing the

scale of the graph as demonstrated in Figure 42 (next page). Again, it should be

mentioned that due to the high thermal conductivity of *RBC*-5400, the raise in

temperature is very small. Therefore, the vertical scale in Figure 42 does not show any difference.
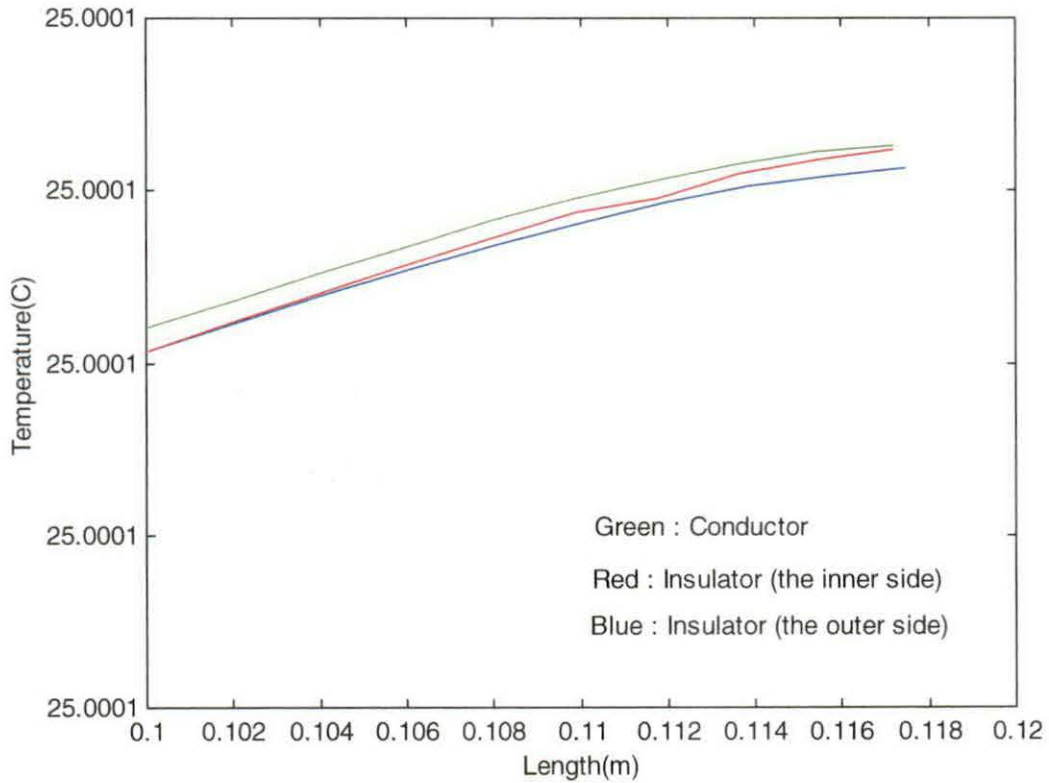
Figure 42. The same figure as Figure 41, but with different scale and showing the bent part of the wire.

Referring to Matrix *node_thy_mat*, the maximum nodal temperature in the conductor is 25.00008862 °C and in the insulator, the inner side and outer side, are 25.00008861°C and 25.00008856°C respectively.

The Impact of the Voltage Surge on the Temperature Distribution

A 50,000 V was applied across the wire. Since the under-study wire was a piece of a long wire in the stator coil winding, this voltage was not applied directly across this small wire, but was applied across the coil. The coil chosen for the current study had 14.9Ω resistance and ability to carry 7.2 A. The length of the wire having the mentioned characteristic was calculated to be approximately 699.5 m, which was rounded to 700. This was the whole length of the wire used to make the stator coil winding.

Therefore, the voltage surge was applied across a 700-m wire. To find the voltage applied across the 0.12-m of the wire was desired, it was needed to know how many of these 0.12-m were contained in the 700-m wire. This was calculated by dividing 700 by 0.12, and the result was approximately 5833.3. This value was then rounded to 5833.

The meaning of this value is that there were 5833 pieces of wires in the 700-m wire, each of which was 0.12 m long. Each of these pieces was treated as a resistor. Therefore, there was a long chain of series resistors. The voltage (in this case, 50,000 V) was divided among 5833 resistors. Consequently, there were 50000/5833 ≈ 8.6 V across each 0.12-m resistor.

In Function *ss_cylinder* (refer to Appendix B), the total amount of the voltage surge was plugged in since the program calculates the voltage across each small resistor itself. Therefore, parameter *sur_volt* (refer to Appendix A-1) was set at 50,000V.

The lines commented in Figure 23 were uncommented in order to implement the surge into the computer program, then Parameters *insl_k* and *arc_ang* (refer to Appendix A-1) were changed to obtain the temperature distribution with different insulators and angle of curvature.

Based on the choice of the insulator and the angle, the following graphs were produced and categorized.

1) Insulator : Epoxy Resin(*RBC*-5520),   Curvature Angle: 15°

The result is demonstrated in Figure 43.
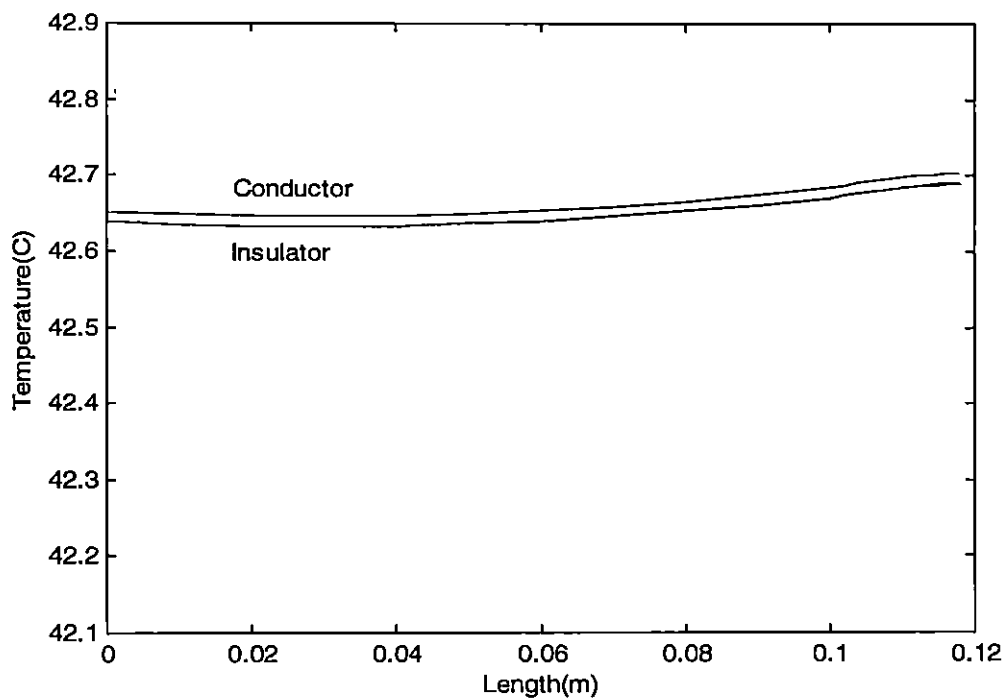
Figure 43. The nodal temperature along the wire (angle = 15°)

As seen, the temperature suddenly increased. When the surge hit the wire, it produced a big current in the wire. This current created extra heat within the wire and, therefore, the temperature increased. As expected, the temperature along the straight part of the wire was almost identical, since the shape of the wire was a cylinder and it had symmetry along its axis. In the bent area, as the curvature increased, the temperature increased as well. Again, the temperature reached its maximum at the very end part of the wire where the curvature was maximum. To better observe, the temperature distribution at the end part of the wire, the node set number three was selected. Then, to obtain the corresponding graph, the parameter *plot_key* (refer to Appendix A-1) in Function *ss_cylinder* (refer to Appendix B) was set to be four.

Figure 44 (next page) demonstrates the temperature across the wire at the far end of it, corresponding to node set number three. At the moment of the surge, the voltage suddenly increased and then gradually decreased.
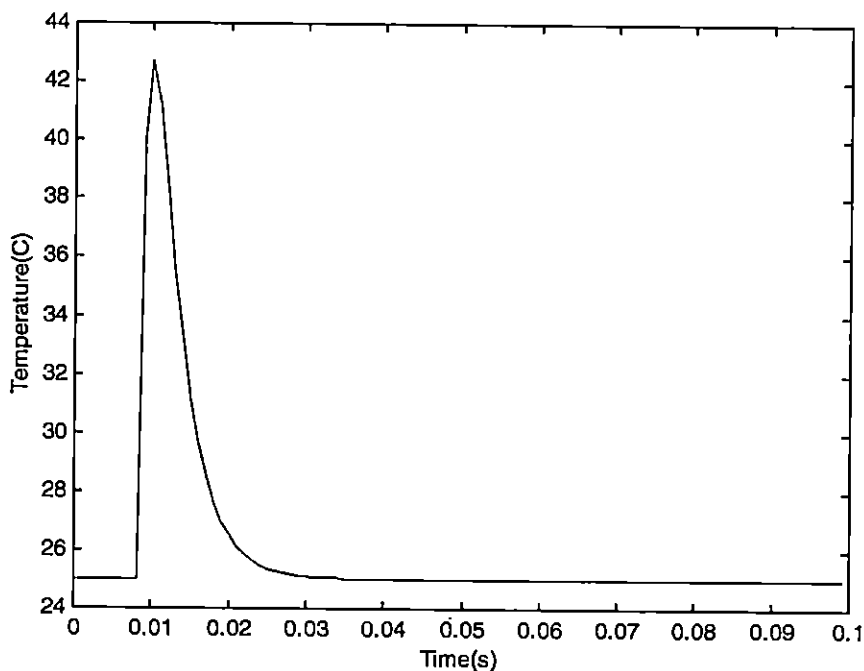
Figure 44. The nodal temperature for the node set number three.

A close look at Figure 44 also reveals that the temperature between the two

sides of the wire (inner and outer sides) in the bent part of the wire was not the same.

Figure 45 (next page) expands and provides a closer view of the bent part. As seen,

there was a slight difference between the temperature of the inner side nodes and the

outer side ones. It is also clear that the inner side part of the insulator is hotter than

the outer side. The inner side of the wire tolerates higher pressure than the outer side,

therefore, causing the temperature to increase.

According to Matrix *node_ths_mat* (refer to Appendix A-2) the maximum and

the minimum temperatures for the conductor were approximately 42.703 °C and

42.652 °C respectively. For the insulator, the maximum and minimum temperature of

the inner side are 42.691°C and 42.638°C and for the outer side are 42.689 °C and

42.638 °C respectively.
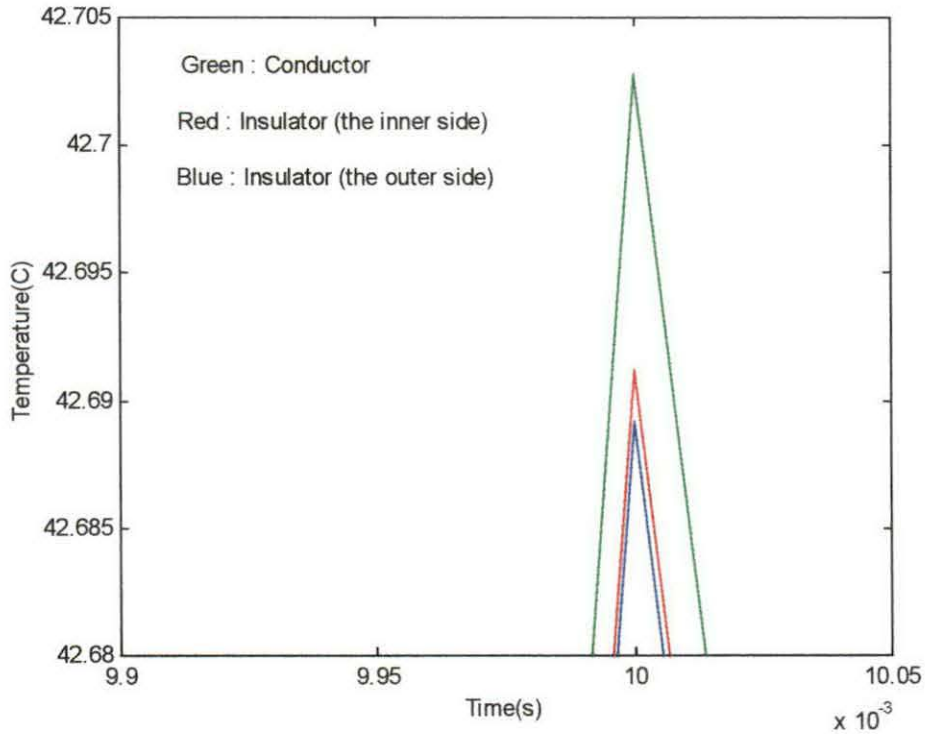
Figure 45. The same distribution as Figure 44 with different scale (angle = 15°).

2) Insulator : Epoxy Resin(*RBC*-5520),   Curvature Angle: 25°

This analysis was the same as analysis number one except the angle is set at

25° instead of 15°. The graph in Figure 46 (next page) demonstrates this case.
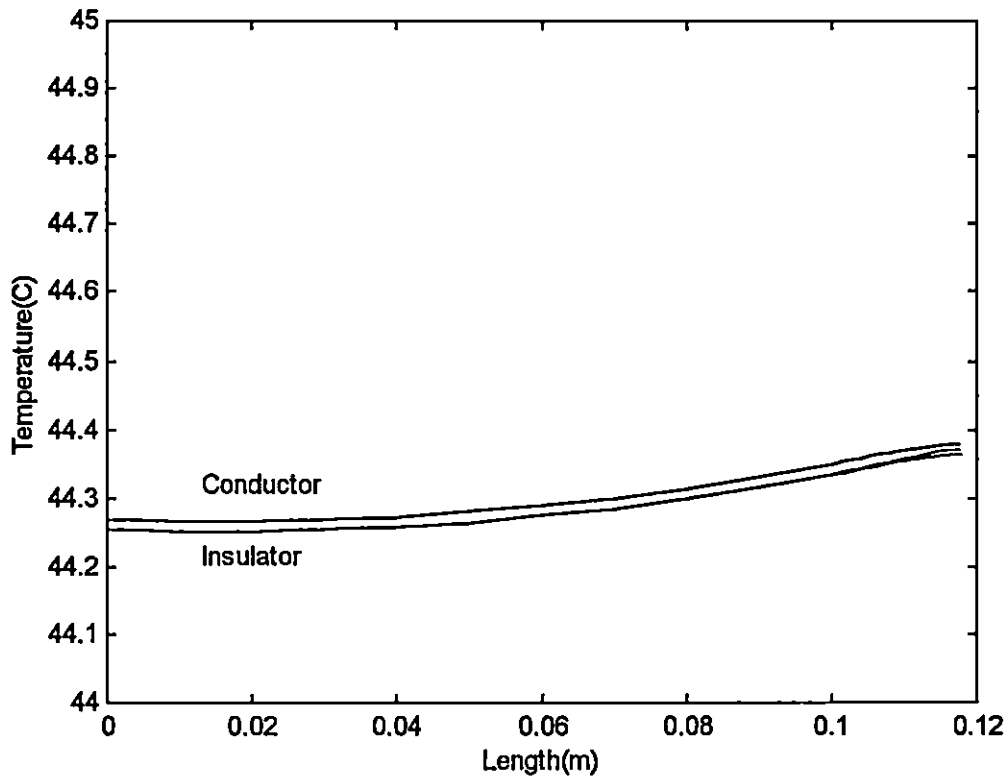
Figure 46. The nodal temperature along the wire (angle = 25°).

Comparing this graph with Figure 43, one sees that the temperature had

increased. The reason lies in the angle increasing. The nodal values contained in

Matrix *node_thy_mat* (refer to Appendix A-2) showed the maximum and minimum

values for the conductor as 44.379 °C and 44.271 °C respectively. For the inner side

nodes of the insulator, the maximum of the temperature was 44.370 °C and the

minimum was 44.253 °C. The outer side temperature of the insulator at its maximum

was 44.364 °C and at its minimum was 44.253 °C.

The temperature of the inner side of the insulator was higher than the outside

temperature of the insulator. To demonstrate this, the scales of the graph in Figure 46

were changed to produce the result in Figure 47.
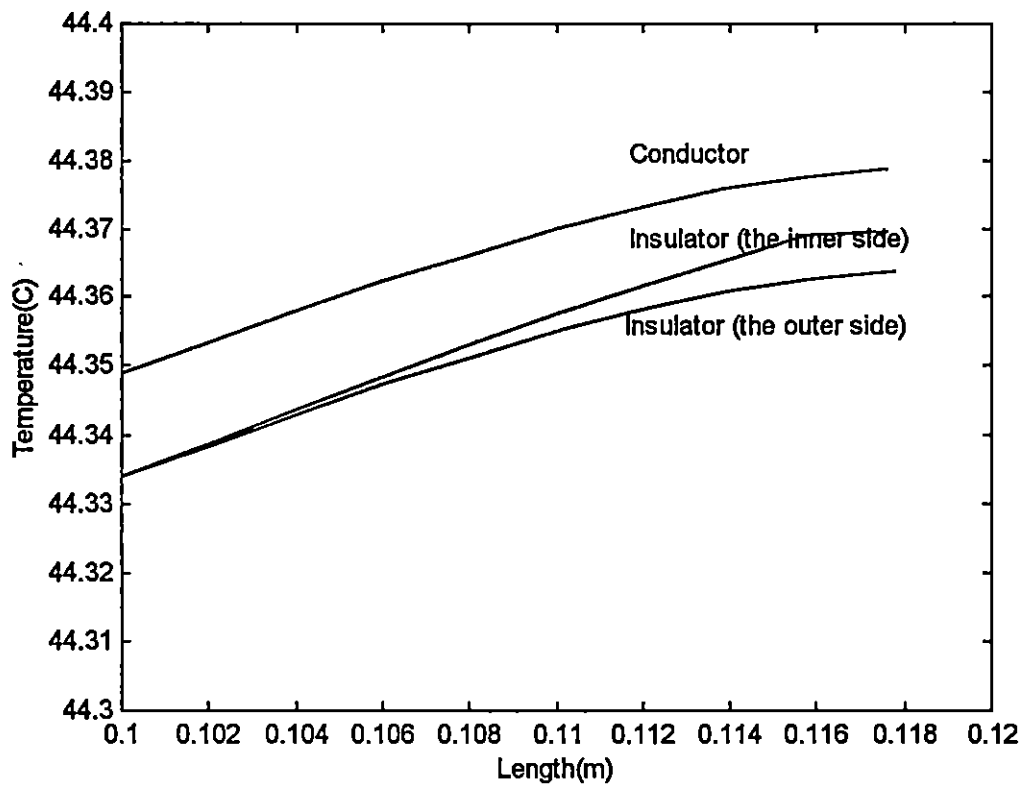
Figure 47. The bent part of the wire shown in Figure 46 (angle = 25°).

Since the maximum occurred at the same area as in the previous analysis

(refer to analysis number one), the temperature varying versus time was obtained

using the same set of node (i.e. node set number three). Figure 48 illustrates the

result.
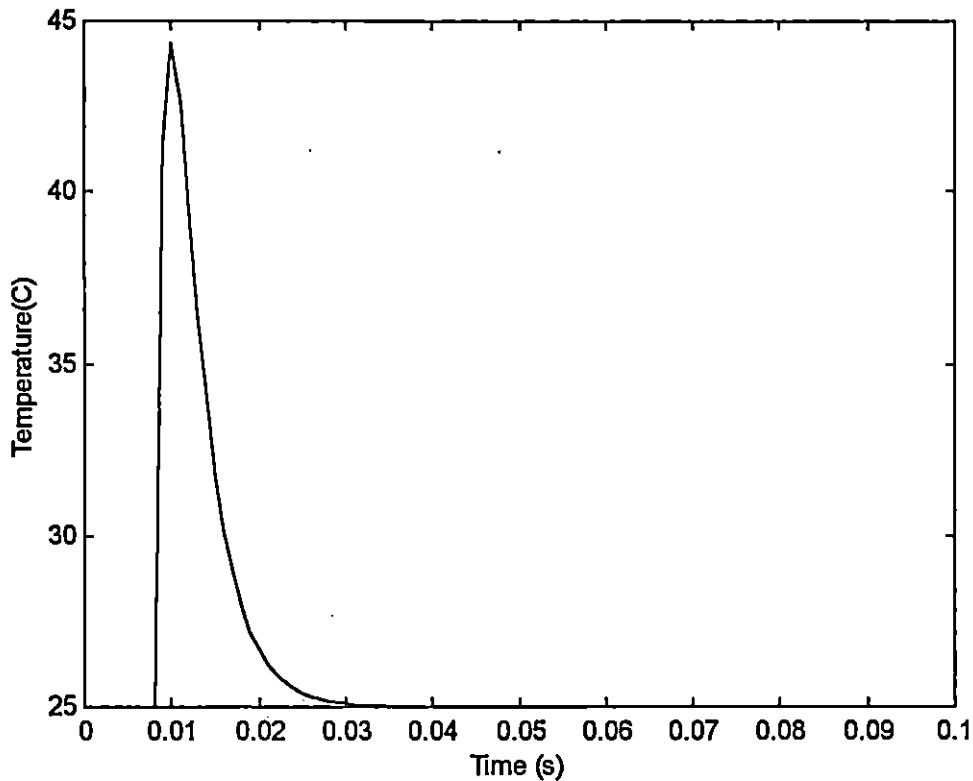
Figure 48. The nodal temperature for the node set number three (angle = 25°).

3) **Insulator : Epoxy Resin(*RBC*-5520),   Curvature Angle: 35°**

The graph in Figure 49 (next page) was produced by changing the angle from

25° to 35°. As seen, the temperature along the wire had increased and was

expected since the angle of the wire was increased. Also, the temperature in the

bent area increased, as was the case in the previous similar analysis.
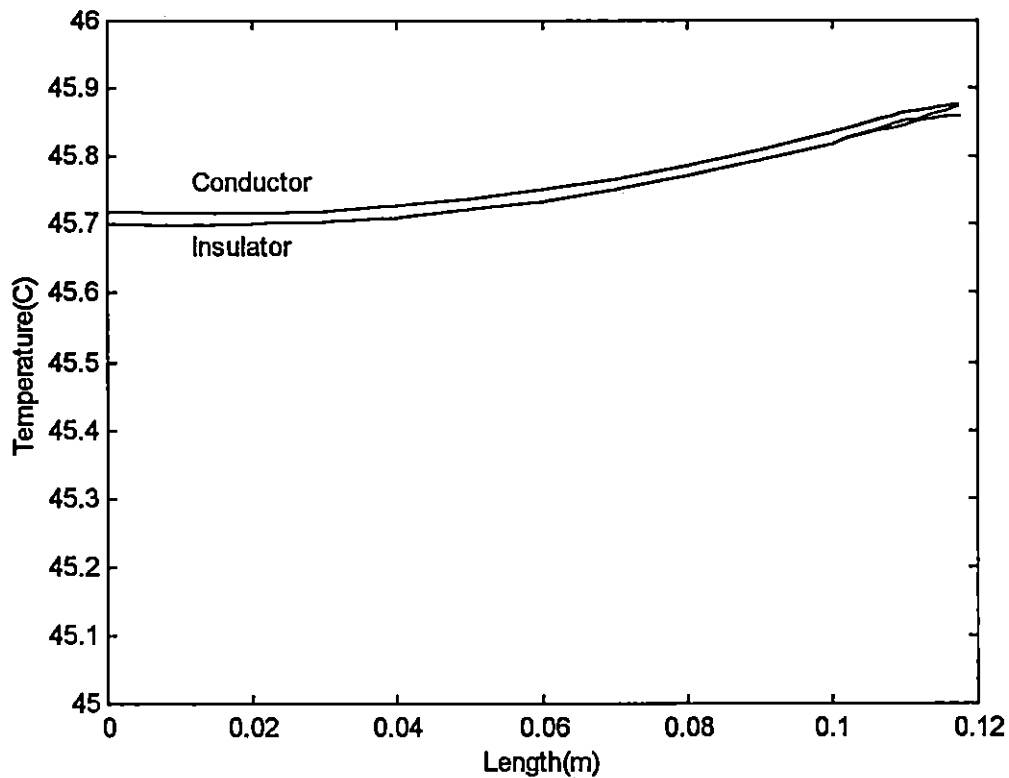
Figure 49. The temperature distribution along the wire (angle = 35°).

The maximum and the minimum values of the temperature in the conductor

were 45.876°C and 45.718 °C. In the insulator, the maximum and the minimum were

45.873°C and 45.720°C. The maximum value here represents the nodal temperature

in the inner side of the insulator. The corresponding maximum values for the outer

side of the insulator was 45.87°C and the minimum was 45.70°C. Figure 50 (next

page) represents the temperature varying in the bent area when the scales were

changed in the graph in Figure 49.
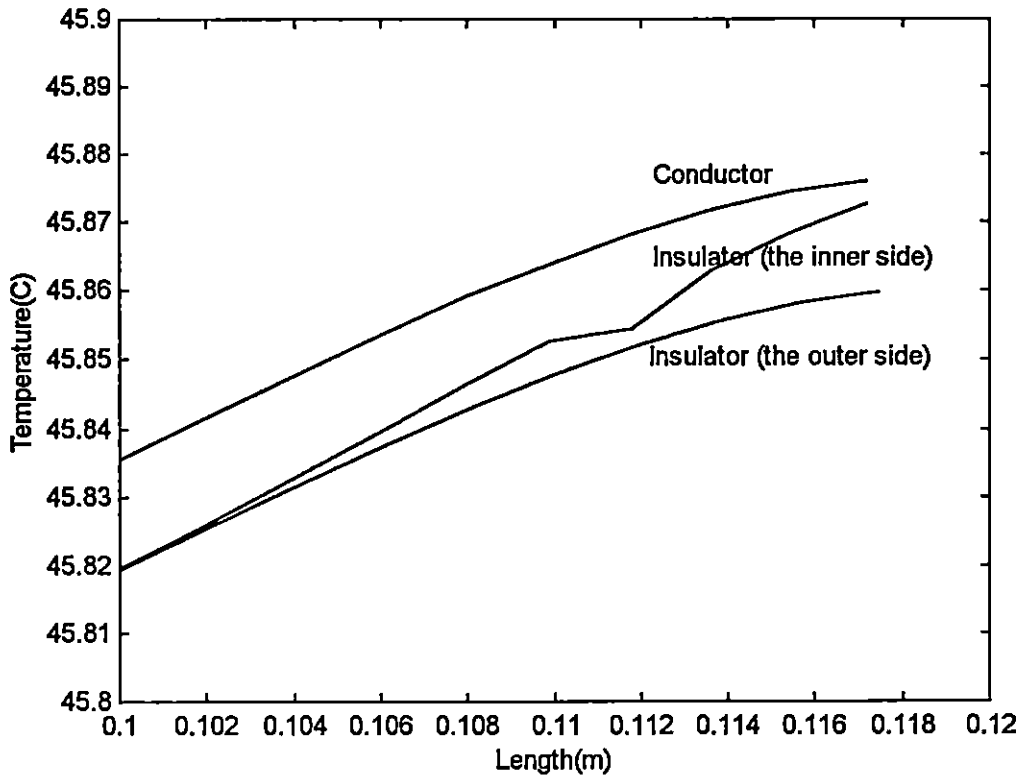
Figure 50. The temperature distribution in the bent area in both conductor and insulator (angle = 35°).

Referring to Figure 22, the node set representing the bent area at far the end of the wire was node set number three. Therefore, the program was run again to calculate the nodal temperatures. Figure 51 (next page) illustrates the result.
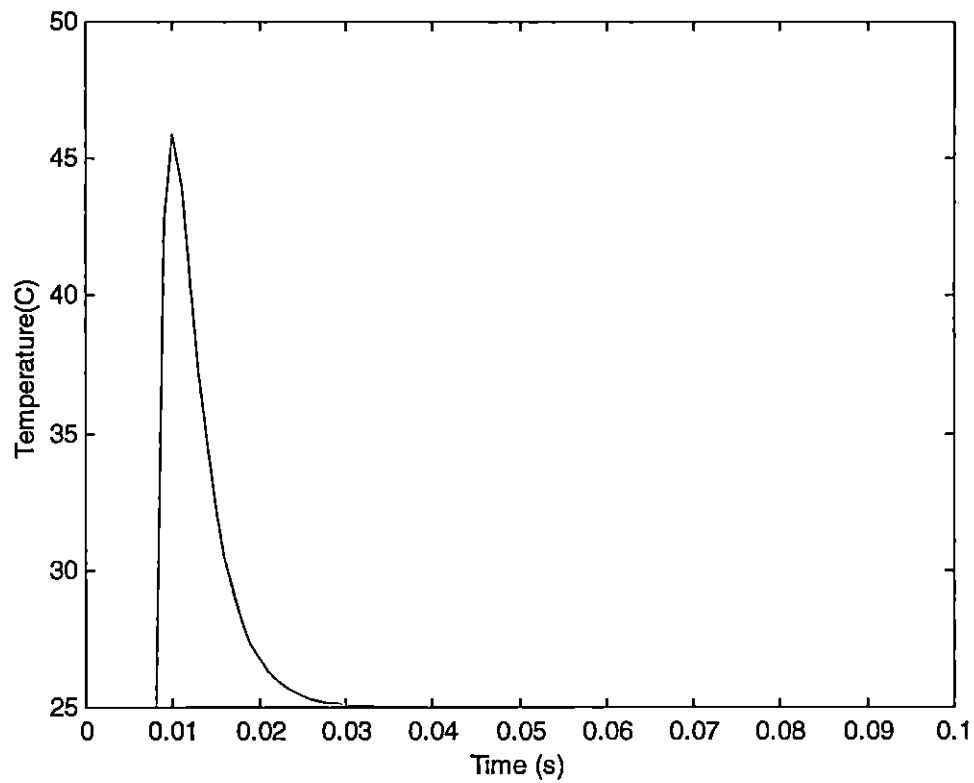
Figure 51. The nodal temperature for the node set number three

By comparing Figure 51 with Figure 48, the deduction can be made that the temperature had increased. Consequently, increasing the angle raised the temperature in both conductor and the insulator. As in analysis number one, a closer view of the figure was needed. Figure 52 (next page) shows the enhanced view of the graph in Figure 51.
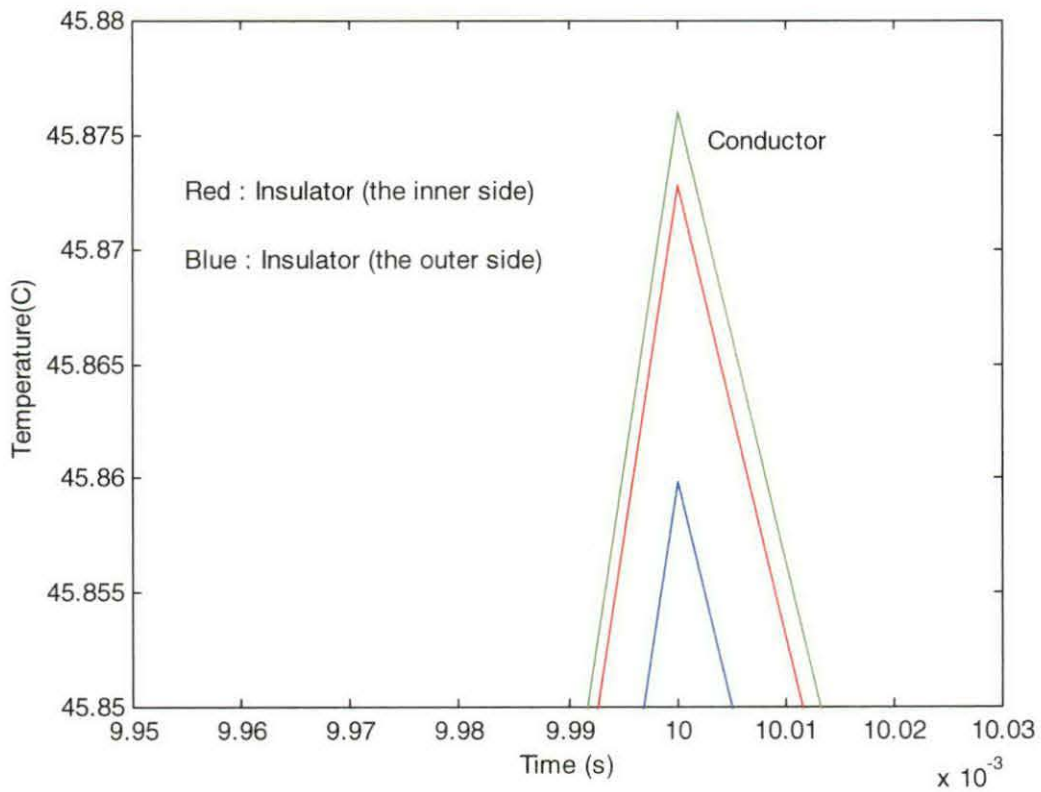
Figure 52. A close look at the peak of the same temperature distribution shown in Figure 51.

Again, the graph revealed that the temperature of the insulator in the inner side of the wire was higher than the outer side. Since the temperature difference was not too much, the difference was not evident in Figure 51.

4) Insulator : Epoxy Resin(*RBC*-5200),   Curvature Angle: 15°

In this case, the material used as the insulator was changed to Epoxy Resin

(*RBC*-5200). Therefore, Parameter *insl_k cylinder* (refer to Appendix A-1) in

Function *ss_* representing this parameter was uncommented and the same parameter

representing the value for Insulator Epoxy Resin (*RBC*-5520) was commented. Also,

the angle was set to its first value, which was 15°. The program was run for the new

values of the parameters. Figure 53 shows the result of the analysis using these new

data.
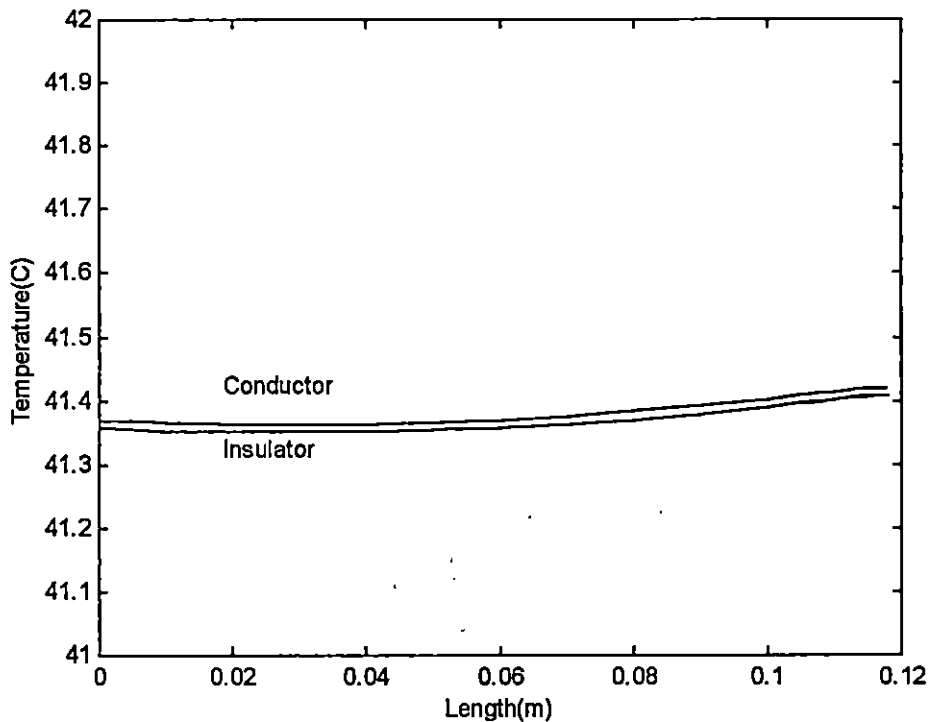
Figure 53. The nodal temperature along the wire (angle = 15°).

This figure shows that the average temperature along the wire had decreased

compared with the similar analysis shown in Figure 43. The thermal conductivity

RBC-5520 is less than RBC-5200 and the rate of loosing temperature in RBC-5520 is

less than RBC-5200. Therefore, under the same experienced circumstances, the wire

that had RBC-5520 was at the higher temperature than the wire that had RBC-5200 as

insulator. Comparing Figures 43 and 53 indicate this correlation.

As shown in Figure 53, the end part of the wire (in the bent area) had the

highest temperature. Figure 54 illustrates the temperature distribution in the bent part

of the wire using node set number three.
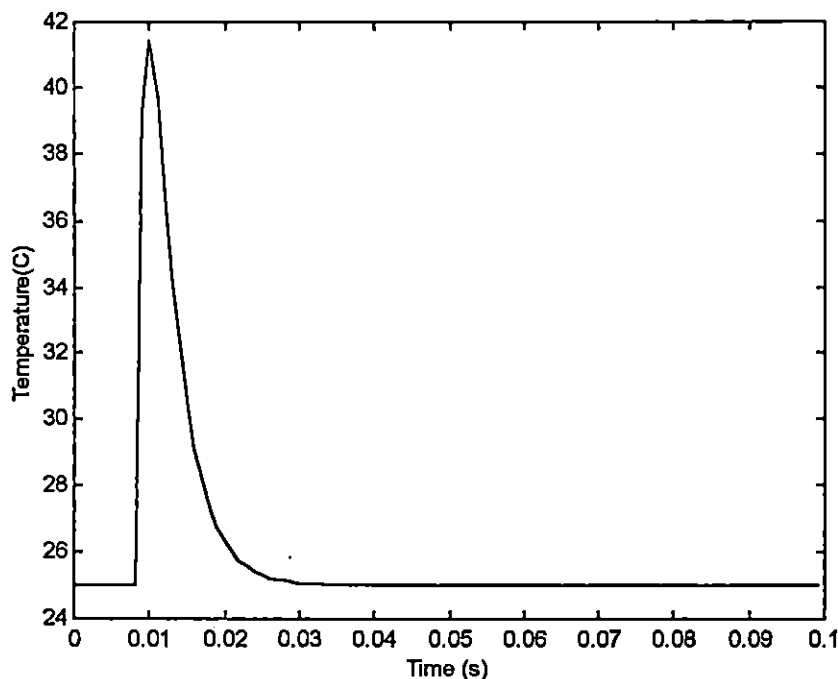
Figure 54. The nodal temperature for the node set number three (angle = 15°).

By comparing Figure 54 with Figure 44, the results show that the peak of the temperature had decreased. Referring to Matrix *node_ths_mat* the maximum value for the temperature was 41.420 °C for the conductor and for the insulator was 41.409°C (in the inner side) and 41.407°C (for the outer side).

Similar to the previous analysis, the temperature of the conductor was the highest. Also, the temperature of the inner side of the insulator was higher than the outer side.

Figure 55 illustrates the same distribution as in Figure 54 using another scale so that the temperature difference can be more readily observed.
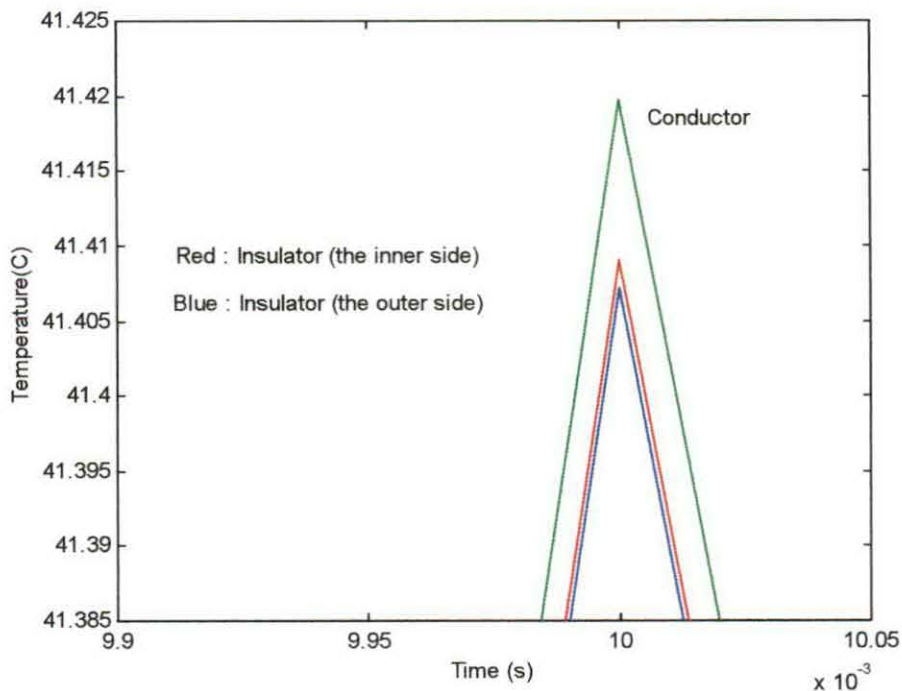
Figure 55. A close look at the peak of the same temperature distribution shown in figure 54 (angle = 15°).

5) Insulator : Epoxy Resin(*RBC*-5200),   Curvature Angle: 25°

In this analysis, the angle was changed to 25° with the rest of the parameters

left unchanged. The temperature distribution along the wire, in both conductor

and insulator, showed the same pattern as the previous similar analysis as shown

in Figure 56.
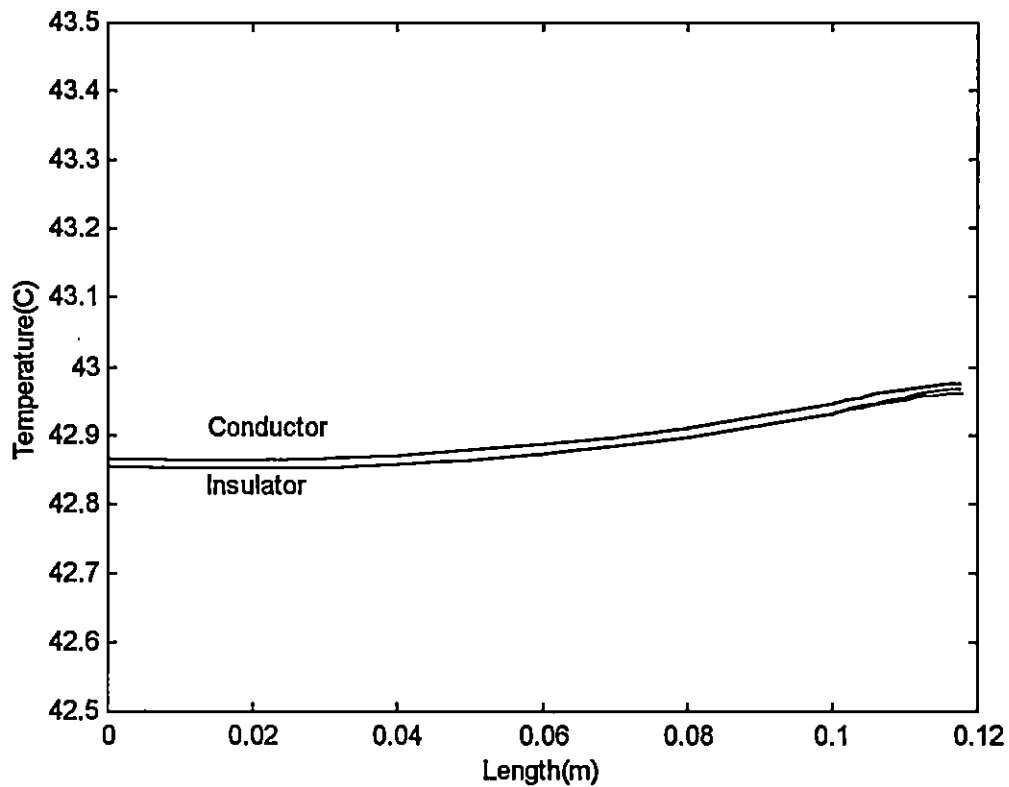
Figure 56. The nodal temperature along the wire (angle = 25°).

Again the same pattern was observed. The shape of the distribution was the same and the temperature increased as the curvature increased. The only difference was that the average temperature had decreased when compared to the results shown in Figure 46. The reason was that the thermal conductivity of *RBC*-5200 was higher than *RBC*-5520.

The nodal values for the node set number three should again be considered since the maximum temperatures occurred in the bent (refer to Figure 56). Figure 57 demonstrates the distribution in this case for node set number three.
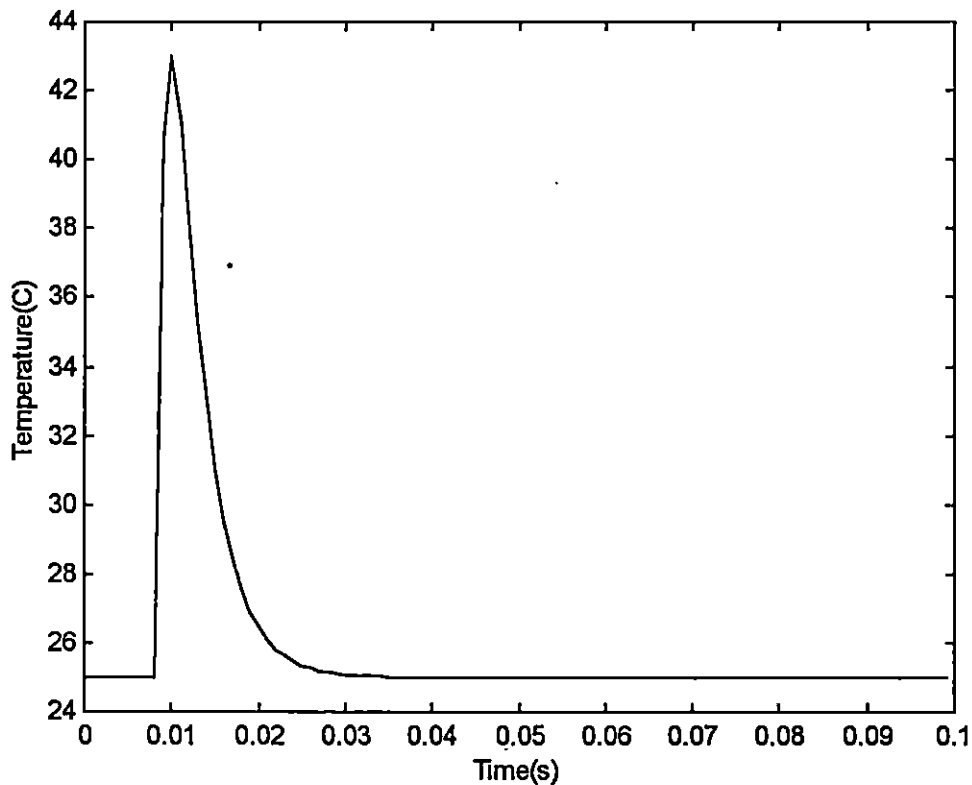
Figure 57. The nodal temperature for the node set number three (angle = 25°).

6) Insulator : Epoxy Resin(*RBC*-5200),   Curvature Angle: 35°

Figure 58 demonstrates the distribution obtained by changing the angle from

25° to 35°. Similar to the previous analysis, just the angle was changed.
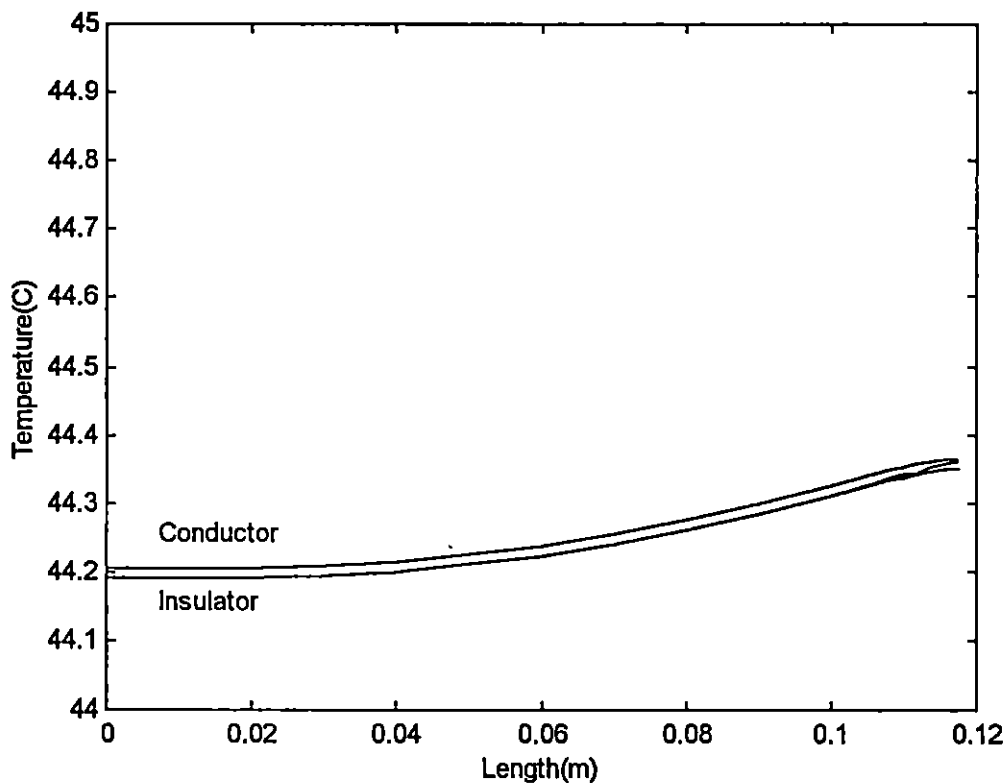
Figure 58. The nodal temperature along the wire (angle = 35°).

Figure 58 shows the pattern was repeated among the similar analysis, but the

temperature changed. In this case, the temperature decreased, compared with Figure

49, in which the same angle was used, but with different insulator material.

Figure 59 represents a different scale for the graph in Figure 58.
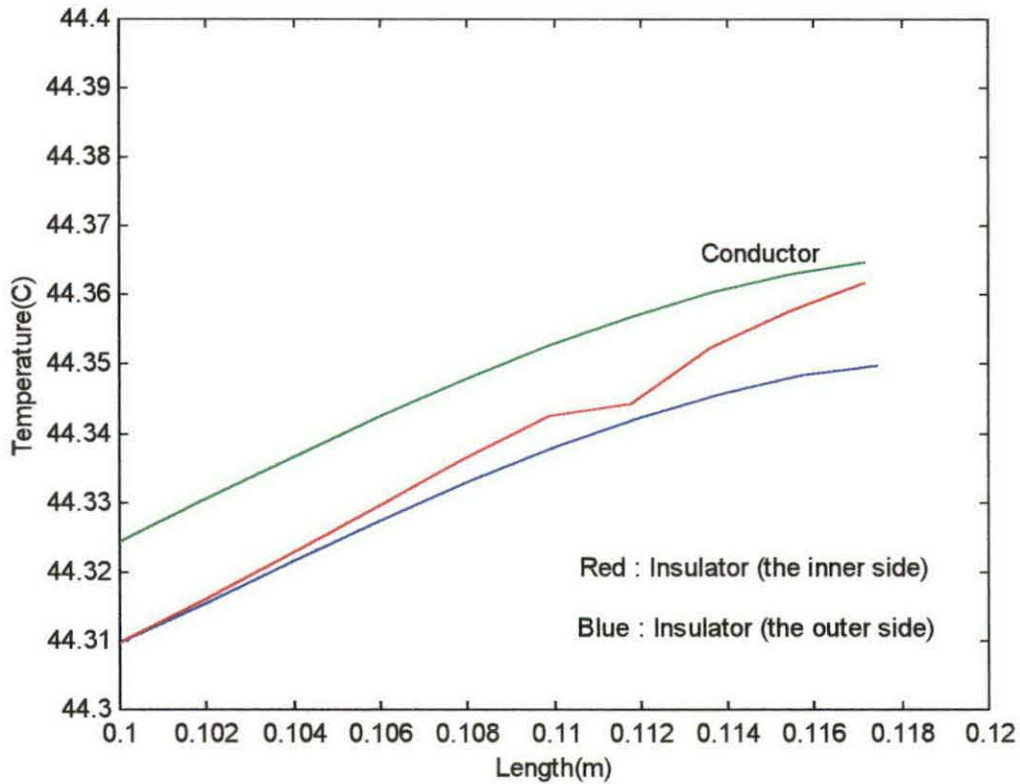
Figure 59. The temperature distribution in the bent area in both conductor and insulator (angle = 35°).

Again, the inner side of the insulator was at a higher temperature than the outer side. Both of them are at a lower temperature than the conductor, which was expected.

7) Insulator : Epoxy Resin(*RBC*-5400),   Curvature Angle: 15°

The last insulator material analyzed was Epoxy Resin (*RBC*-5400). This

material has a very good thermal conductivity as compared with the two previously

used. The analysis started using the angle of 15° as the curvature and the rest of the

parameters were kept unchanged. Figure 60 shows the result of this analysis.
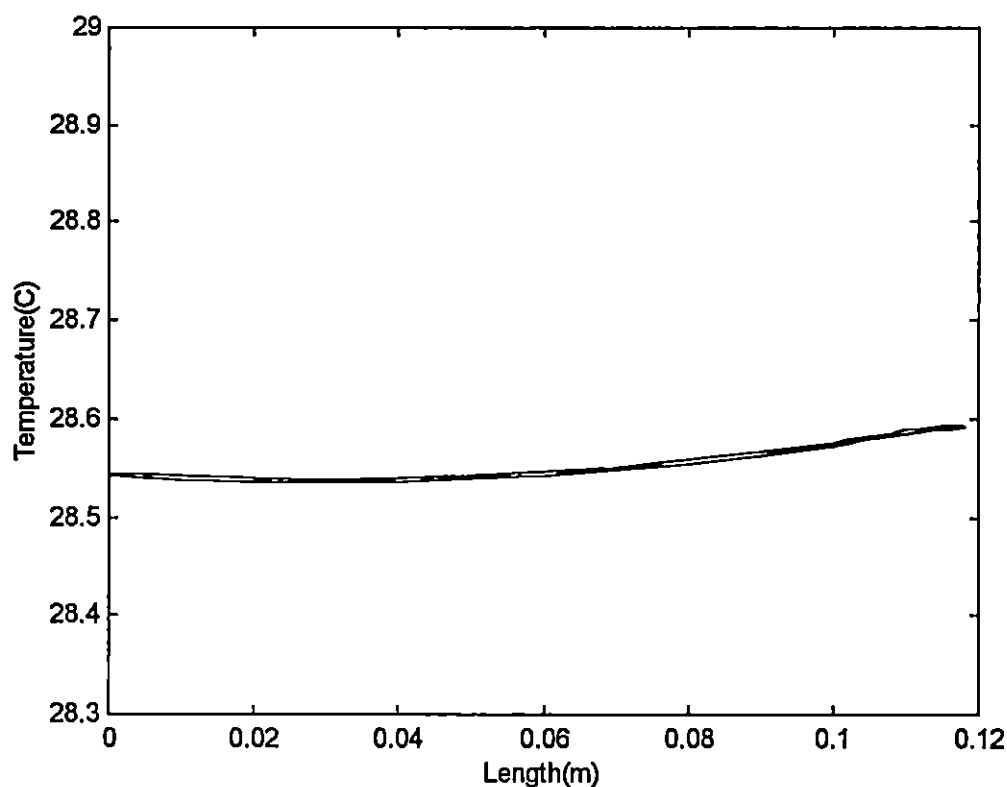
Figure 60. The temperature distribution along the wire (angle = 15°).

It is obvious that the temperature decreased. This is reasonable since the thermal conductivity of *RBC*-5400 is high, which allows it to conduct the heat faster and more than *RBC*-5520 and *RBC*-5200. By changing the scale of the above figure, the graph in Figure 61 was generated, showing the temperature distribution in the bent area of the wire.
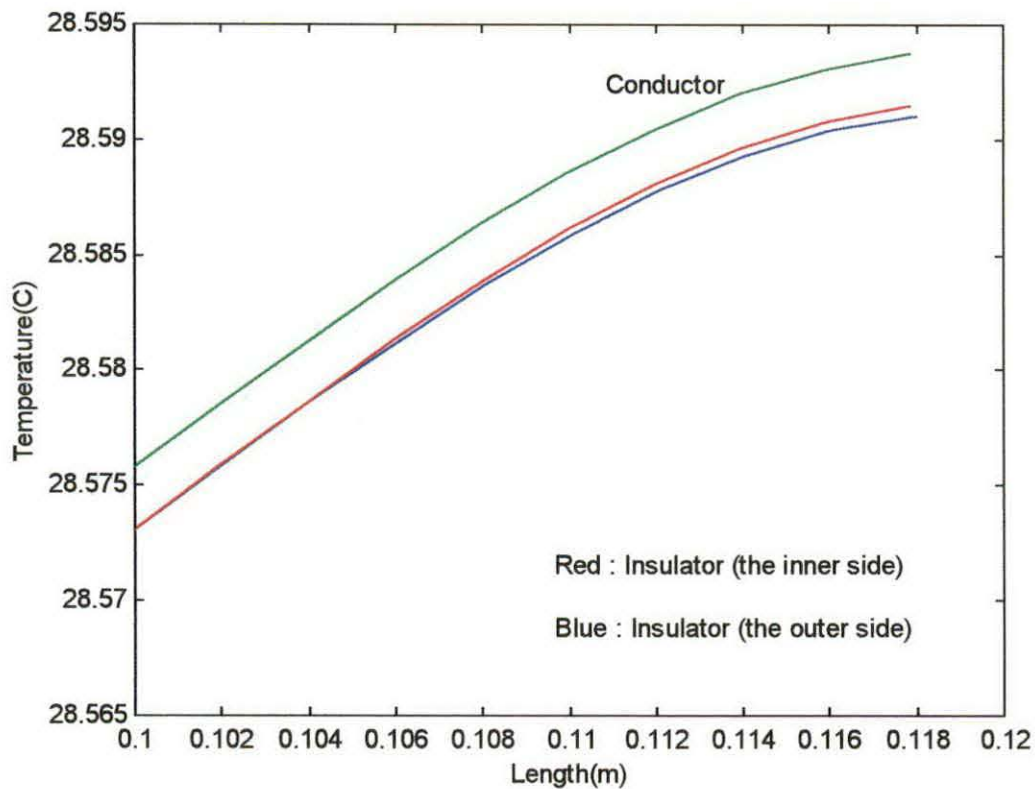
Figure 61. The same distribution as Figure 60 but using different scales to see the distribution in the bent area (angle = 15°).

Again, the same pattern was observed. The temperature in the conductor was the highest one and the temperature in the inner side of the insulator was higher than the outer side. Since the maximum temperature was in the bent area of the wire, again, node set number three was chosen. The results of this analysis are shown in the graph in Figure 62.
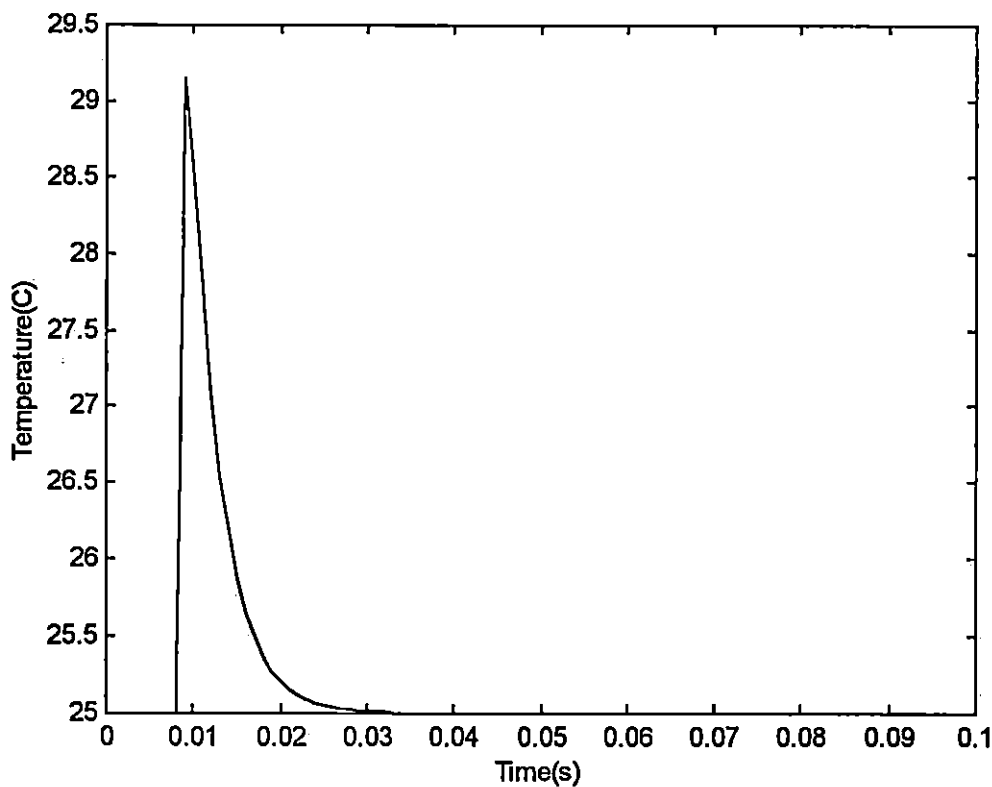
Figure 62. The nodal temperature for the node set number three (angle = 15°).

By changing the scale, it was possible to observe the temperature varying at the peak of the above figure. Figure 63 (next page) illustrates this observation. As

seen in this figure, the temperature of the inner side was higher than the outer side,

the same distribution as with the other insulators. The only thing changed was the

maximum temperature. Referring to Matrix *node_ths_mat*, this maximum was

29.143 °C for the conductor and for the insulator, it was 29.141°C for the inner side

and 29.140°C for the outer side.
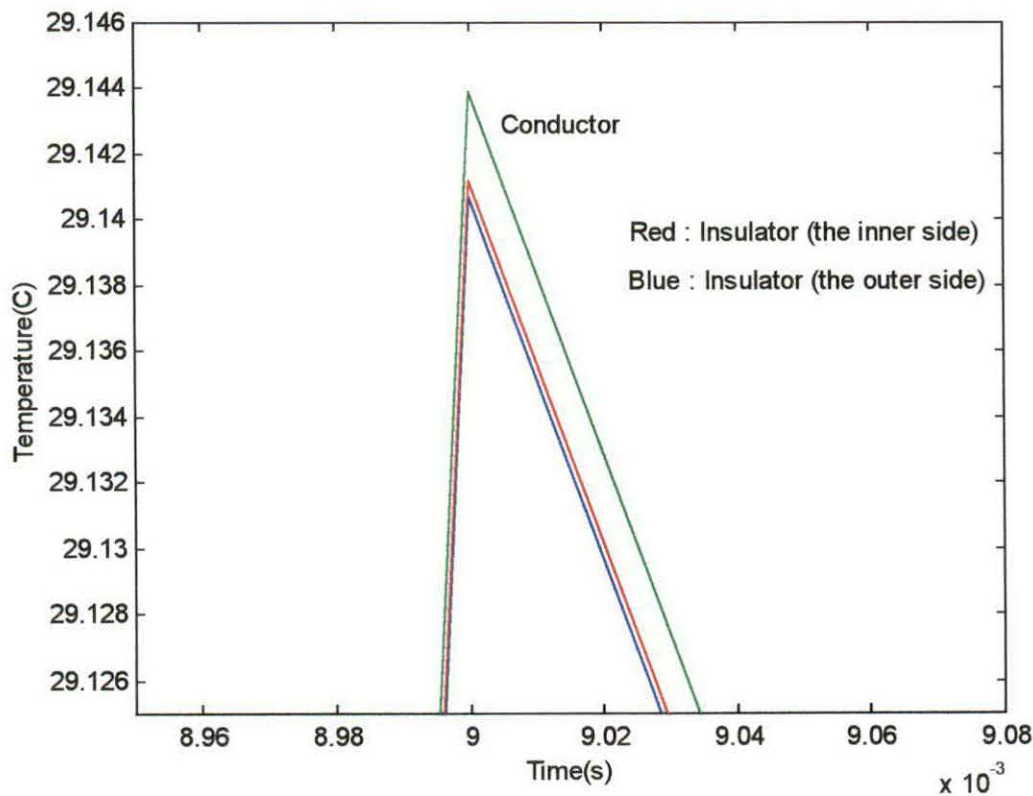
Figure 63. A closer view of the peak shown in Figure 62 (angle = 15°).

Another interesting result obtained from Figure 63 was when the temperature

raised, the rise occurred in both insulator and conductor almost simultaneously. At

the peak, the temperature of the conductor increased more than the insulator.

Therefore, when the voltage surge decreased the temperature of both conductor and

insulator decreased (the right-hand side of Figure 63), but the temperature difference

between the conductor and the insulator was now more than the increasing time (the

left-hand side of Figure 63).

8) Insulator : Epoxy Resin(*RBC*-5400),   Curvature Angle: 25°

In this case, just the angle was changed. Figure 64 illustrates the result.
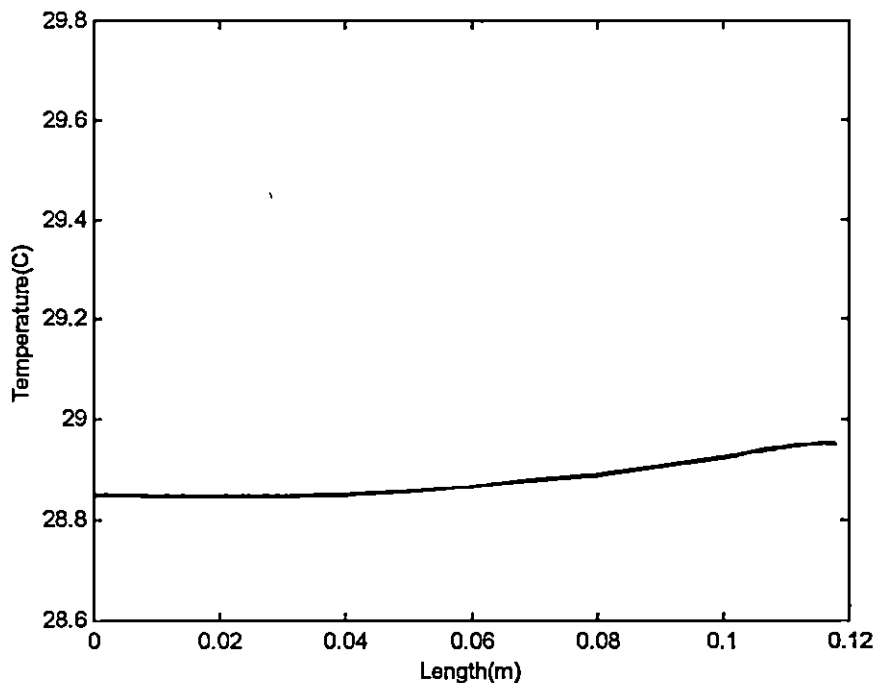
Figure 64. The nodal temperature along the wire (angle = 25°).

Figure 65 shows the same distribution with a different scale in the bent part of the wire. It was completed by choosing the proper scales. It is obvious that the nodal temperature decreased compared to Figure 47 due to the high thermal conductivity of *RBC*-5400.
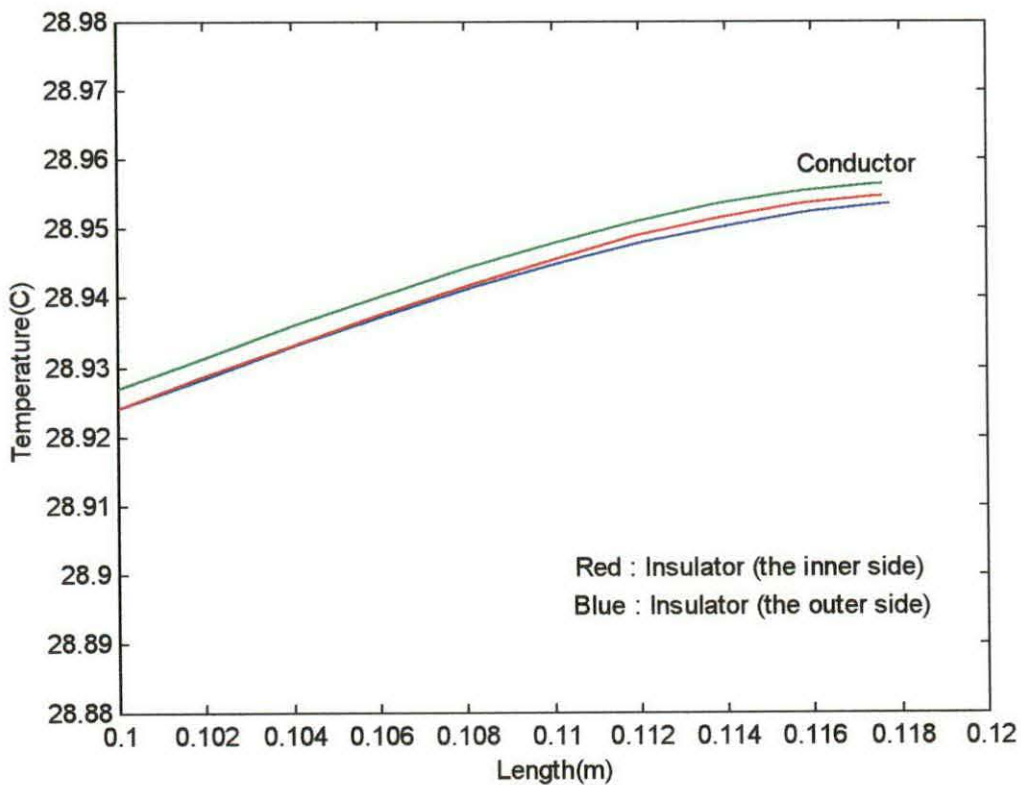
Figure 65. The same distribution as Figure 64 but using different scales to see the distribution in the bent area (angle = 25°).

9) Insulator : Epoxy Resin(*RBC*-5400),   Curvature Angle: 35°

The last analysis was performed by setting the angle of the curvature to be

35°. The result is shown in Figure 66. Due to the close nodal temperatures of

both the conductor and the insulator, the difference was not obvious in this figure.
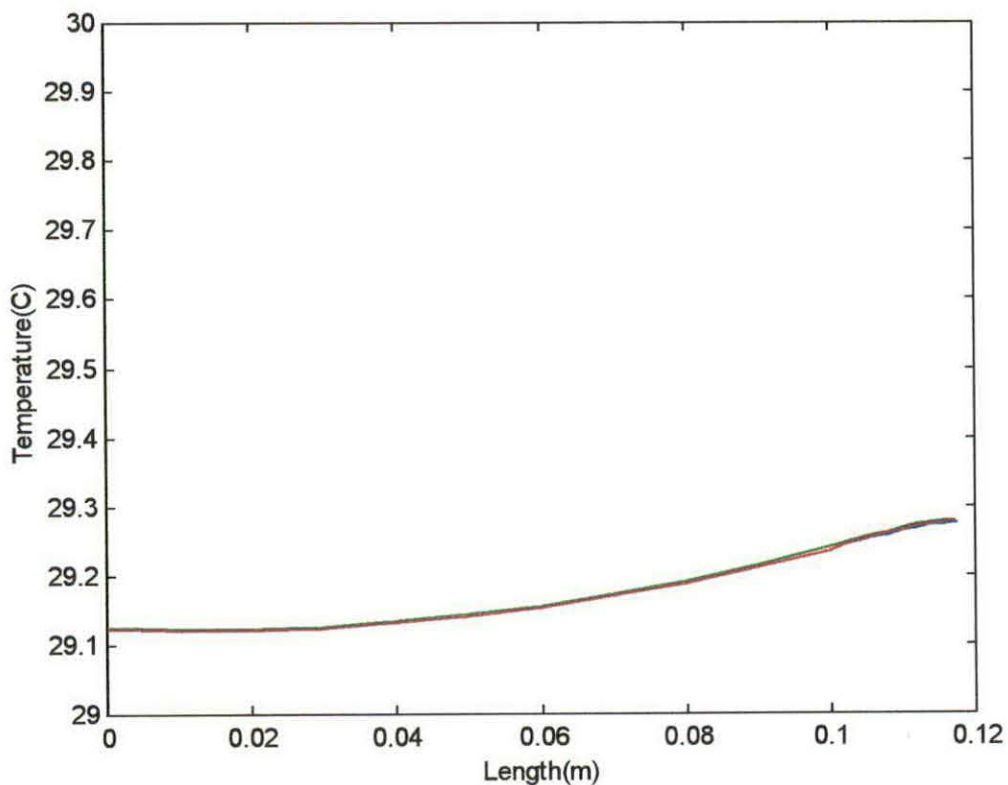
Figure 66. The temperature distribution along the wire (angle = 35°).

A closer view of Figure 66 is shown in Figure 67 (next page). Like the

previous cases, this graph was generated in the bent part of the wire. At first glance,

it appears that the slope of the curves was more than the other similar analysis (refer to Figure 50), but actually they had the same slope. The only thing different was that the temperature difference between conductor and insulator in the present analysis was less than other analysis. This was acceptable since the thermal conductivity of *RBC*-5400 was the maximum one among the insulators chosen, therefore, the heat passed through the insulator faster.
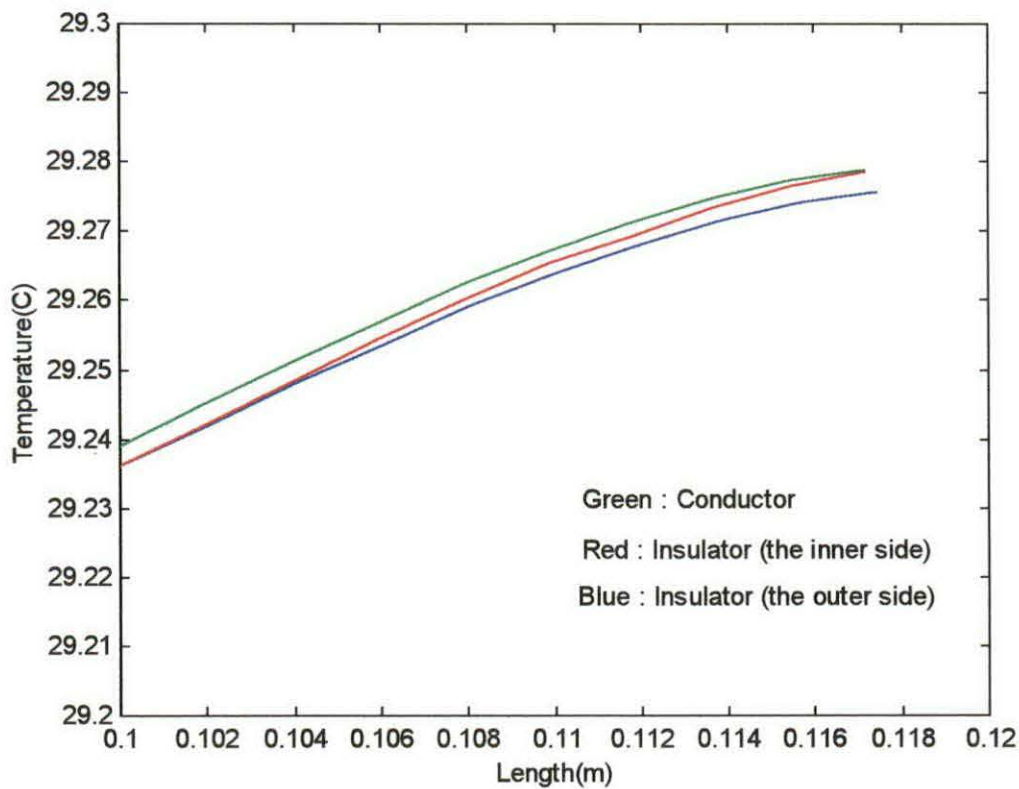
Figure 67. The bent part of the wire analyzed in Figure 66 (angle = 35°).

Summary and Conclusion

In this chapter, the results of the different analyses were shown. Each of the analyses produced for a particular angle of curvature and the material used as an insulator. The graphs were detailed and discussed, and the impact of changing each of the parameters, such as material and angle of curvature, were addressed. Three research questions presented in this Thesis with respective answers are as follows:

1- Where on the wire does the failure happen due to the over-voltage?

As the analysis showed, when the voltage (not the voltage surge) was applied across the wire, the temperature in both conductor and insulator increased. The temperature in the insulator was less than the conductor since the insulator blocked the heat flowing out of the conductor toward the ambient. Consequently, the temperature of the conductor increased. Also, the temperature in the straight part of the wire was less than the bent part because, in the bent area, the cross-section of the wire was decreased, therefore increasing the resistance, which led to increasing the temperature.

In less than 10 ms (refer to Figure 27), the temperature established in both conductor and insulator, and did not increase. When the voltage surge was applied, the temperature of both the conductor and the insulator increased suddenly. As the voltage surge decreased, the temperature was decreased too. The analysis showed that the temperature was increased and that the increment was more in the bent area

of the wire. The analysis did not show any significant increment in the temperature, in either conductor or insulator, which led to over heat the insulator or conductor. In this study, just the impacts of the thermoelectrical effects were observed. Since the wires in the stator coil winding experience some mechanical impacts, these impacts could be led to the failure in the insulators. On the other hand, the vibration of the coils in the stator effects the insulators. This effect can appear as a mechanical damage to the insulator layers or even some thermal effect, such as temperature increment.

Despite all of these effects, it can be said that the temperature in the bent area of the wire, where the wire is bent to go out from one slot or even where it goes into another slot, reaches its maximum value. Therefore, these areas in the stator coil winding are most likely the places where the damages occur.

2- What is the impact of the bent on the heat distribution within the wire?

The temperature of the wire in the straight part was smooth. In this part, the corresponding nodes in the inner side and outer side had almost the same temperatures, due to the symmetry of the straight part, which is basically a cylinder. In the bent area, the temperature variation was a function of the curvature. When the angle of curvature either increased or decreased, the nodal temperature also increased or decreased. The more the angle, the more the temperature increment.

When the angle increased the temperature difference between conductor and insulator increased. And, the temperature of the inner side of the insulator (refer to

Figure 65) was higher than the outer side, which can lead to failure in this area of the wire.

3- What is the impact of the insulator material on the heat distribution within the wire?

Since each insulator had its own thermal conductivity, the impact of conducting the heat to the ambient was different among the insulators. The present analysis showed that the amount of the thermal conductivity had direct impact on the nodal temperature in both the conductor and the insulator. When the thermal conductivity increased, the temperature increased as well. Therefore, choosing the material, which had good thermal conductivity was essential. But, at the same time, the mechanical behavior of the material chosen should be considered, since there are some mechanical effects in the stator coil winding.

Suggestions and recommendations

Based on the results of this study, the following are recommended for the next study:

1- Since this study just considered the thermal-electrical effect, it is recommended to consider the mechanical impact on the heat distribution.

2- The method used for analyzing the present study was actually two-dimensional with the two-dimensional element used to discretize the domain. Also, just a cross-section of the wire was studied. To obtain more details and

more accurate results, the three-dimensional analysis is recommended, with the three-dimensional element used to mesh the wire. For instance, a hexahedral element (either with 8 nodes or 20) could be used.

3- Using some well-known engineering packages, such as ANSYS, could assist in seeing and observing the results in three dimensions.

4- One practical problem is the change of the physical properties with the temperature increment. Most of the physical parameters are not constant during the temperature increasing/decreasing. To obtain a better more realistic answer, it is recommended to include the variation or fluctuation of some properties such as resistance, thermal convection, and thermal conductivity.

References

Arfken, G. (1971). Mathematical methods for physics. (2nd ed.). New York: Academic Press.

Armor, A. F., Chari, M. V. K. (1976). Heat flow in the stator core of large turbine-generators, by the method of three-dimensional finite elements. IEEE Transactions on Power Apparatus and Systems, PAS-95, pp. 1648-1662.

Byron, F. W., Jr., & Fuller, R. W. (1969). Mathematics of classical and quantum mechanics (Vol. 1).(1st ed.). MA: Addison Wesley.

Carslaw, H. S., & Jaeger, J. C. (1959). Conduction of heat in solids (2nd.). London: Oxford University Press.

Devries, P. L. (1994). A first course in computational physics (1st ed.). New York: John Wiley and Sons.

Floyd, T. L. (1995). Electric circuits fundamentals (3rd ed.). Englewood Cliffs, N.J. :Prentice Hall.

Halliday, D., & Resnick, R. (1986). Fundamental of physics (2nd ed., rev. ed.). New York: John Wiley & Sons.

Hoole, S. R. H. (1989). Computer -aided analysis and design of electromagnetic devices (1st ed.). New York: Elsevier Science.

Huebner, K. H., Thornton, E. A., & Byrom, T. G. (1995). The Finite element method for engineers (3rd ed.). New York: John Wiley & Sons.

Kwon, Y. W., & Bang, H. (1997). The Finite element method using matlab (1ˢᵗ ed.). FL: CRC.

Liu,Y. (1998) . Introduction to Finite Element Method - I & II (Chapter 1, Lecture 1: Introduction to FEM)[On-line] . Available: http://urbana.mie.uc.edu/yliu/FEM-525/FEM-525.htm.

Malik, N. H., Al-Arainy, A. A., & Qureshi, M. I. (eds.) . (1998) . Electrical insulation in power systems (1ˢᵗ ed.). New York: Marcel Dekker.

Marriam-Webster's collegiate dictionary . (2000) . [On-line]. Available: http://www.m-w.com.

MATALB user's guide. (1993). Natick, MA: The MathWorks.

Narang, A., Gupta, B. K., Dick, E. P., & Sharma, D. K. (1989) . Measurement and analysis of surge distribution in motor stator windings. IEEE Transactions on Energy Conversion, 4, pp. 126-134.

Nasar, S. A., & Unnewehr, L., E. (1979) . Electromechanics and electric machines. New York: John Wiley & Sons.

Oyegoke, B. S. (1997) . A comparative analysis of methods for calculating the transient voltage distribution within the stator winding of an electric machine subjected to steep-fronted surge. IEE Conference, 444, pp. 294-298.

Özisik, M. N. (1980) . Heat conduction. New York: John Wiley & Sons.

Rajagopal, M. S., Seetharamu, K. N., & Ashwathnarayana, P. A. (1998) . Transient thermal analysis of induction motors. IEEE Transaction on Energy Conversion, 13, 62-69.

RBC Industries (Electronics Products Division). (1997). Resin selector chart . [Brochure] . Warwick, RI: RBC Industries.

Sarkar, D., Mukherjee, P. K., & Sen, S. K. (1991) . Use of 3-dimensional finite element for computation of temperature distribution in the stator of an induction motor. IEE Proceedings-B, 138, pp. 75-86.

Sears, F. W. (1958) . Mechanics, wave motion, and heat. Readings MA: Addison-Wesley.

Silvester, P., (1969) . A general high-order finite element waveguide analysis program. IEEE Transactions on Microwave Theory and Techniques, MTT-17, pp. 204-209.

Silvester, P. (1969) . High-order polynomial triangular finite elements for potential problems. International Journal of Engineering Scince, 7, pp. 849-861.

Symon, K. R. (1964) . Mechanics (2nd ed.). MA: Addison -Wesley.

Zienkiewicz, O. C., Lyness, J., & Owen, D. R. J. (1977) . Three-dimensional magnetic field determination using a scalar potential – A finite element solution. IEEE Transactions on Magnetics, MAG-13, pp. 1649-1656.

Appendix A

Table 1

The Name of all the Variables Used in the MATLAB Programs

Variable	Description
amb_temp	The ambient temperature
arc_ang	The angle of the arc (in degree)
arc_len	The length of the arc
cap	The capacitance of the capacitor in the RC circuit
con_area	The cross-section area of the conductor
con_k	The thermal conductivity of the conductor
con_res	The resistance of the wire
con_ro	The volume density of the conductor
con_spec	The conductor thermal specific heat
counter, counter1, i, k	The counter of the loops
cyl_hei	The height of the cylinder
el_con	The parameter which determines if the element is conductor or insulator
el_num	The element number
ele_dof	Degree of freedom in each element

Table 1 (Continued)

fin_time	The final time (the time which the computation is stopped)
flux_side_len	The length of the side which have the flux passing through it
ini_time	The initial time (the time that the computation is started)
insl_conv	The convection of the insulator to the ambient
insl_k	The thermal conductivity of the first insulator around the conductor
n_time	The number of time intervals in the time domain
node_coor	The node coordinate
node_dof	Degree of freedom in each node
node_num	The node number
node_wanted	The node which its time-history is desired
num_element	The number of elements in the system
num_flux_node	The number of nodes in the conductor
num_flux_node	The number of nodes which have the flux boundary conditions
num_node_sys	The total number of nodes in the system
num_node_el	The number of node per element

Table 1 (Continued)

plot_key	The parameter determining the kind of desired graph
r_flux_node	The r-coordinate of the node which has flux
res	The resistance of the resistor in the RC circuit
sur_volt	The voltage across the capacitor in the RC circuit (the voltage surge)
sys_dof	The system degree of freedom
time	The time parameter in the surge equation
time_int	The time interval for each computation
time_wanted	The time that the history of the node is desired
tri_area	The area of the triangle
wire_c	The specific thermal of the wire
wire_cur	The current passes through the wire
wire_dia	The diameter of the wire
wire_row	The volume density of the wire
wire_sig	The electrical conductivity of the wire
wire_temp	The wire temperature at any time

Table 2

The Name of all the Matrices and Vectors Used in the MATLAB Programs

Name	Description
bc_vec1	The boundary condition vector
con_node_mat	The matrix including the nodes of the conductor part of the wire
con_node_num	The matrix including constrained node numbers
con_node_val	The vector including constrained node values
el_flux_mat	The nodes with flux boundary condition
el_mat	The element matrix (time independent)
el_vec	The element vector
node_coor_mat	The matrix containing the coordinate of the nodes
node_num_mat	The matrix containing the number dedicated to each node in each element
node_ths_mat	The matrix containing the time history solution of the nodes
node_thy_mat	The matrix containing the y-position history solution of the node at the particular time given
sol_vec	The vector containing the solution of each node
sys_mat	The system matrix

Table 2 (continued)

sys_vec	The system vector
td_el_mat	The time-dependent element matrix
td_sys_mat	The time-dependent system matrix
u_w	The last matrix in the formula

Table 3

The Name of all the Functions Used in the MATLAB Programs

Name	Description
asemble_mat1	Assembles the time-independent element matrix and vector into system matrix and system vector
asemble_t_mat1	Assembles the time-dependent element matrix into system matrix
com_node_coor1	Computes the nodes coordinates
con_el_mat1	Constructing the element matrix (time-independent)
con_el_vec1	Constructing the element vector
con_td_el_mat1	Constructing the element matrix (time-dependent)
giv_nod_num1	Assigns number to the nodes
node_t_h	setting the report type (temperature along the wire or temperature across the wire)
ss_cylinder	The main function. It calls other functions and graphs the results.

APPENDIX B

The Source Code of the MATLAB Programs

```
%
% the last date of modification:10-30-00
%-----------------------------------------------------------
% Function: ss_cylinder (the main function)
% This program calculates the temperatures among a one-
layer cylindrical wire carrying
% electricity  (the transient response)
%-----------------------------------------------------------


%-----------------------------------------------------------
%
%node_coor_mat(a , b) = c -> Global Cartesian coordinates
%                   |   |
%      Node number  The node coordinate (x,y)
%
% node_num_mat(a , b) = c -> Global node number
%                 |   |
% Element number    Local node number associated with the
                    element
%
%-----------------------------------------------------------
% NOTE: ALL THE VALUES ARE CONSIDERED IN THE SI SYSTEM
%-----------------------------------------------------------
clear;
%-----------------------------------------------------------
% Initialing the variables, vectors, and matrices
%-----------------------------------------------------------
amb_temp    = 25;
arc_ang     = 25;
arc_len     = 0.02;
cap         = 470e-006; %10 47-mf capacitors with 4.5 kV
con_area    = 7.85e-007;
con_dia     = 0.001;           %AWG = 18
con_k       = 401;
con_res     = 0.0026;
con_ro      = 8920;
con_spec    = 386;
cyl_hei     = 0.1;
el_con      = 0;
ini_time    = 0;
insl_conv   = 5;
%insl_k  = 0.20;  % Silicon rubber(RBC-5520)  ,Temp
                    range :-65,Max.100
```

```
%insl_k     = 0.22;   % Silicon rubber(RBC 5200)  ,Temp
                        range :-65,Max.100
insl_k      = 1.13;% Silicon rubber(RBC 5400)  ,Temp
                        range :-65,Max.100
ele_dof     = 3;
fin_time    = 0.1;
node_dof    = 1;
node_wanted = 3;
num_con_el  = 200;
num_con_node= 126;
num_flux_node = 70;
num_node_el = 3;
num_element = 600;
num_node_sys= 336;
plot_key    = 1;
sur_volt    = 50000;
sys_dof     = node_dof*num_node_sys;
time        = 0;
time_int    = 0.001;
wire_cur    = 7.2;
wire_dia    = 0.0015;
wire_res    = 14.9;
wire_sig    = 5.98e+007;
%
n_time = (fin_time - ini_time)/time_int;
time_wanted    = n_time - 89;
%
con_node_mat = zeros(num_con_node,1);
con_node_val = zeros(num_con_node,1);
conduct_mat  = zeros(num_con_el,1);
node_num_mat = zeros(num_node_sys,3);
node_coor_mat =zeros(num_node_sys,2);
el_flux_mat  = zeros(num_flux_node-2, 2);
el_vec       = zeros(ele_dof, 1);
sys_vec      = zeros(sys_dof, 1);
el_mat       = zeros(ele_dof, ele_dof);
td_el_mat    = zeros(ele_dof, ele_dof);
td_sys_mat   =  zeros(sys_dof, sys_dof);
sys_mat      = zeros(sys_dof, sys_dof);
sol_vec      = zeros(num_node_sys,1);
node_ths_mat = zeros(20,round(n_time));
node_thy_mat = zeros(3, 20);
```

```
%
%-----------------------------------------------------------
%  Construction the conductor element matrix
%-----------------------------------------------------------
%
m = 5;
j = 1;
for counter = 1:num_con_el
    conduct_mat(counter,1) = m + j;
    j = j + 1;
    if j == 6
        m = m + 15;
        j = 1;
    end
end
%
%-----------------------------------------------------------
%  The Main Program
%-----------------------------------------------------------
%
%Assigning number to the nodes
node_num_mat = giv_nod_num1(node_num_mat);

% Computing the node coordinates
node_coor_mat =
com_node_coor1(node_coor_mat,con_dia,wire_dia,cyl_hei,arc
_len,arc_ang);
%
m = 0;
for counter=1:num_element
    tri_area  = (1/2)*det([1,
    node_coor_mat(node_num_mat(counter,1),1),
    node_coor_mat(node_num_mat(counter,1),2); 1,
    node_coor_mat(node_num_mat(counter,2),1),
    node_coor_mat(node_num_mat(counter,2),2); 1,
    node_coor_mat(node_num_mat(counter,3),1),
    node_coor_mat(node_num_mat(counter,3),2)]);
    el_mat   =
    con_el_mat1(el_mat,node_coor_mat,node_num_mat,counter,
    tri_area,con_k,insl_k,m);
    td_el_mat = con_td_el_mat1(td_el_mat,tri_area);
    if counter >= m + 6
        if counter <= m + 10
            el_vec  =
            ((wire_cur)^2/(con_ro*con_spec*(con_area)^2*wire
```

```
          _sig))*con_el_vec1(el_vec, node_coor_mat,
          node_num_mat, counter,tri_area);
        else
            el_vec = [0;0;0];
        end
    end
   [sys_mat,sys_vec] =
   asemble_mat1(sys_mat,node_num_mat,el_mat,el_vec,sys_ve
   c,counter);
   [td_sys_mat]=
   asemble_t_mat1(td_sys_mat,td_el_mat,node_num_mat,counte
   r);
   if counter >= 15 + el_con
        el_con = el_con + 15;
        m = m + 15;
   end
end
%
%------------------------------------------------------------
% Computing the flux at the boundaries and adding it to
%the system matrices and vector
%------------------------------------------------------------
%               el_flux_mat( a, b)
%                             |  |
%the counter representing   the number of the node
%the number of the element
%
el_flux_mat(1,1)  = 1;   el_flux_mat(1,2)  = 17;
el_flux_mat(2,1)  = 17;  el_flux_mat(2,2)  = 33;
el_flux_mat(3,1)  = 33;  el_flux_mat(3,2)  = 49;
el_flux_mat(4,1)  = 49;  el_flux_mat(4,2)  = 65;
el_flux_mat(5,1)  = 65;  el_flux_mat(5,2)  = 81;
el_flux_mat(6,1)  = 81;  el_flux_mat(6,2)  = 97;
el_flux_mat(7,1)  = 97;  el_flux_mat(7,2)  = 113;
el_flux_mat(8,1)  = 113; el_flux_mat(8,2)  = 129;
el_flux_mat(9,1)  = 129; el_flux_mat(9,2)  = 145;
el_flux_mat(10,1) = 145; el_flux_mat(10,2) = 161;
el_flux_mat(11,1) = 161; el_flux_mat(11,2) = 177;
el_flux_mat(12,1) = 177; el_flux_mat(12,2) = 193;
el_flux_mat(13,1) = 193; el_flux_mat(13,2) = 209;
el_flux_mat(14,1) = 209; el_flux_mat(14,2) = 225;
el_flux_mat(15,1) = 225; el_flux_mat(15,2) = 241;
el_flux_mat(16,1) = 241; el_flux_mat(16,2) = 257;
el_flux_mat(17,1) = 257; el_flux_mat(17,2) = 273;
el_flux_mat(18,1) = 273; el_flux_mat(18,2) = 289;
```

```
el_flux_mat(19,1) = 289; el_flux_mat(19,2) = 305;
el_flux_mat(20,1) = 305; el_flux_mat(20,2) = 321;
el_flux_mat(21,1)  = 16; el_flux_mat(21,2)  = 32;
el_flux_mat(22,1)  = 32; el_flux_mat(22,2)  = 48;
el_flux_mat(23,1)  = 48; el_flux_mat(23,2)  = 64;
el_flux_mat(24,1)  = 64; el_flux_mat(24,2)  = 80;
el_flux_mat(25,1)  = 80; el_flux_mat(25,2)  = 96;
el_flux_mat(26,1)  = 96; el_flux_mat(26,2)  = 112;
el_flux_mat(27,1)  = 112;el_flux_mat(27,2)  = 128;
el_flux_mat(28,1)  = 128;el_flux_mat(28,2)  = 144;
el_flux_mat(29,1)  = 144;el_flux_mat(29,2)  = 160;
el_flux_mat(30,1) = 160; el_flux_mat(30,2) = 176;
el_flux_mat(31,1) = 176; el_flux_mat(31,2) = 192;
el_flux_mat(32,1) = 192; el_flux_mat(32,2) = 208;
el_flux_mat(33,1) = 208; el_flux_mat(33,2) = 224;
el_flux_mat(34,1) = 224; el_flux_mat(34,2) = 240;
el_flux_mat(35,1) = 240; el_flux_mat(35,2) = 256;
el_flux_mat(36,1) = 256; el_flux_mat(36,2) = 272;
el_flux_mat(37,1) = 272; el_flux_mat(37,2) = 288;
el_flux_mat(38,1) = 288; el_flux_mat(38,2) = 304;
el_flux_mat(39,1) = 304; el_flux_mat(39,2) = 320;
el_flux_mat(40,1) = 320; el_flux_mat(40,2) = 336;
el_flux_mat(41,1) = 336; el_flux_mat(41,2) = 335;
el_flux_mat(42,1) = 335; el_flux_mat(42,2) = 334;
el_flux_mat(43,1) = 334; el_flux_mat(43,2) = 333;
el_flux_mat(44,1) = 333; el_flux_mat(44,2) = 332;
el_flux_mat(45,1) = 332; el_flux_mat(45,2) = 331;
el_flux_mat(46,1) = 331; el_flux_mat(46,2) = 330;
el_flux_mat(47,1) = 330; el_flux_mat(47,2) = 329;
el_flux_mat(48,1) = 329; el_flux_mat(48,2) = 328;
el_flux_mat(49,1) = 328; el_flux_mat(49,2) = 327;
el_flux_mat(50,1) = 327; el_flux_mat(50,2) = 326;
el_flux_mat(51,1) = 326; el_flux_mat(51,2) = 325;
el_flux_mat(52,1) = 325; el_flux_mat(52,2) = 324;
el_flux_mat(53,1) = 324; el_flux_mat(53,2) = 323;
el_flux_mat(54,1) = 323; el_flux_mat(54,2) = 322;
el_flux_mat(55,1) = 322; el_flux_mat(55,2) = 321;
el_flux_mat(56,1) = 1;   el_flux_mat(56,2) = 2;
el_flux_mat(57,1) = 2;   el_flux_mat(57,2) = 3;
el_flux_mat(58,1) = 3;   el_flux_mat(58,2) = 4;
el_flux_mat(59,1) = 4;   el_flux_mat(59,2) = 5;
el_flux_mat(60,1) = 5;   el_flux_mat(60,2) = 6;
el_flux_mat(61,1) = 6;   el_flux_mat(61,2) = 7;
el_flux_mat(62,1) = 7;   el_flux_mat(62,2) = 8;
el_flux_mat(63,1) = 8;   el_flux_mat(63,2) = 9;
```

```
el_flux_mat(64,1) = 9;    el_flux_mat(64,2) = 10;
el_flux_mat(65,1) = 10;   el_flux_mat(65,2) = 11;
el_flux_mat(66,1) = 11;   el_flux_mat(66,2) = 12;
el_flux_mat(67,1) = 12;   el_flux_mat(67,2) = 13;
el_flux_mat(68,1) = 13;   el_flux_mat(68,2) = 14;
el_flux_mat(69,1) = 14;    el_flux_mat(69,2) = 15;
el_flux_mat(70,1) = 15;    el_flux_mat(70,2) = 16;
%
for i = 1:(num_flux_node)
    if i > 40
        el_mat1 = [0,0;0,0];
        el_vec1 = [0;0];
    else
        r1_flux_node = node_coor_mat(el_flux_mat(i, 1),1);
        r2_flux_node = node_coor_mat(el_flux_mat(i, 2),1);
        z1_flux_node = node_coor_mat(el_flux_mat(i, 1),2);
        z2_flux_node = node_coor_mat(el_flux_mat(i, 2),2);
        flux_side_len = sqrt((r2_flux_node -
        r1_flux_node)^2 + (z2_flux_node - z1_flux_node)^2);
        el_mat1 =
        insl_k*insl_conv*(flux_side_len/6)*[2,1;1,2];
        el_vec1 =
        insl_k*insl_conv*amb_temp*[flux_side_len/2;flux_sid
        e_len/2];
    end
    [sys_mat,sys_vec] =
    asemble_mat1(sys_mat,el_flux_mat,el_mat1,el_vec1,sys_
    vec,i);
end
%
%-----------------------------------------------------------
% loop for the time integration
%-----------------------------------------------------------
%
for counter1 = 1: num_node_sys
    sol_vec(counter1,1) = 25;
end
yyy = sys_vec;
sys_mat = td_sys_mat + time_int*sys_mat;
for counter = 1:n_time
    %if counter < (n_time - 90)
        r_side = time_int*sys_vec + td_sys_mat*sol_vec;
    %else
    %    for counter1 = 1:length(conduct_mat)
```

```
%    tri_area  = (1/2)*det([1,
     node_coor_mat(node_num_mat(conduct_mat(counter1,1
     ),1),1),
     node_coor_mat(node_num_mat(conduct_mat(counter1,1
     ),1),2); 1,
     node_coor_mat(node_num_mat(conduct_mat(counter1,1
     ),2),1),
     node_coor_mat(node_num_mat(conduct_mat(counter1,1
     ),2),2); 1,
     node_coor_mat(node_num_mat(conduct_mat(counter1,1
     ),3),1),
     node_coor_mat(node_num_mat(conduct_mat(counter1,1
     ),3),2)]);
%    sur_cur = (sur_volt*exp(-
     1*time/(wire_res*cap)))/wire_res;
%    el_vec  =
     ((sur_cur)^2/(con_ro*con_spec*(con_area)^2*wire_s
     ig))*con_el_vec1(el_vec, node_coor_mat,
     node_num_mat, conduct_mat(counter1,1),tri_area);
%    for i = 1:3
%       counter2 =
        node_num_mat(conduct_mat(counter1,1),i);
%       sys_vec(counter2,1) = yyy(counter2,1) +
        el_vec(i,1);
%    end
%  end
%  r_side = time_int*sys_vec + td_sys_mat*sol_vec;
%  time = time + time_int;
%end
%
sol_vec = sys_mat\r_side;
%
switch plot_key
case 1              % Temperature variation along the
                    wire at Time = time_wanted
   node_ths_mat = node_t_h (node_ths_mat, sol_vec,
   counter,node_wanted);
   if counter == time_wanted
       node_thy_mat(1,:) = node_ths_mat(:,
       time_wanted)';
   end
  node_ths_mat = node_t_h (node_ths_mat, sol_vec,
  counter,node_wanted + 5);
   if counter == time_wanted
```

```matlab
          node_thy_mat(2,:) = node_ths_mat(:,
          time_wanted)';
        end
      node_ths_mat = node_t_h (node_ths_mat, sol_vec,
      counter,node_wanted + 11);
       if counter == time_wanted
          node_thy_mat(3,:) = node_ths_mat(:,
          time_wanted)';
        end
    case 2                                   % Node set # 1
       node_ths_mat(1,counter) = sol_vec(83,1);
       node_ths_mat(2,counter) = sol_vec(88,1);
       node_ths_mat(3,counter) = sol_vec(94,1);

    case 3                                    % Node set # 2
      node_ths_mat(1,counter) = sol_vec(179,1);
       node_ths_mat(2,counter) = sol_vec(184,1);
       node_ths_mat(3,counter) = sol_vec(190,1);
    case 4                                    % Node set # 3
       node_ths_mat(1,counter) = sol_vec(307,1);
       node_ths_mat(2,counter) = sol_vec(312,1);
       node_ths_mat(3,counter) = sol_vec(318,1);
    end
end
%
%-------------------------------------------------------------
% Plot the result
%-------------------------------------------------------------
%
switch plot_key
case 1
    counter = node_wanted;
    for k = 1: length(node_thy_mat)
      x_pos(1,k) = node_coor_mat(counter,2);
       counter = counter + 16;
    end
    counter = node_wanted + 5;
    for k = 1: length(node_thy_mat)
       x_pos(2,k) = node_coor_mat(counter,2);
       counter = counter + 16;
    end
    counter = node_wanted + 11;
    for k = 1: length(node_thy_mat)
       x_pos(3,k) = node_coor_mat(counter,2);
       counter = counter + 16;
```

```
    end
    plot(x_pos(1,:),node_thy_mat(1,:),'-
',x_pos(2,:),node_thy_mat(2,:),'-
',x_pos(3,:),node_thy_mat(3,:),'-');
case  {2,3,4}
    time = ini_time:time_int:(fin_time - time_int);
    plot(time,node_ths_mat(1,:),'-
',time,node_ths_mat(2,:),'-',time,node_ths_mat(3,:),'-');
end
axis auto;
ylabel('Temperature(C)');
clear;
```

```
%---------------------------------------------------------------
% the last date of modification:10-14-00
% Function: giv_nod_num1
% Assigning number to the nodes in the system (Transient
%analysis
% with a 1-layer cylinder)
%
% node_num_mat(a , b) = c -> Global node number
%                   |   |
% Element number  Local node number associated with the
element
%---------------------------------------------------------------
function[node_num_mat] = giv_node_nume1(node_num_mat);
%
% Insulator 1
   node_num_mat(1,1)   = 1;      node_num_mat(1,2)   = 2;
   node_num_mat(1,3)  = 18;
   node_num_mat(2,1)   = 2;      node_num_mat(2,2)   = 3;
   node_num_mat(2,3)  = 19;
   node_num_mat(3,1)   = 3;      node_num_mat(3,2)   = 4;
   node_num_mat(3,3)  = 20;
   node_num_mat(4,1)   = 4;      node_num_mat(4,2)   = 5;
   node_num_mat(4,3)  = 21;
   node_num_mat(5,1)   = 5;      node_num_mat(5,2)   = 6;
   node_num_mat(5,3)  = 22;
   node_num_mat(16,1) = 1;       node_num_mat(16,2) = 18;
   node_num_mat(16,3) = 17;
   node_num_mat(17,1) = 2;       node_num_mat(17,2) = 19;
   node_num_mat(17,3) = 18;
   node_num_mat(18,1) = 3;       node_num_mat(18,2) = 20;
   node_num_mat(18,3) = 19;
   node_num_mat(19,1) = 4;       node_num_mat(19,2) = 21;
   node_num_mat(19,3) = 20;
   node_num_mat(20,1) = 5;       node_num_mat(20,2) = 22;
   node_num_mat(20,3) = 21;
% Conductor
   node_num_mat(6,1)   = 6;      node_num_mat(6,2)   = 7;
   node_num_mat(6,3)  = 23;
   node_num_mat(7,1)   = 7;      node_num_mat(7,2)   = 8;
   node_num_mat(7,3)  = 24;
   node_num_mat(8,1)   = 8;      node_num_mat(8,2)   = 9;
   node_num_mat(8,3)  = 25;
   node_num_mat(9,1)   = 9;      node_num_mat(9,2)   = 10;
   node_num_mat(9,3)  = 26;
```

```
node_num_mat(10,1) = 10; node_num_mat(10,2) = 11;
node_num_mat(10,3)= 27;
node_num_mat(21,1) = 6;      node_num_mat(21,2) = 23;
node_num_mat(21,3) = 22;
node_num_mat(22,1) = 7;      node_num_mat(22,2) = 24;
node_num_mat(22,3) = 23;
node_num_mat(23,1) = 8;      node_num_mat(23,2) = 25;
node_num_mat(23,3) = 24;
node_num_mat(24,1) = 9;      node_num_mat(24,2) = 26;
node_num_mat(24,3) = 25;
node_num_mat(25,1) = 10; node_num_mat(25,2) = 27;
node_num_mat(25,3) = 26;
%  Insulator 1
node_num_mat(11,1) = 11; node_num_mat(11,2) = 12;
node_num_mat(11,3) = 28;
node_num_mat(12,1) = 12; node_num_mat(12,2) = 13;
node_num_mat(12,3) = 29;
node_num_mat(13,1) = 13; node_num_mat(13,2) = 14;
node_num_mat(13,3) = 30;
node_num_mat(14,1) = 14; node_num_mat(14,2) = 15;
node_num_mat(14,3) = 31;
node_num_mat(15,1) = 15; node_num_mat(15,2) = 16;
node_num_mat(15,3) = 32;
node_num_mat(26,1) = 11; node_num_mat(26,2) = 28;
node_num_mat(26,3) = 27;
node_num_mat(27,1) = 12; node_num_mat(27,2) = 29;
node_num_mat(27,3) = 28;
node_num_mat(28,1) = 13; node_num_mat(28,2) = 30;
node_num_mat(28,3) = 29;
node_num_mat(29,1) = 14; node_num_mat(29,2) = 31;
node_num_mat(29,3) = 30;
node_num_mat(30,1) = 15; node_num_mat(30,2) = 32;
node_num_mat(30,3) = 31;
%
l = 30;
for i = 1: 19
   for j = 1:15
      node_num_mat(j+l,1)    = node_num_mat(j+l-15,3);
      node_num_mat(j+l,2)    = node_num_mat(j+l-15,2);
      node_num_mat(j+l,3)    = node_num_mat(j+l-15,2)+ 16;
   end
   for k = 1:15
      node_num_mat(k+j+l,1) = node_num_mat(k+j+l-15,1);
      node_num_mat(k+j+l,2) = node_num_mat(k+j+l-15,3);
```

```
        node_num_mat(k+j+1,3) = node_num_mat(k+j+1-15,1)
        +16;
    end
    1 = 1 + 30;
end
%
```

```
%------------------------------------------------------------
%     the last date of modification:10-14-00
%     Function: com_node_coor1
%     Computing the coordinates of the nodes in the
%     system(transient analysis with a 1-layer cylinder)
%
%node_coor_mat(a , b) = c -> Global Cartesian coordinates
%                     |   |
%     Node number  The node coordinate (x,y)
%------------------------------------------------------------
function[node_coor_mat]  =
com_node_coor1(node_coor_mat,con_dia,wire_dia,cyl_hei,
arc_len, arc_ang);
%
%------------------------------------------------------------
%     The variables used in this program:
%arc_rad                :The main radios of the torus
                         (measured form the central arc of the
                         turos)
%diff_ang               :The difference between the angles of
                          the two successive out_seg_lens
%in_arc_rad             :The inner radius of the torus
%in_seg_len             :The length of the inner segment
                         separated from the inner circle of
                         the torus
%out_arc_rad            :The outer radius of the torus
%out_seg_len            :The length of the outer segment
                         separated from the outer circle of
                         the torus
%sub_ang                :The angle of each secant of the
torus
%sub_wire_dia           :A fraction part of the wire diameter
%
%------------------------------------------------------------
%
%     The cylindrical part
%
node_coor_mat(1,1) = 0;  node_coor_mat(1,2) = 0;
m = 1;
for i = 1:11
   for j = 1:5
     node_coor_mat(j+m,1) = node_coor_mat(j+m-1,1) +
     ((wire_dia - con_dia)/2)/5;
      node_coor_mat(j+m,2) = node_coor_mat(j+m-1,2);
   end
```

```
  for j = 6:10
    node_coor_mat(j+m,1) = node_coor_mat(j+m-1,1) +
    (con_dia)/5;
     node_coor_mat(j+m,2) = node_coor_mat(j+m-1,2);
  end
  for j = 11:15
    node_coor_mat(j+m,1) = node_coor_mat(j+m-1,1) +
    ((wire_dia - con_dia)/2)/5;
    node_coor_mat(j+m,2) = node_coor_mat(j+m-1,2);
  end
  m = m + 16;
  node_coor_mat(m,1) = 0;
  node_coor_mat(m,2) = node_coor_mat(m-16,2) +
cyl_hei/10;
end
%
%    The curved part
%
sub_ang = arc_ang/10;
diff_ang = 0;
arc_rad = (arc_len*180) / (arc_ang*3.14);
in_arc_rad = arc_rad  - (wire_dia/2);
out_arc_rad = arc_rad + (wire_dia/2);
in_seg_len    = in_arc_rad*(sub_ang*pi/180);
out_seg_len   = out_arc_rad*(sub_ang*pi/180);
b_angle = (180 - sub_ang)/2;
%
m = 177;
for i =1 :10
   node_coor_mat(m,1) = node_coor_mat(m - 16,1) +
out_seg_len*cos((b_angle - diff_ang)*pi/180);
   node_coor_mat(m,2) = node_coor_mat(m - 16,2) +
out_seg_len*sin((b_angle - diff_ang)*pi/180);
   for j = 1:5
     node_coor_mat(j+m,1) = node_coor_mat(j+m-16,1) +
     (out_seg_len/out_arc_rad)*(out_arc_rad - j*(wire_dia
     - con_dia)/10)*cos((b_angle-diff_ang)*pi/180);   .
     node_coor_mat(j+m,2) = node_coor_mat(j+m-16,2) +
     (out_seg_len/out_arc_rad)*(out_arc_rad - j*(wire_dia
     - con_dia)/10)*sin((b_angle-diff_ang)*pi/180);
   end
   jj = 1;
   for j = 6:10
     node_coor_mat(j+m,1) = node_coor_mat(j+m-16,1) +
     ((out_seg_len/out_arc_rad)*(out_arc_rad - ((wire_dia
```

```
    - con_dia)/2 + (jj*con_dia)/5)))*cos((b_angle-
    diff_ang)*pi/180);
    node_coor_mat(j+m,2) = node_coor_mat(j+m-16,2) +
    ((out_seg_len/out_arc_rad)*(out_arc_rad - ((wire_dia
    - con_dia)/2 + (jj*con_dia)/5)))*sin((b_angle-
    diff_ang)*pi/180);
    jj = jj + 1;
  end
  jj = 1;
  for j = 11:15
    node_coor_mat(j+m,1) = node_coor_mat(j+m-16,1) +
    ((out_seg_len/out_arc_rad)*(out_arc_rad - ((wire_dia
    - con_dia)/2 + (con_dia)/5 + jj*(wire_dia -
    con_dia)/10)))*cos((b_angle-diff_ang)*pi/180);
    node_coor_mat(j+m,2) = node_coor_mat(j+m-16,2) +
    ((out_seg_len/out_arc_rad)*(out_arc_rad - ((wire_dia
    - con_dia)/2 + (con_dia)/5 + jj*(wire_dia -
    con_dia)/10)))*sin((b_angle-diff_ang)*pi/180);
    jj = jj + 1;
  end
  m = m + 16;
  diff_ang = diff_ang + sub_ang;
end
```

```
%------------------------------------------------------------
% the last date of modification:10-14-00
% Function: con_el_mat1
% Constructing the element matrix
%
%    node_num_mat(a , b) = c -> Global node number
%                         |   |
%    Element number  Local node number associated with
the element
%----------------------------------------------%function[el_mat]  =
el_mat_fun1(el_mat,node_coor_mat,node_num_mat,el_num,
tri_area,con_k,insl_k,m);
function[el_mat] =
con_el_mat1(el_mat,node_coor_mat,node_num_mat,counter,tri
_area,con_k,insl_k,m);
%
   r1 = node_coor_mat(node_num_mat(counter,1),1);
   z1 = node_coor_mat(node_num_mat(counter,1),2);
   r2 = node_coor_mat(node_num_mat(counter,2),1);
   z2 = node_coor_mat(node_num_mat(counter,2),2);
   r3 = node_coor_mat(node_num_mat(counter,3),1);
   z3 = node_coor_mat(node_num_mat(counter,3),2);
   switch counter
   case {m+1, m+2, m+3, m+4, m+5}
       cc = insl_k*(1/(4*tri_area));
   case {m+6, m+7, m+8, m+9, m+10}
        cc =  con_k*(1/(4*tri_area));
   case {m+11, m+12, m+13, m+14, m+15}
       cc = insl_k*(1/(4*tri_area));
   end
   el_mat(1,1)  = cc*((r3 - r2)^2+(z2 - z3)^2);
   el_mat(1,2)  = cc*((r3 - r2)*(r1 - r3)+(z2 - z3)*(z3 -
   z1));
   el_mat(1,3)  = cc*((r3 - r2)*(r2 - r1)+(z2 - z3)*(z1 -
   z2));
   el_mat(2,1)  = el_mat(1,2);
   el_mat(2,2)  = cc*((r1 - r3)^2+(z3 - z1)^2);
   el_mat(2,3)  = cc*((r1 - r3)*(r2 - r1)+(z3 - z1)*(z1 -
   z2));
   el_mat(3,1)  = el_mat(1,3);
   el_mat(3,2)  = el_mat(2,3);
   el_mat(3,3)  = cc*((r2 - r1)^2+(z1 - z2)^2);
%
```

```
%----------------------------------------------------------------
%  the last date of modification:10-14-00
%  Function: con_td_el_mat1
%  Constructing the time_dependent element matrix
(transient analysis with a 1-layer cylinder)
%----------------------------------------------------------------
%
function[td_el_mat] =
    con_td_el_mat1(td_el_mat,tri_area);
%
td_el_mat = [2,1,1;1,2,1;1,1,2];
td_el_mat = (tri_area/12)*td_el_mat;
```

```
%----------------------------------------------------------------
% the last date of modification:10-14-00
% Function: con_el_vec1
% Constructing the element vector (transiant analysis
%with a 1-layer cylinder)
%
% node_num_mat(a , b) = c -> Global node number
%                  |   |
% Element number  Local node number associated with the
element
%
%----------------------------------------------------------------
%
function [el_vec] = con_el_vec1(el_vec, node_coor_mat,
node_num_mat, counter, tri_area);
%
r1 = node_coor_mat(node_num_mat(counter,1),1);
r2 = node_coor_mat(node_num_mat(counter,2),1);
r3 = node_coor_mat(node_num_mat(counter,3),1);
z1 = node_coor_mat(node_num_mat(counter,1),2);
z2 = node_coor_mat(node_num_mat(counter,2),2);
z3 = node_coor_mat(node_num_mat(counter,3),2);
%
f1 = (1/(2*tri_area))*(r2 - r1)*(z3 - z1);
% The Hi is treated as the multiplication of the form
of:h1 = f1 * f2

% Computing h1
f2 = (r2*z3 - r3*z2) + (1/2)*(r1 + r2)*(z2 - z3) +
(1/2)*(r3 - r2)*(z3 + z1) ;
el_vec(1,1) = f1*f2;

% Computing h2
f2 = r3*z1 - r1*z3 + (1/2)*(r1 + r2)*(z3 - z1) +
(1/2)*(r1 - r3)*(z3 + z1);
el_vec(2,1) = f1*f2;

% Computing h3
f2 = r1*z2 - r2*z1 + (1/2)*(r1 + r2)*(z1 - z2) +
(1/2)*(r2 - r1)*(z1 + z3);
el_vec(3,1) = f1*f2;
%
```

```
%---------------------------------------------------------------
%  the last date of modification:10-14-00
%  Function: asemble_mat1
%  Constructing the time-independent system matrix
%---------------------------------------------------------------
function[sys_mat,sys_vec]   =
asemble_mat1(sys_mat,node_num_mat,el_mat,el_vec,sys_vec,c
ounter);
%
mat_len = length(el_mat);
vec_len = length(el_vec);
for i = 1:vec_len
    counter1 = node_num_mat(counter,i);
    sys_vec(counter1) = sys_vec(counter1) + el_vec(i);
    for j = 1:mat_len
        counter2 = node_num_mat(counter,j);
        sys_mat(counter1,counter2) =
    sys_mat(counter1,counter2) + el_mat(i,j);
    end
end
```

```
%
%-------------------------------------------------------
% the last date of modification:7-12-00
% Function: asemble_t_mat1
% Constructing the time-dependent system matrix
%-----------------------------------------------
function[td_sys_mat]=
asemble_t_mat1(td_sys_mat,td_el_mat,node_num_mat,counter)
;
%
%--------------------------------------------
% Assembling time-dependent matrix elements
%--------------------------------------------
%
td_sys_mat(node_num_mat(counter,1),node_num_mat(counter,1
))=
td_sys_mat(node_num_mat(counter,1),node_num_mat(counter,1
)) + td_el_mat(1,1);

td_sys_mat(node_num_mat(counter,1),node_num_mat(counter,2
))=
td_sys_mat(node_num_mat(counter,1),node_num_mat(counter,2
)) + td_el_mat(1,2);

td_sys_mat(node_num_mat(counter,1),node_num_mat(counter,3
))=
td_sys_mat(node_num_mat(counter,1),node_num_mat(counter,3
)) + td_el_mat(1,3);

td_sys_mat(node_num_mat(counter,2),node_num_mat(counter,1
))=
   td_sys_mat(node_num_mat(counter,2),node_num_mat(counte
r,1)) + td_el_mat(2,1);

td_sys_mat(node_num_mat(counter,2),node_num_mat(counter,2
))=
   td_sys_mat(node_num_mat(counter,2),node_num_mat(counte
r,2)) + td_el_mat(2,2);

td_sys_mat(node_num_mat(counter,2),node_num_mat(counter,3
))=
   td_sys_mat(node_num_mat(counter,2),node_num_mat(counte
r,3)) + td_el_mat(2,3);
```

```
td_sys_mat(node_num_mat(counter,3),node_num_mat(counter,1
)) =
    td_sys_mat(node_num_mat(counter,3),node_num_mat(counte
r,1)) + td_el_mat(3,1);

td_sys_mat(node_num_mat(counter,3),node_num_mat(counter,2
)) =
    td_sys_mat(node_num_mat(counter,3),node_num_mat(counte
r,2)) + td_el_mat(3,2);

td_sys_mat(node_num_mat(counter,3),node_num_mat(counter,3
)) =
td_sys_mat(node_num_mat(counter,3),node_num_mat(counter,3
)) + td_el_mat(3,3);
```

```
%
%------------------------------------------------------------
%
% the last date of modification:10-14-00
% Function: node_t_h
% Making the time-history of the chosen node(s) and
filling Matrix node_ths_mat
%
%------------------------------------------------------------
%
function[node_ths_mat] =
node_t_h(node_ths_mat,sol_vec,counter,node_wanted,plot_ke
y);
    j = 0;
   for i = 1:20
      node_ths_mat(i,counter)  = sol_vec(node_wanted +
      j,1);
       j = j + 16;
    end
```